12-2002

Geoelectrical Response of an Aged LNAPL Plume: Implications for Monitoring Natural Attenuation

Douglas D. Werkema Jr.
Western Michigan University

GEOELECTRICAL RESPONSE OF AN AGED LNAPL PLUME: IMPLICATIONS FOR MONITORING NATURAL ATTENUATION

by

Douglas D. Werkema, Jr.

A Dissertation
Submitted to the
Faculty of The Graduate College
in partial fulfillment of the
requirements for the
Degree of Doctor of Philosophy
Department of Geosciences

Western Michigan University
Kalamazoo, Michigan
December 2002

GEOELECTRICAL RESPONSE OF AN AGED LNAPL PLUME: IMPLICATIONS FOR MONITORING NATURAL ATTENUATION

Douglas D. Werkema, Jr., Ph.D.

Western Michigan University, 2002

The geoelectric stratigraphy at a site impacted with light non-aqueous phase liquids (LNAPLs) is investigated for its link to natural biodegradation, its contribution to the conductive model for aged (i.e. mature) LNAPL contaminated sites, and the relationship to the natural hydrologic regime. The highest conductivities (lowest resistivities) were observed in portions of soils where LNAPL was in residual and free phase. Corroborating evidence from bacteria enumeration from soil close to the vertical resistivity probe (VRP) installations show orders-of-magnitude increase in both heterotrophic and oil degrading microbes at the depths where the conductivity was at a maximum. The coincidence of peak microbial populations with zones of high conductivity provides circumstantial evidence linking the anomalous high conductivity to microbial degradation of LNAPLs.

A simple analysis using Archie's Law reveals that large pore water saturation and a large pore water conductivity enhancement is necessary to produce the VRP field results from the contaminated locations. These results support the conductive model at aged LNAPL contaminated sites due to the effects of enhanced mineral dissolution of the aquifer materials resulting from biodegradation of the contaminant mass.

Further comparison of the temporal conductivity variation and water table fluctuations are also presented. The VRP results suggest that the conductivity response is inversely related to water table elevations at locations of LNAPL contamination and directly related at the non-contaminated location.

Overall, this study demonstrates the potential of geoelectrical investigations as a tool for assessing the microbial degradation of LNAPL impacted soils. The results will guide biogeochemical investigations to discrete zones where, physical changes are occurring, and provide the basis for model calibration at sites with mature LNAPL contamination.

INFORMATION TO USERS

This manuscript has been reproduced from the microfilm master. UMI films the text directly from the original or copy submitted. Thus, some thesis and dissertation copies are in typewriter face, while others may be from any type of computer printer.

The quality of this reproduction is dependent upon the quality of the copy submitted. Broken or indistinct print, colored or poor quality illustrations and photographs, print bleedthrough, substandard margins, and improper alignment can adversely affect reproduction.

In the unlikely event that the author did not send UMI a complete manuscript and there are missing pages, these will be noted. Also, if unauthorized copyright material had to be removed, a note will indicate the deletion.

Oversize materials (e.g., maps, drawings, charts) are reproduced by sectioning the original, beginning at the upper left-hand corner and continuing from left to right in equal sections with small overlaps.

ProQuest Information and Learning
300 North Zeeb Road, Ann Arbor, MI 48106-1346 USA
800-521-0600

ACKNOWLEDGMENTS

The following are just a few who contributed to the completion of this dissertation. First, to the members of my committee, Dr. Estella Atekwana, Dr. William Sauck, Dr. Daniel Cassidy, and Dr. Anthony Endres I extend my sincere appreciation for their guidance, support and patience. Also the various funding institutions which supported this work financially: AAPG Grants-In-Aid, NASA through the Michigan Space Grant Consortium, the Doctoral Dissertation Fellowship through the Graduate College at Western Michigan University, and the American chemical Society-Petroleum Research Fund Grant (PRF# 31594-AC2).

Second, I thank Joe Duris for his help in the field and his contribution to the microbiological investigations, and Dr. Sylvia Rossbach for her collaboration in microbiology.

Third, I thank Tyler Knoll, Andy Nicholls and Jeff Locey for their technical assistance in the field.

I thank my family especially my parents Douglas Werkema and Marcia Werkema whose support and unconditional love cannot be overstated. Thank you.

Finally, I thank my wife Stephanie for her support, encouragement and for being the best wife, friend and mother to our daughter, Grace, that anyone could dream for.

Douglas D. Werkema, Jr.

TABLE OF CONTENTS

LIST OF TABLES

LIST OF FIGURES

CHAPTER 2

CHAPTER 3

CHAPTER 1

INTRODUCTION

Geophysical investigations, predominantly using electrical methods such as electromagnetic induction, ground penetrating radar, resistivity, and spontaneous potential, have been commonly applied to characterize the subsurface geology and contaminant distribution at sites contaminated with petroleum hydrocarbons such as light non-aqueous phase liquids (LNAPLs) (Daniels et al., 1992; Maxwell and Schmok, 1995; Benson et al., 1997; Bermejo et al., 1997; Vanhala, 1997). These methods are applicable because the LNAPL contaminated zone is electrically different from the surrounding material thus presenting anomalies suggestive of their location. Specifically, most of the geoelectrical investigations and modeling at LNAPL impacted sites are based on the insulating layer model where the more resistive petroleum hydrocarbon occupies the pore space and results in a geoelectrically resistive anomaly (Mazác et al., 1990; De Ryck et al., 1993; Redman et al., 1994; Osiensky, 1997; Blacic and Arulanandan, 1999). However, these investigations have not included how the LNAPL contaminated zone or impacted areas change over time due to natural hydrologic and biogeochemical reactions, such as those reported by numerous geochemical and microbial studies (Cozzarelli et al., 1990; Bennett et al., 1993; McMahon et al., 1995).

The natural microbial degradation of petroleum hydrocarbon contamination has been accepted as a viable means to deal with such contamination (Davee and Sanders, 2000). Natural biodegradation of the LNAPL reduces its extent and eventually removes

it altogether as natural microbes metabolize the hydrocarbon. This process of resident microbes capable of breaking down hydrocarbons has been well established in the geochemistry and microbial literature (Baedecker et al., 1987; Cozzarelli et al., 1990; Baedecker et al., 1993; Bennett et al., 1993; Eganhouse et al., 1993; Davee and Sanders, 2000). Through the microbially mediated breakdown of the hydrocarbons, the microbes produce carbonic and organic acids and biosurfactants. One of the end products of this transformation is CO_2, which reacts with pore waters to produce carbonic acid. This acid production enhances mineral dissolution of the resident aquifer sediment (McMahon et al., 1995). Furthermore, the production of biosurfactants emulsify the hydrocarbon which further changes the physical and chemical composition of the hydrocarbon impacted area (Hudak, 2001; Cassidy et al., 2002). Most of these processes are fairly well understood; however, it is not known how the microbial degradation and subsequent biogeochemical processes alters the electrical properties of the impacted zone. Therefore, the application of geoelectrical methods cannot be interpreted until a fundamental understanding of these processes and the resulting affect on the geoelectrical properties of the subsurface is obtained.

Present geophysical studies report contradictory results based on the state of degradation of the LNAPL. Some short term and controlled spill studies show a more resistive LNAPL impacted zone (De Ryck et al., 1993; Redman et al., 1994; Campbell et al., 1996), while many case studies and field investigations of more mature LNAPL impacted sites reveal the opposite with a more geoelectrically conductive response (Benson et al., 1997; Sauck et al., 1998; Atekwana et al., 2000; Werkema et al., 2000). A more recent geoelectrical model developed by Sauck et al., (1998) with continual support

by other studies (Atekwana et al., 2002; Atekwana et al., 1998; Atekwana et al., 2000; Sauck, 2000; Werkema et al., 2000; Cassidy et al., 2001) accounts for these dynamic changes and the resulting effect on the geoelectrical response. Not only has this new conductive plume model (Sauck, 2000) been initially supported by the field studies listed above, but also biogeochemical investigations (Duris et al., 2000; Hudak, 2001; Duris et al., 2001; Legall, 2002). However, these studies have only begun to describe the geophysical changes occurring at an aged (i.e. mature) LNAPL contaminated site, and a clear link between the conductive response to biogeochemical modifications of the LNAPL impacted zone has yet to be made. Furthermore, no studies have addressed how natural hydrologic events (i.e. groundwater recharge) alter the geoelectrical signature at such sites.

Therefore, this study is designed to: (a) test the conductive plume model at a mature hydrocarbon contaminated site; (b) investigate how the geoelectrical response changes with time both vertically and horizontally across the site; and (c) investigate the influence of hydrologic processes on the conductivity.

This study will provide insights into the foundation necessary for the development of more robust models that will adequately address the influence of microbial processes on geophysical signatures. Such a model will allow for the potential development of geophysical techniques as sensors of the presence of intrinsic bioremediation and provide an understanding of biogeochemical processes associated with natural attenuation processes.

1.0 References

Atekwana, E., Rowe, R. S., Atekwana, E. A, Werkema, D. D., and Legall, F. D. Total Dissolved Solids in Groundwater and its Relationship to Bulk Conductivity of Soils Contaminated with Hydrocarbon. Journal of Environmental and Engineering Geophysics, in review. 2002.

Atekwana, E. A, Sauck, W. A., and Werkema, D. D. Investigations of geoelectrical signatures at a hydrocarbon contaminated site. Journal of Applied Geophysics, 44, 167-180. 2000.

Atekwana, E. A., Sauck, W. A., and Werkema, D. D. Characterization of a Complex Refinery Groundwater Contaminant Plume using Multiple Geoelectric Methods. Proceedings of the Symposium on the Application of Geophysics to Engineering and Environmental Problems (SAGEEP '98), 427-436. 1998.

Baedecker, M. J., Cozarelli, I. M, and Eganhouse, R. P. The composition and fate of hydrocarbons in a shallow glaical-outwash aquifer. United States Geological Survey Open File Report, 87-109. 1987.

Baedecker, M. J., Cozarelli, I. M, Eganhouse, R. P., Siegel, D. I., and Bennett, P. C. Crude oil in a shallow sand and gravel aquifer: III. Biogeochemical reactions and mass balance modeling in anoxic groundwater. Applied Geochemistry, 8, 569-586. 1993.

Bennett, P. C., Siegel, D. I., Baedecker, M. J., and Hult, M. F. Crude oil in a shallow sand and gravel aquifer: I. Hydrogeology and inorganic geochemistry. Applied Geochemistry, 8, 529-549. 1993.

Benson, A. K., Payne, K. L., and Stubben, M. A. Mapping Groundwater Contamination using DC Resistivity and VLF Geophysical Methods - A Case Study. Geophysics, 62[1], 80-86. 1997.

Bermejo, J. L, Sauck, W. A., and , Atekwana E. A. Geophysical Discovery of a New LNAPL Plume at the Former Wurtsmith AFB, Oscoda, Michigan. Ground Water Monitoring & Remediation, XVII[4], 131-137. 1997.

Blacic and Arulanandan, K. Identification of Contaminated Soils by Dielectric Constant and Electrical Conductivity. Journal of Environmental Engineering, 103-105. 1999.

Campbell, D. L., Lucius, J. E., Ellefson, K. J., and Desczcs-Pan, M. D. Monitoring of a Controlled LNAPL Spill Using Ground Penetrating Radar. Proceedings of the Symposium on the Application of Geophysics to Engineering and Environmental Problems (SAGEEP '96), Keystone, Colorado, 511-517. 1996.

Cassidy, D. P., Hudak, A., Werkema, D. D., Atekwana, E., Rossbach S., Duris, J. W., Atekwana, E. A, and Sauck, W. A. *In Situ* Rhamnolipid Production At An Abandoned Petroleum Refinery. Soil and Sediment Contamination: an International Journal, In press. 2002.

Cassidy, D. P., Werkema, D. D., Sauck, W. A., Atekwana, E. A., Rossbach, S., and Duris, J. The effects of LNAPL biodegradation products on electrical conductivity measurements. Journal of Environmental and Engineering Geophysics, 6, 47-52. 2001.

Cozzarelli, I. M, Eganhouse, R. P., and Baedecker, M. J. Transformation of monoaromatic hydrocarbons to organic acids in anoxic groundwater environment. Environmental Geology and Water Science, 16[2], 135-141. 1990.

Daniels, J. J., Roberts, D., and Vendl, M. Site Studies of Ground Penetrating Radar for Monitoring Petroleum Product Contaminants. Proceedings of the Symposium on the Application of Geophysics to Engineering and Environmental Problems (SAGEEP '92), Oak Brook IL., 597-609. 1992.

Davee, K. W. and Sanders, D. A. Petroleum Hydrocarbon Monitored Natural Attenuation: Essential Framework for Remedial Managers. Environmental Geosciences, 7[4], 190-202. 2000.

De Ryck, S. M., Redman, J. D., and Annan, A. P. Geophysical Monitoring of a Controlled Kerosene Spill. Proceedings of the Symposium on the Application of Geophysics to Engineering and Environmental Problems (SAGEEP'93), San Diego, CA, 5-20. 1993.

Duris, J. W., Werkema, D. D., Atekwana A., Eversole, R., Beuving, L., and Rossbach S. Microbial Communities and Their Effects on Silica Structure & Geophysical Properties in Hydrocarbon Impacted Sediments. Geological Society of America Annual Meeting Abstracts, Reno, NV, A190. 2000.

Duris, J. W., Werkema, D. D., Davis, J., Eversole, R., Beuving, L., Atekwana A., and Rossbach S. Shifts in Microbial Community Structure in Hydrocarbon Impacted Sediments Associated with Alterations in Physical Parameters of Soil. Abstracts: American Society for Microbiology 101st General Meeting.ASM Press, Washington D.C., 655. 2001.

Eganhouse, R. P., Baedecker, M. J., Cozarelli, I. M, Aiken, G. R., Thorn, K. A., and Dorsey, T. F. Crude oil in a shallow sand and gravel aquifer: II. Organic geochemistry. Applied Geochemistry, 8, 551-567. 1993.

Hudak, A. In situ biosurfactant production at Carson City Park, MI. M.S.Thesis, Western Michigan University. 2001.

Legall, F. D. unpublished data, personal communication. 2002.

Maxwell, M and Schmok, J. Detection and Mapping of an LNAPL Plume using GPR: A Case Study. Proceedings of the Symposium on the Application of Geophysics to Engineering and Environmental Problems (SAGEEP '95), 15-23. 1995.

Mazác, O., Benes, L., Landa, I., and Maskova, A. Determination of the extent of oil contamination in groundwater by geoelectrical methods. Geotechnical and Environmental Geophysics, vol II, S.H.Ward editor, 107-112. 1990. Tulsa, OK., Society of Exploration Geophysicists.

McMahon, P. B., Vroblesky, D. A., Bradely, P. M., Chapelle, F. H., and Gullet, C. D. Evidence for enhanced mineral dissolution in organic acid-rich shallow ground water. Ground Water, 33[2], 207-216. 1995.

Osiensky, J. L. Ground Water Modeling of mise-a-la-masse Delineation of Contaminated Ground Water Plumes. Journal of Hydrology, 146-165. 1997.

Redman, J. D., De Ryck, S. M, and Annan, A. P. Detection of LNAPL Pools with GPR: Theoretical Modelling and Surveys of a Controlled Spill. Proceedings of the Fifth International Conference on Ground Penetrating Radar (GPR'94), Kitchener, Ontario, 1283-1294. 1994.

Sauck, W. A. A model for the resistivity structure of LNAPL plumes and their environs in sandy sediments. Journal of Applied Geophysics, 44/2-3, 151-165. 2000.

Sauck, W. A., Atekwana, E. A., and Nash, M. S. High Conductivities Associated with an LNAPL Plume Imaged by Integrated Geophysical Techniques. Journal of Environmental and Engineering Geophysics, Vol. 2, No. 3, 203-212. 1998.

Vanhala, H. Mapping Oil-Contaminated Sand and Till with the Spectral Induced Polarization (SIP) Method. Geophysical Prospecting, 45, 303-326. 1997.

Werkema, D. D., Atekwana A., Sauck, W., Rossbach.S., and Duris J. Vertical Distribution of Microbial Abundances and Apparent Resistivity at an LNAPL Spill Site. Proceedings of the Symposium on the Application of Geophysics to Engineering and Environmental Problems (SAGEEP 2000). 2000.

CHAPTER 2

IN SITU APPARENT RESISTIVITY MEASUREMENTS AND MICROBIAL POPULATION DISTRIBUTION AT A HYDROCARBON CONTAMINATED SITE: IMPLICATIONS FOR THE ASSESSMENT OF INTRINSIC BIOREMEDIATION

2.0 Introduction

Light non-aqueous phase liquids (LNAPLs) contamination of soils remains a major problem of global environmental concern. The task of locating and quantifying the amount of LNAPL present and its subsequent degradation in soils has presented significant challenges to scientists and engineers involved in soil cleanup and remediation. The partitioning of hydrocarbons in the subsurface into various phases (vapor, residual, free, and dissolved phase) and their spatial and temporal nature is difficult to characterize, thus compounding the problem of soil remediation (Davis et al., 1993).

Geophysical techniques hold great promise as inexpensive and non-invasive sensors of subsurface LNAPL contamination. As such, geophysical techniques including ground penetrating radar (GPR), electromagnetic induction, and electrical resistivity have been widely used to detect hydrocarbon-impacted zones in the subsurface (Mazác et al., 1990; Annan et al., 1991; Daniels et al., 1992; Schneider and Greenhouse, 1992; Davis et al., 1993; Redman et al., 1994; Benson and Stubben, 1995; Grumman and Daniels, 1995; Endres and Greenhouse, 1996; Bermejo et al., 1997; Sauck et al., 1998; Atekwana et al., 2000). The theoretical basis for the use of electrical resistivity methods for the detection of LNAPL contaminants in the subsurface is dependent on the contrasting electrical

properties of the LNAPLs versus the pore and ground water displaced by LNAPL plumes. According to Archie's law (Archie, 1942), the resistivity of porous geologic material (in the absence of clays) can be described by:

$$\rho_b = a\,\phi^{-m}\,S_w^{-n}\,\rho_W \quad \text{.....(1)}$$

Where ρ_b is the bulk resistivity, ϕ is the fractional pore volume (porosity), S_w is the fraction of the pores containing water, ρ_W is the pore water resistivity and n, a and m are constants.

With LNAPL contamination, S_w is lowered due to the partial replacement of pore waters with LNAPL and results in an increase in ρ_b of the impacted media. This basic scenario forms the basis for the "insulating layer model" supported by short-term laboratory and controlled hydrocarbon spill experiments (De Ryck et al., 1993), as well as petrophysical modeling (Endres and Redman, 1996). It is on the basis of the above model that geoelectrical data have been interpreted from many hydrocarbon-contaminated sites.

2.0.1 Effect of Biodegradation

LNAPL-impacted sites investigated are rarely "fresh" spills, as depicted by the above controlled studies, but more often, have undergone some degree of physical alteration and/or microbial degradation resulting in changes in the aquifer geochemistry. The LNAPL contaminant, the microbial degradation products, and subsequent geochemical reactions with the hydrologic media and geologic host material may result in time-dependent changes in the geoelectrical properties of the impacted soils and pore

fluids. For example, geochemical investigations at hydrocarbon-contaminated sites suggest that major metabolic products of hydrocarbon biodegradation are carbonic and volatile organic acids. These products enhance mineral dissolution in soils when released by microbes into pore water. Additionally, these products are directly generated at soil particle surfaces during microbial colonization of those surfaces (Cozzarelli et al., 1990; Hiebert and Bennett, 1992; Cozzarelli et al., 1994; McMahon et al., 1995; Cozzarelli et al., 1995; Bennett et al., 1996). We suggest that increases in dissolved ion concentrations in pore water accompanying enhanced mineral dissolution should increase the electrical conductivity of the impacted media lowering its resistivity (Sauck, 2000). Indeed, surface geophysical investigations at several "aged" LNAPL impacted sites show anomalous low apparent resistivities (high conductivities) coincident with contaminated subsurface regions (Benson and Stubben, 1995; Gajdos and Král, 1995; Monier-Williams, 1995; Sauck et al., 1998; Atekwana et al., 2000). Further, other studies have documented attenuated GPR reflections probably due to increased conductivities in regions with subsurface hydrocarbon contamination (Maxwell and Schmok, 1995; Bermejo et al., 1997; Sauck et al., 1998).

It is of particular importance to geophysical investigations at LNAPL-contaminated sites is the need to understand how microbial LNAPL degradation influences soil mineralogy and groundwater geochemistry that could be observed by geophysical methods. It is apparent that the full potential of geophysical techniques cannot be exploited until they are calibrated with biogeochemical and physical changes that occur during the biodegradation of these contaminants. Thus, we envision this to

become a very active research area for environmental geophysicists in the very near future.

Despite the apparent connection between microbial degradation of hydrocarbon and possible changes in the geoelectrical properties of soils, no studies have been conducted to document this relationship. In this study, we simultaneously investigated resistivity variations, the heterotrophic and oil degrading microbial population distribution, and water quality parameters indicative of pore fluid conductivity changes at an "aged" LNAPL-impacted site as a first attempt to establish this relationship. The broader implications of this study were to assess geoelectrical methods as sensors of subsurface hydrocarbon contamination and the potential use of these techniques in the assessment of in-situ microbial degradation of LNAPL in soils.

2.0.2 Site Description

This study was focused on a LNAPL plume from a former refinery (Crystal Refinery) located in Carson City, Michigan, USA (Fig. 1). Hydrocarbon releases from storage facilities and pipelines resulted in the seepage of hydrocarbons into the subsurface, impacting soils and groundwater. In 1945, the Department of Conservation (now the Michigan Department of Environmental Quality (MDEQ)) first observed evidence of hydrocarbon contamination in the nearby creek (Fish Creek). Subsequent site characterization documented a northern (crude oil) and southern (refined oil) plume emanating from the refinery property (Dell Engineering, 1992; Snell Environmental Group, 1994). The southern plume, extending from the property southwesterly into the neighboring Carson City Park (Fig. 1) is the focus of this study. In 1994, the plume was

approximately 229 m long and 82 m wide with a free product thickness between 0.3 m to 0.6 m (Dell Engineering, 1992; Snell Environmental Group, 1994).

Geologically, the very near surface (upper 10 meters) of the site is characterized by unconsolidated glacial outwash. The aquifer below the site is approximately 4.6 m to 6.1 m of fine to medium sands, coarsening with depth to gravel. A clay aquitard unit 0.6 m to 3.1 m thick underlies the aquifer. Depth to the water table varies from 0.6 m to 0.9 m west of the study site next to Fish Creek to 4.6 m to 5.8 m east of the study area. Generally, groundwater gradient direction is west-southwest towards Fish Creek with a hydraulic gradient magnitude of 0.0015 m/m and a velocity of 1.68 m/day.

2.0.3 Field Investigations

In this study, we determined the distribution of LNAPL phase, sediment grain size distribution, and measured soil apparent resistivity, heterotrophic and oil degrading microbial populations, volatile organic acids, and soil water and groundwater specific conductance in contaminated and uncontaminated portions of soils at the study area. Each monitoring location consisted of an instrument cluster that included a Vertical Resistivity Probe (VRP), multilevel lysimeters, and multilevel piezometers (Fig. 1).

2.0.3.1 Subsurface LNAPL Phase Distribution

Subsurface LNAPL phase distribution was determined from sediment cores. Sediment cores were collected using 5.05 cm diameter, 122 cm long acetate liners for direct push coring with a Geoprobe™ drill rig. The sediment cores were visually examined for the vertical distribution of hydrocarbon by observing staining of the sediments, and for the presence of hydrocarbon free product.

2.0.3.2 Sediment Grain Size Distribution

The sediment grain size distribution was measured in the same cores used for LNAPL phase characterization from the study area. The grain size distribution consisted of determining the percentage gravel, sand and silt/clay fractions. The gravel (> 4.75 mm), sand (4.75 – 0.0625 mm) and silt/clay (< 0.0625mm) were determined for selected depth intervals by sieve analysis, after drying the sediments at 105 °C. The select depth intervals were either 15 or 30 cm depending on visual inspection of the changes in grain size.

2.0.3.3 In Situ Resistivity Measurements

Vertical resistivity probes (VRPs) were constructed and installed throughout the study site as part of ongoing geophysical investigations of LNAPL-contaminated soils (VRPs 1, 2, & 3 were installed Aug., 1997; VRPs 4, 5, 6, 7 & 8 were in Fall 1998, VRPs 9 & 10 were in June, 1999). The VRPs consist of 3.8 cm inner diameter (ID) PVC dry wells with 1.3 cm long stainless steel screws installed at 2.54 cm intervals. The screw heads on the outer portion of the dry PVC wells serve as the electrode contact with the geologic formation; the threaded ends inside the wells enable measurements with

resistivity equipment. Installation of these probes included a small bentonite slurry annulus, which facilitated installation below the saturated zone and decreased the contact resistance with the surrounding geologic formation in the unsaturated zone. A total of ten VRPs are currently installed at this site. Apparent resistivity measurements were collected for a 5.08 cm Wenner array along the probes using a Syscal R2 resistivity meter with an automated/semi-automated switching system for switching between the electrodes (Werkema et al., 1998; Werkema et al., 2000). In order to allow the bentonite slurry to equilibrate, the resistivity data were collect about one year after installation (Groncki, 1999). The locations of the VRPs used in this study are shown in Figure 1.

2.0.3.4 Microbial Sampling and Cell Extraction

The total hetrorotrophic and oil degrading microbial populations were enumerated for soil collected about 1 m from each VRP. Soil cores were obtained using a 2.54 cm diameter by 61 cm long acetate liners for direct push coring (using a manual Geoprobe^{TM}system). Prior to soil sampling, the acetate liners and liner caps were disinfected in the laboratory with an 80% ethanol solution and dried in a laminar flow hood. In the field, liners were again disinfected and the soil cores were aseptically collected, capped and placed on ice and out of direct sunlight. The soil samples were subsequently transported to the laboratory and stored at 4° C until analysis. The holding time prior to microbial enumeration did not exceed 10 days.

Sub-sampling of the soil for microbial enumeration was conducted at ~15 cm intervals. Prior to sampling the core, the outside of the sleeve was disinfected with 80% ethanol. A sterilized razor blade was used to cut a 2 x 2 cm portion of the core sleeve,

exposing the soil. The outer portion of soil was aseptically removed and about 1 gram of soil was collected and placed in sterile 15 ml polypropylene tubes for extraction of microbial cells and subsequent enumeration of microbes. Determination of the total heterotrophic and oil degrading microorganisms was performed using a modification of a previously reported procedure (VanElsas and Smalla, 1997). A solution of 9.5 ml 0.1% sodium pyrophosphate was added to 1 gram of soil, shaken for 30 minutes and centrifuged at ~ 900 g for 10 minutes. The most probable number of bacteria (MPN/g of soil) was determined from aliquots of the supernatant using the 96-well plate method with 10% TSB (Tryptic Soy Broth) medium to enumerate the total heterotrophic microorganisms and with Bushnell-Haas (B-H) medium (Becton Dickinson, Detroit, MI) supplemented with hexadecane to enumerate the hydrocarbon degrading microorganisms (Salama et al., 1978; Klee, 1993; Haines et al., 1996; Wrenn and Venosa, 1996). After each plate from the 96-well plate had been scored, the number of positive wells at each serial dilution was entered into a computer program (Klee, 1993) to determine the most probable number of bacteria/g soil and the 95% confidence limits at each sample point. The computer program provided MPN numbers that were corrected for positive bias in published MPN charts (Salama et al., 1978).

2.0.3.5 Pore Water and Groundwater Specific Conductance and Volatile Organic Acids

Soil water and groundwater specific conductance was measured by microelectrode using a HydroLab™ multi-parameter probe. Soil water was collected in lysimeters and groundwater was sampled at 30 cm depth intervals from 0.64 cm PVC tubing fitted with 10 cm nylon screens. The pore water from lysimeters was evacuated

using standard techniques. Groundwater from the multilevel piezometers was pumped to the surface using a peristaltic pump. Volatile organic acids were determined using the chromatographic separation method for organic acids. The values are reported as acetic acid in mg/l.

2.1 Results

Results of the grain size analyses, distribution of LNAPL phases, apparent resistivity and microbial populations are also presented graphically in Figures 2, 3, and 4. We present below the results from three representative monitoring locations: two from contaminated locations and one from a background site with no detectable hydrocarbons but comparable soil characteristics (see Figure 1).

2.1.1 Location With No LNAPL Contamination

Two VRP locations contain no evidence of LNAPL contamination and are considered the control locations at this site. Figure 2 shows the results from one such location (VRP 9). All depths reported in this study are below ground surface. The geology at this location consists of unconsolidated fine to medium sands, which coarsen with depth below 150 cm to coarse sand with gravel. Depth to water fluctuates from 200 to 260 cm with an average at 212 cm at this location.

The apparent resistivity measured for soils at this location ranged from 1158 to 9394 Ωm within the unsaturated zone and 56 to 313 Ωm within the saturated zone (Table 1). Higher and more variable resistivities characterize the vadose zone. A slight increase in resistivity values is observed above the water table (150 cm) coincident with increased gravel content (see grain size distribution, Fig. 2). The apparent resistivity gradually

decreased from about 190 cm through the transition zone to a depth of 250 cm, remaining relatively constant (~ 67 Ωm) below this depth to the base of the aquifer.

The heterotrophic microbe population ranged from 2.4 x 10^2 to 2.5 x 10^6 MPN/g soil. The microbes capable of hydrocarbon degradation (oil degraders) ranged from 7.0 x 10^1 to 2.5 x 10^5 MPN/g soil in soils at this location. Heterotrophic populations of 1.1 x 10^4 to 2.5 x 10^6 MPN/g soil and oil degrading microorganisms from 2.9 x 10^2 to 2.5 x 10^5 MPN/g of soil were measured in the unsaturated zone. Heterotrophic populations from 2.4 x 10^2 to 3.8 x 10^5 MPN/g soil and oil degrading microorganism populations ranged from 7.0 x 10^1 to 2.1 x 10^3 MPN/g of soil in the saturated zone. Plots depicting the microbial numbers showed slight decreases with depth for both microbial population types (Fig. 2). The oil degrading bacterial population were essentially constant at ~5.6% of the total heterotrophic population. There was a slight peak in the heterotrophic and oil degrading microbial population (3.6 x 10^2 to 3.77 x 10^5 MPN/g of soil) below the saturated zone at 260 cm, but only 0.5% of the population were capable of hydrocarbon degradation.

Specific groundwater conductance values from the multilevel piezometers show lower values ranging from 78 to 380 μS/cm characterizing the transition zone, and higher values (764 to 877μS/cm) at the base of the aquifer (Table 1). However, volatile organic acids were below detectable levels. No pore water samples were recovered from the lysimeters at VPR 9.

2.1.2 Locations With LNAPL Contamination

A total of five VRPs are installed in locations where variable thicknesses (or amounts) of free product are observed. Amounts of free product observed range from a few inches to almost 2 feet (60.96 cm). Results from LNAPL-impacted soils at the study site are from locations VRP5 and VRP4 (see Fig. 1 for locations). The soils at VRP5 were primarily medium sands within the unsaturated zone, which coarsened to coarse sands and gravels at depths below 300 cm. Depth to water at this location fluctuated from 250 – 310 cm with an average of 280 cm. LNAPL distribution showed a residual product zone 100 cm thick between depths of 150 and 250 cm. The residual product zone consisted of moist light gray-colored, fine to medium, oil-stained sands with hydrocarbon odor between 150 to 180 cm and a dark gray to black-colored coarse sand and gravel layer between 180 and 250 cm that was moist and had a very strong hydrocarbon odor. A 30 cm-thick free product zone characterized by medium grained sands extended from a depth of 250 to 280 cm. The dissolved phase occupied the entire saturated zone based on measured total hydrocarbon (benzene, ethylbenzene, toluene and xylene) (Legall, 2002).

The vertical resistivity measured for this location ranged from 20 to 7394 Ωm within the unsaturated zone and 33 to 77 Ωm within the saturated zone. The apparent resistivity at this location was highest (>3000 Ωm) in the upper portions of the unsaturated zone between 0-150 cm. At a depth of ~150 cm and coincident with the upper zone of residual LNAPL contamination, the apparent resistivity decreased abruptly from ~3500 Ωm to < 200 Ωm. The apparent resistivity continued to decrease to 45 Ωm to the boundary between the residual and free product zones at ~250 cm. Below this

depth, a relatively large amplitude alternating polarity Wenner array response corresponding to the LNAPL free-product/water-saturated zone interface was observed indicative of a sharp boundary (Telford, 1990). It is important to note that the lowest resistivity values occurred within the free product zone. Below the free product zone and within the saturated zone, apparent resistivity values increased slightly but remained steady (between 33 and 77 Ωm) to the base of the aquifer, with an average of ~ 50 Ωm.

Heterotrophic microorganisms from soils near VRP 5 ranged from 2.4×10^2 to 1.3×10^7 MPN/g soil in the unsaturated zone. The oil degrading microorganisms ranged from 3.1×10^1 to 5.6×10^4 MPN/g of soil in the unsaturated zone. In the saturated zone the heterotrophic microorganisms ranged from 4.0×10^2 to 1.5×10^4 MPN/g soil and the oil degrading microorganisms from 3.2×10^2 to 2.2×10^3 MPN/g of soil. The total heterotrophic microbial population increased with depth to 50 cm and then decreased slightly but remained between 8.7×10^4 to 1.3×10^7 MPN/g of soil to a depth of 220 cm. Except for an increase (2.6×10^6 MPN/g of soil) at a depth of 244 cm, the total heterotrophic bacterial population decreases within the lower portion of the residual LNAPL product and the entire free phase LNAPL zones. The population of oil degrading bacteria was steady (between 2.0×10^4 and 5.6×10^4 MPN/g of soil) from the surface to a depth of 60 cm, and then decreased to 3.6×10^1 MPN/g of soil at a depth of about 122 cm, just above the residual product zone. The oil degrading bacteria increased in numbers, peaking at 3.1×10^4 MPN/g of soil at 244 cm within the residual LNAPL product zone. There was a decrease from the above peak population to 3.1×10^1 MPN/g soil within the free product zone. Another peak population in the oil degraders (2.1×10^3

MPN/g soil) was observed at 305 cm in the upper portions of the saturated zone within the dissolved LNAPL product phase.

Specific groundwater conductance values from the VRP 5 location also show a variation with depth. However, values from the upper parts of the aquifer within the dissolved product zone are significantly higher (842 μS/cm) compared to values (78 - 380 μS/cm) from the background location (VRP 9). Specific conductance values remain high to the base of the aquifer (Table 1). Pore water samples obtained from one lysimeter at this location show a specific conductance value of 538 μS/cm from within the residual product zone (200 cm depth). Also volatile organic acids are detectable and range in value from 12.9 – 16.2 mg/l.

The subsurface at VRP 4 consists of fine to medium sands, coarsening to coarse sand and gravel at depths below 108 cm. LNAPL distribution showed a residual product zone of 10 cm between depths of 102 to 112 cm. This zone was distinguished by moist medium to coarse sands, which were dark to black in color, and of hydrocarbon odor. A free product zone of 40 cm was located between 112 and 152 cm. This zone was predominantly coarse sand with gravel, black in color and saturated with free product. The dissolved phase occupied the entire saturated zone based on measured total hydrocarbon (benzene, ethylbenzene, toluene and xylene) (Legall, 2002).

The vertical resistivity measured for VRP 4 ranged from 104 to 6708 Ωm within the unsaturated zone and from 27 to 105 Ωm within the saturated zone. The apparent resistivity values were higher within the uncontaminated unsaturated zone (1193 to 6604 Ωm). A decrease in the apparent resistivity was observed between 50 and 80 cm. At the base of the residual LNAPL product zone the apparent resistivity decreased abruptly from

2159 Ωm to 910 Ωm. The apparent resistivity values continued to decrease reaching a minimum of 104 Ωm within the free product zone (~112 – 152 cm). Below the free product zone and within the water-saturated zone, the apparent resistivity values decreased further reaching a minimum of 27 Ωm at 210 cm of depth. A slight increase in apparent resistivity values was observed below 210 cm to the base of the aquifer, with an average resistivity value of ~40 Ωm.

The heterotrophic microorganisms ranged from 9.9×10^4 to 4.6×10^6 MPN/g soil and oil degrading microorganisms ranged from and 5.1×10^3 to 2.5×10^5 MPN/g of soil, in the unsaturated zone. In the saturated zone the heterotrophic microorganisms ranged from 5.2×10^3 to 1.3×10^6 MPN/g soil and the oil degrading microorganisms ranged from 2.0×10^2 to 3.7×10^5 MPN/g of soil. The heterotrophic microorganisms population remained steady from the surface into the residual LNAPL product zone at 112 cm, but decreased below this depth within the free LNAPL product zone although a slight increase in populations is observed at the top of the saturated zone (Fig. 4).

At the first encounter with LNAPL contamination within the residual product zone at a depth of 102 cm, more than a ten-fold increase in the population of the oil degraders (from 9.1×10^3 to 2.5×10^5 MPN/ g soil) was observed while the population of the total heterotrophs remained steady between 3.5×10^5 and 4.6×10^5 MPN/g of soil across this interface. A sharp increase in both the oil degrading (3.7×10^5 MPN/g soil) and heterotrophic populations (1.2×10^6 MPN/g of soil) was observed within the dissolved product phase (198 cm) and was coincident with the zone of lowest resistivity at this location.

The highest specific groundwater conductance values were obtained from this VRP location (990 to 1014μS/cm) with values increasing to the base of the aquifer consistent with observations at the other VRP locations (Table 1). Pore water samples obtained from the unsaturated zone (50 cm) at this location show a specific conductance value of 705 μS/cm. No data are available for volatile organic acids at VRP 4.

2.2 Discussion

The results show significant resistivity decreases associated with zones of LNAPL contamination. The data reveal three zones where low apparent resistivity measurements were observed: 1) in the unsaturated zone within residual LNAPL product phase, 2) within the free LNAPL product pool, and 3) in the upper parts of the saturated zone contaminated with dissolved LNAPL product. The low apparent resistivity observed in hydrocarbon-contaminated soils at the study site can result from several factors including aquifer heterogeneity (especially in the presence of clays), changes in moisture content, and increase in the soil water and groundwater conductivity due to dissolution of aquifer minerals resulting from biodegradation of the contaminant mass. Grain size analyses indicate that the soils in the unsaturated zone consisted of poorly graded fine to medium sands (with relatively little clay). Soils within the saturated zone were typically well-graded medium to coarse sand with gravel. The apparent resistivity variations in soils at the site do not correlate with grain size variation with depth (see Figs. 2, 3 and 4). Hence, the observed changes in resistivity cannot be explained solely in terms of aquifer heterogeneity. Apparent resistivity fluctuations in the unsaturated zone at VRP9 and in the unsaturated zone with no visible LNAPL contamination at VRP5 and VRP4 may be

attributed to saturation effects. Increased saturation due to a moving infiltration front will reduce the apparent resistivity of soils. However, it is important to note that the observed reduction in the apparent resistivity resulted in values that were still significantly higher than corresponding values in the unsaturated zone impacted with LNAPL (Figs. 3 and 4). Within the saturated zone, the lowest resistivities in uncontaminated groundwater ranged from 56 to 313 Ωm at VRP9 compared to lower values of 27 to 77 Ωm at VRP5 and VRP4. When compared to the uncontaminated unsaturated and saturated soils, the low apparent resistivities at the contaminated locations appear to be related to the presence of LNAPL contamination. This is inconsistent with the expected increase in resistivity due to the presence of the more resistive LNAPLs at the contaminated locations (equation 1 and per the resistive model). Thus, it seems likely that the reduction in resistivities may be associated with biodegradation.

Corroborating evidence is provided by the microbial population data, which showed that microbes capable of degrading hydrocarbon were present in the soils at the study site. In uncontaminated soils from the background location (VRP9), the oil degrading microorganisms comprised 5% and 0.5% of the total heterotrophic microbial population in the unsaturated and saturated zones, respectively. At contaminated locations, oil-degrading microbes constituted 2.7, 1.7, 8.8 and 35% of the total heterotrophic populations in the unsaturated zone above the residual phase, the residual, free, and dissolved phase LNAPL zones respectively, at VRP5 and 6.2, 55.4, 53.3% and 22.5% at VRP4. The microbial population distribution varied significantly in the soil profile on scales of 15 cm or less and is similar to vertical profiles reported in other studies (Bekins et al., 1999). Although the MPN method utilized in this study is a

culture-based method and probably underestimates absolute microbial numbers, the trends in MPN with depth can provide qualitative information from which hydrocarbon degradation can be inferred and the resistivity data explained.

In the saturated zone with dissolved phase LNAPL, the oil-degrading microbe numbers were more than 15 to 50% higher compared to the uncontaminated saturated zone at VRP 9 (<1%). Further, the contaminated unsaturated zone at VRP4 showed more oil-degrading microbes (6.2 to 55%) compared to 5.6% in the unsaturated zone at VRP9. However, the soils at VRP5 had lower oil degrading microbes (1.7 and 2.7%) except in the free phase (8.8%) zone compared to the unimpacted unsaturated zone at VRP9. Although microbial enumeration as presented in this study does not conclusively indicate the presence of biodegradation, they do provide circumstantial evidence linking the lower resistivities of the contaminated locations to possible degradation effects.

To corroborate our observations, measurements of groundwater specific conductance (or conductivity) values from the upper parts of the saturated zone (dissolved phase) at contaminated locations (VRP4 and VRP5) show significantly higher values (842 to 990 μS/cm) compared to 78 to 380 μS/cm at VRP 9, the background site. Although at all VRP locations, specific conductance values (see Table 1) increased with depth to the base of the aquifer, values from contaminated locations were still higher than values from the background location (VRP9). Further, volatile organic acids that show significant difference between contaminated and background locations complement these results. Volatile organic acids were not detected at VRP9 but were detected at VRP5 and other contaminated locations at the site. These observations are consistent with results from other hydrocarbon contamination sites (McMahon et al., 1995). Thus, the presence

of organic acids and conductive zones coincident with elevated levels of oil degrading bacterial populations provide circumstantial evidence linking anomalous low apparent resistivities to biodegradation of LNAPL in both the saturated and unsaturated zones. These results are consistent with observations from a recent laboratory study of geoelectrical properties during microbial degradation of diesel fuel that showed considerable changes in pore water biogeochemistry with a significant increase in volatile organic acids and a five-fold increase in total dissolved solids and pore water conductivity (Cassidy et al., 2001).

It is also important to note that we observed no significant increase in apparent resistivities associated with the free phase LNAPL zone. This finding is significant, as intuitively this zone is expected to have the highest resistivities, since oil is an insulator and we expect to have significant oil saturation within this zone. A recent study at this site (Cassidy et al., 2002) suggested *in-situ* biosurfactant production by resident microbial populations at the contaminated locations. This observation is consistent with laboratory findings that reported the production of biosurfactants under both aerobic and anaerobic conditions, resulting in significant emulsification of diesel fuel (Cassidy et al., 2001). We suggest that the emulsion of LNAPL due to *in-situ* biosurfactant production during biodegradation would break up the initial continuous LNAPL layer providing conductive leachate pathways for the electrical current flow. Recently, surfactant producing organisms and the presence of biosurfactants has been identified from the study site corroborating our above explanation (Cassidy et al., 2002). We believe that this phenomenon offers a reasonable explanation as to why soils within the residual and free phase zones were conductive and not resistive. Hence, our conceptual model is that the

decrease in apparent resistivities observed at many "aged" LNAPL impacted sites may be the combined effect of increases in dissolved ion concentrations (from enhanced mineral dissolution by acids) and apparent emulsification of LNAPLs (accompanying biosurfactant production) during biodegradation. However, further studies are required to investigate the effects of biosurfactant on geoelectrical signatures.

Accordingly, the geoelectrical response measured in LNAPL-contaminated soils is the end product of a complex interaction between biological, chemical, hydrological, and geological processes. It is expected that infiltration and recharge events will periodically flush conductive soil water and degradation byproducts from the unsaturated zone into the saturated zone contributing to the higher groundwater conductance values and byproducts added to the dissolved phase degradation activities. Thus, we infer from this study that hydrocarbon-degrading environments are complex, and that research methods that combine physical, biological, geochemical, and hydrologic information may provide greater insights and understanding of hydrocarbon degradation in natural field settings.

2.2.1 Implications of the *In Situ* Geoelectrical Measurements to Natural Attenuation

Over the past several years, natural attenuation has become increasingly accepted as a remedial alternative for many hydrocarbon-contaminated sites, partly because of its relatively lower cost. However, the implementation of natural attenuation as a remedial strategy at a site often requires a demonstration that natural attenuation is occurring through several lines of evidence. One such line of evidence is the demonstration of the potential for intrinsic bioremediation. Because biodegradation is expected to cause

predictive changes in groundwater chemistry (Cozzarelli et al., 1990; Cozzarelli et al., 1994; Cozzarelli et al., 1995; Fang et al., 2000), traditional methods for assessing an area for the potential of intrinsic bioremediation have relied heavily on extensive sampling and analyses of groundwater and soil vapor for intermediates of biological hydrocarbon metabolism, depletion of terminal electron acceptors, and assessment of microbial communities capable of metabolizing the hydrocarbons. Such investigations can be very expensive, labor intensive, and provide little data to interpret remediation activities at specific subsurface locations and do not span the entire spatial and temporal scales associated with the remediation processes. Thus, it is not surprising that the collection, preparation, and analysis of solid, liquid and gas samples from LNAPL-contaminated sites constitute a major portion of the total cost for remediation, and also involves health risk concerns (Granato and Smith, 1999). Given the fact that many of these sites will have to be monitored for decades to come, there is a need for the development non-invasive methods that can serve as surrogates for much of the ground water sampling and analysis to monitor the cleanup of contaminated sites. Such methods will have tremendous potential to reduce cleanup costs and reduce health risks to humans and the environment. We submit that conductive zones as depicted by the VRPs may represent areas of active biodegradation and demonstrate the potential for electrical geophysical techniques to be used as an independent proxy for the assessment of intrinsic bioremediation at LNAPL-contaminated sites. However, fundamental geophysical research at both the lab- and field-scale are needed to understand how microbial mediated processes of LNAPL-impacted soils influence their geoelectrical response.

2.3 Acknowledgments

This work was funded in part by the American Chemical Society-Petroleum Research Fund Grant (PRF # 31594-AC2). Geophysical equipment used during this study was funded through a NSF Grant DUE-9550974 and Western Michigan University. We thank Craig Smith and Andy Nichols for excellent technical assistance. M. Mormile reviewed an earlier version of this manuscript.

2.4 References

Annan, A. P., Bauman, P., Greenhouse, J. P., and Redman, J. D. Geophysics and DNAPLS: Groundwater Management #5. Proceedings of the Fifth Annual Outdoor Action Conference on Aquifer Restoration, Groundwater Monitoring, and Geophysical Methods, Las Vegas, NV. 1991.

Archie, G. E. The Electrical Resistivity Log as an Aid in Determining Some Reservoir Characteristics. Transactions of the American institute of Mining, Metallurgical and Petroleum Engineers, 146, 54-62. 1942.

Atekwana, E. A, Sauck, W. A., and Werkema, D. D. Investigations of geoelectrical signatures at a hydrocarbon contaminated site. Journal of Applied Geophysics, 44, 167-180. 2000.

Bekins, B. A., Godsy, E. M., and Warren, E. Distribution of microbial physiologic types in an aquifer contaminated by crude oil. Microbial Ecology, 37, 263-275. 1999.

Bennett, P. C., Hiebert, F. K., and Choi, W. J. Microbial colonization and weathering of silicates in a petroleum-contaminated groundwater. Chemical Geology, 45-53. 1996.

Benson, A. K. and Stubben, M. A. Interval resistivities and very low frequency electromagnetic induction - an aid to detecting groundwater contamination in space and time: a case study. 0. Environmental Geosciences, 2, 74-84. 1995.

Bermejo, J. L, Sauck, W. A., and , Atekwana E. A. Geophysical Discovery of a New LNAPL Plume at the Former Wurtsmith AFB, Oscoda, Michigan. Ground Water Monitoring & Remediation, XVII[4], 131-137. 1997.

Cassidy, D. P., Hudak, A., Werkema, D. D., Atekwana, E., Rossbach S., Duris, J. W., Atekwana, E. A, and Sauck, W. A. *In Situ* Rhamnolipid Production At An

Abandoned Petroleum Refinery. Soil and Sediment Contamination: an International Journal, In press. 2002.

Cassidy, D. P., Werkema, D. D., Sauck, W. A., Atekwana, E. A., Rossbach, S., and Duris, J. The effects of LNAPL biodegradation products on electrical conductivity measurements. Journal of Environmental and Engineering Geophysics, 6, 47-52. 2001.

Cozzarelli, I. M, Eganhouse, R. P., and Baedecker, M. J. Transformation of monoaromatic hydrocarbons to organic acids in anoxic groundwater environment. Environmental Geology and Water Science, 16[2], 135-141. 1990.

Cozzarelli, I. M, Eganhouse, R. P., Baedecker, M. J., and Goerlitz, D. F. The geochemical evolution of low-molecular-weight organic acids derived from the degradation of petroleum contaminants in groundwater. Geochim.Cosmochim.Acta., 58, 863-877. 1994.

Cozzarelli, I. M, Herman, J. S., and Baedecker, M. J. Fate of microbial metabolites of hydrocarbons in a coastal plain aquifer: the role of electron acceptors. Environmental Science and Technology, 29, 458-469. 1995.

Daniels, J. J., Roberts, D., and Vendl, M. Site Studies of Ground Penetrating Radar for Monitoring Petroleum Product Contaminants. Proceedings of the Symposium on the Application of Geophysics to Engineering and Environmental Problems (SAGEEP '92), Oak Brook IL., 597-609. 1992.

Davis, G. B., Johnston, C. D., Thierrin, J., Power, T. R., and Patterson, B. M. Characterizing the distribution of dissolved and residual NAPL petroleum hydrocarbons in unconfined aquifers to effect remediation. ASGO J Geol.Geophy., 14, 89-94. 1993.

De Ryck, S. M., Redman, J. D., and Annan, A. P. Geophysical Monitoring of a Controlled Kerosene Spill. Proceedings of the Symposium on the Application of Geophysics to Engineering and Environmental Problems (SAGEEP'93), San Diego, CA, 5-20. 1993.

Dell Engineering. Remedial Action Plan for Crystal Refining Company, 801 North Williams Street, Carson City, MI. Report DEI No.921660, Holland, Michigan. 1992.

Endres, A. L. and Greenhouse, J. P. Detection and monitoring of chlorinated solvent contamination by thermal neutron logging. Ground Water, 34, 283-292. 1996.

Endres, A. L. and Redman, J. D. Modelling the Electrical Properties of Porous Rocks and Soils Containing Immiscible Contaminants. Journal of Environmental and Engineering Geophysics, 0, 105-112. 1996.

Fang, J., Barcelona, M. J., Krishnamurthy, R. V., and Atekwana, E. A. Stable carbon biogeochemistry of a shallow sand aquifer contaminated with fuel hydrocarbons. Applied Geochemistry, 15, 157-169. 2000.

Gajdos, V. and Král, V. Influence of hydrocarbon pollution to soil conductivity. Proceedings of the Symposium on the Application of Geophysics to Engineering and Environmental Problems (SAGEEP '95), 785-789. 1995.

Granato, G. E. and Smith, K. P. Robowell:, An automated process for monitoring ground water quality using established sampling protocols. Ground Water Monitoring & Remediation, 81-89. 1999.

Groncki, J. M. Calibration, installation techniques, and initial measurements for vertical resistivity probes in hydrogeologic investigations. M.S.Thesis, -122. 1999.

Grumman, D. L. and Daniels, J. J. Experiments on the Detection of Organic Contaminants in the Vadose Zone. Journal of Environmental and Engineering Geophysics, 0, 31-38. 1995.

Haines, J., Wrenn, B. A., Holder, E., Strohmeier, K., Herrington, R., and Venosa, A. Measurment of hydrocarbon-degrading microbial populations by a 96-well plate most-probably-number procedure. Journal of Industrial Microbiology, 16, 36-41. 1996.

Hiebert, F. K. and Bennett, P. C. Microbial control of silicate weathering in organic-rich ground water. Science, 258, 278-281. 1992.

Klee, A. J. A computer program for the determination of most probable number and its confidence limits. Journal of Microbiological Methods, 18, 91-98. 1993.

Legall, F. D. unpublished data, personal communication. 2002.

Maxwell, M and Schmok, J. Detection and Mapping of an LNAPL Plume using GPR: A Case Study. Proceedings of the Symposium on the Application of Geophysics to Engineering and Environmental Problems (SAGEEP '95), 15-23. 1995.

Mazác, O., Benes, L., Landa, I., and Maskova, A. Determination of the extent of oil contamination in groundwater by geoelectrical methods. Geotechnical and Environmental Geophysics, vol II, S.H.Ward editor, 107-112. 1990. Tulsa, OK., Society of Exploration Geophysicists.

McMahon, P. B., Vroblesky, D. A., Bradely, P. M., Chapelle, F. H., and Gullet, C. D. Evidence for enhanced mineral dissolution in organic acid-rich shallow ground water. Ground Water, 33[2], 207-216. 1995.

Monier-Williams, M. Properties of light non-aqueous phase liquids and detection using commonly applied shallow sensing geophysical techniques. Proceedings of the

Symposium on the Application of Geophysics to Engineering and Environmental Problems (SAGEEP '95).Orlando, FL, 1-13. 1995.

Redman, J. D., De Ryck, S. M, and Annan, A. P. Detection of LNAPL Pools with GPR: Theoretical Modelling and Surveys of a Controlled Spill. Proceedings of the Fifth International Conference on Ground Penetrating Radar (GPR'94), Kitchener, Ontario, 1283-1294. 1994.

Salama, I. A., Koch, G. G., and Tolley, H. D. On the estimation of the most probable number in a serial dilution technique. Commun.Stat.Theor.Metholol., A, 1267. 1978.

Sauck, W. A. A model for the resistivity structure of LNAPL plumes and their environs in sandy sediments. Journal of Applied Geophysics, 44/2-3, 151-165. 2000.

Sauck, W. A., Atekwana, E. A., and Nash, M. S. High Conductivities Associated with an LNAPL Plume Imaged by Integrated Geophysical Techniques. Journal of Environmental and Engineering Geophysics, Vol. 2, No. 3, 203-212. 1998.

Schneider, G. W. and Greenhouse, J. P. Geophysical detection of perchloroethylene in a sandy aquifer using resistivity and nuclear logging techniques. Proceedings of the Symposium on the Application of Geophysics to Engineering and Environmental Problems (SAGEEP'92), Oakbrook, IL., 619-628. 1992.

Snell Environmental Group. Technical Memorandum Task 1B-IRAP Evaluation, Crystal Refinery, Carson City, Michigan, MERA ID #59003. 1994. Michigan Department of Natural Resources, Grand Rapids District Office.

Telford, W. M. Geldart, L. P. and Sheriff, R. E. Applied Geophysics . Second, 558. 1990. Cambridge University Press.

VanElsas, J. D. and Smalla, K. Methods for sampling soil microbes. Manual of Environmental Microbology, 383-390. 1997. C.J. Hurst (eds.). Washington, D.C.: ASM Press.

Werkema, D. D., Atekwana, E.A., Sauck W. A., and Asumadu, J. A Versatile Windows Based Multi-Electrode Acquisition System for DC Electrical Methods Surveys. Environmental Geosciences, 5[4], 196-206. 1998.

Werkema, D. D., Atekwana, E. A., and Asumadu, J. A. A generic automated and semi-automated digital multi-electrode instrument for field resistivity measurements. IEEE Transaction on Instrumentation and Measurement, 49, 1249-1253. 2000.

Wrenn, B. A. and Venosa, A. D. Selective enumberation of aromatic and aliphatic hydrocarbon degrading bacteria by a most-probable-number procedure. Canadian Journal of Microbiology, 42, 252-258. 1996.

Table 1. Soil Depth, Apparent Resistivity, Heterotrophic and Oil Degrading Microorganism Population Numbers, Volatile Organic Acids, and Specific Groundwater Conductance Measurements.

VRP 9					VRP 5					VRP 4				
Depth (cm)	Resistivity Ohm. m	Heterotrophs (MPN/g soil)	Oil Degraders (MPN/g soil)	Conductance	Depth (cm)	Resistivity Ohm. m	Heterotrophs (MPN/g soil)	Oil Degraders (MPN/g soil)	Conductance	Depth (cm)	Resistivity Ohm. m	Heterotrophs (MPN/g soil)	Oil Degraders (MPN/g soil)	Conductance
7.6	9394.5	-	-	-	12.7	1843.8	-	-	-	15.2	-	4.60E+06	4.33E+04	-
15.2	-	2.47E+06	2.47E+05	-	15.2	-	5.64E+04	5.63E+04	-	27.9	2148.9	-	-	-
17.8	1158.1	-	-	-	17.8	2350.6	-	-	-	30.5	-	4.18E+05	1.10E+05	-
22.9	440.9	-	-	-	22.9	4333.5	-	-	-	38.1	6098.2	-	-	-
27.9	392.4	-	-	-	27.9	4877.8	-	-	-	45.7	-	1.03E+06	2.42E+04	-
30.5	-	1.33E+06	1.09E+05	-	30.5	-	1.90E+05	2.32E+04	-	48.3	5483.2	-	-	-
33.0	320.7	-	-	-	38.1	7393.7	-	-	-	50.2	-	-	-	705
38.1	314.4	-	-	-	43.2	6178.5	-	-	-	53.3	6708.1	-	-	-
43.2	309.4	-	-	-	45.7	-	3.88E+06	1.97E+04	-	61.0	-	1.19E+06	6.11E+04	-
45.7	-	2.49E+05	2.49E+04	-	48.3	6034.3	-	-	-	63.5	1416.9	-	-	-
48.3	321.2	-	-	-	61.0	-	2.18E+06	3.05E+04	-	68.6	1235.8	-	-	-
53.3	335.9	-	-	-	76.2	-	5.89E+05	4.90E+03	-	73.7	1193.3	-	-	-
58.4	302.2	-	-	-	83.8	4122.7	-	-	-	78.7	1351.4	-	-	-
61.0	-	1.76E+05	1.44E+05	-	88.9	3164.6	-	-	-	83.8	1672.0	-	-	-
63.5	237.7	-	-	-	91.4	-	1.25E+07	1.63E+02	-	88.9	2974.8	-	-	-
68.6	265.9	-	-	-	94.0	3238.8	-	-	-	91.4	-	3.45E+05	9.08E+03	-
73.7	226.6	-	-	-	99.1	6542.4	-	-	-	94.0	2500.2			-
78.7	294.9	-	-	-	100.1	-	-	-	NR	99.1	3550.6			-
83.8	278.5	-	-	-	104.1	1887.4	-	-	-	104.1	2158.9			-
88.9	382.2	-	-	-	106.7	-	8.73E+04	3.73E+01	-	106.7	-	4.53E+05	2.51E+05	-
91.4	-	2.03E+05	3.49E+03	NR	109.2	3867.2	-	-	-	109.2	1763.1	-	-	-
94.0	392.4	-	-	-	114.3	4908.9	-	-	-	114.3	910.2	-	-	-
99.1	357.4	-	-	-	119.4	3723.7	-	-	-	119.4	428.5	-	-	-
104.1	309.3	-	-	-	121.9	-	1.25E+06	3.64E+01	-	121.9	-	9.92E+03	5.08E+03	-
106.7	-	2.20E+05	5.36E+03	-	124.5	2262.5	-	-	-	124.5	185.2	-	-	NR-
109.2	220.0	-	-	-	129.5	3342.7	-	-	-	125.1	-	-	-	
114.3	249.4	-	-	-	134.6	4088.6	-	-	-	129.5	123.3	-	-	-
119.4	227.9	-	-	-	137.2	-	3.71E+05	1.79E+03	-	134.6	105.3	-	-	-
121.9	-	4.29E+04	7.73E+03	NR	139.7	4029.9	-	-	-	137.2	-	4.41E+04	2.44E+04	-
124.5	209.0	-	-	-	144.8	3797.5	-	-	-	139.7	104.7	-	-	-
129.5	200.8	-	-	-	149.9	3675.3	-	-	-	144.8	103.8	-	-	-
134.6	190.3	-	-	-	152.4	-	4.38E+05	2.95E+02	-	149.9	107.6	-	-	-
139.7	224.3	-	-	-	154.9	3032.7	-	-	-	152.4	-	8.89E+04	3.38E+03	-
144.8	258.1	-	-	-	160.0	1485.7	-	-	-	154.9	96.1	-	-	-
149.9	327.2	-	-	-	165.1	513.2	-	-	-	160.0	98.1	-	-	-
152.4	-	3.56E+05	5.29E+03	-	167.6	-	2.26E+06	2.58E+03	-	165.1	104.7	-	-	-
154.9	434.3	-	-	-	170.2	215.2	-	-	-	167.6	-	7.97E+03	3.03E+03	-
160.0	455.6	-	-	-	175.3	111.2	-	-	-	170.2	89.7	-	-	-
165.1	534.3	-	-	-	180.3	194.5	-	-	-	175.3	100.8	-	-	-
167.6	-	5.42E+04	5.63E+03	-	182.9	-	8.24E+05	1.37E+03	-	178.4	-	-	-	?
170.2	666.2	-	-	-	185.4	225.5	-	-	-	180.3	61.6	-	-	-
175.3	557.7	-	-	-	190.5	153.4	-	-	-	182.9	-	3.78E+04	2.10E+04	-
180.3	630.1	-	-	-	195.6	191.1	-	-	-	185.4	53.8	-	-	-
182.9	-	2.66E+05	3.59E+03	-	198.1	-	4.73E+06	4.12E+03	-	190.5	40.1	-	-	-
185.4	446.8	-	-	78	199.1	-	-	-	538	195.6	49.0	-	-	-
190.5	699.7	-	-	-	200.7	122.9	-	-	-	198.1	-	1.25E+06	3.72E+05	-
195.6	694.0	-	-	-	205.7	177.1	-	-	-	200.7	39.7	-	-	-
200.7	626.9	-	-	-	210.8	168.0	-	-	-	205.7	27.3	-	-	-
205.7	517.2	-	-	-	213.4	-	2.15E+06	2.81E+02	-	210.8	27.4	-	-	-
210.8	359.1	-	-	-	215.9	130.2	-	-	-	213.4	-	6.74E+03	2.56E+02	-
213.4	-	4.35E+05	1.15E+03	-	221.0	95.1	-	-	-	215.9	28.6	-	-	-
215.9	313.4	-	-	-	226.1	95.6	-	-	-	221.0	35.5	-	-	-
221.0	214.6	-	-	-	228.6	-	7.80E+03	6.39E+02	-	224.0	-	-	-	990
226.1	171.7	-	-	-	231.1	64.2	-	-	-	226.1	32.4	-	-	-
228.6	-	2.86E+05	2.86E+02	-	236.2	85.4	-	-	-	228.6	-	5.22E+03	1.98E+02	-
231.1	176.8	-	-	-	241.3	52.7	-	-	-	231.1	44.6	-	-	-
234.6	-	-	-	389	243.8	-	2.55E+06	3.07E+04	-	236.2	34.7	-	-	-
236.2	160.1	-	-	-	246.4	45.3	-	-	-	241.3	39.7	-	-	-
241.3	142.3	-	-	-	251.5	90.6	-	-	-	246.4	42.6	-	-	-
243.8	-	1.10E+04	5.23E+02	-	256.5	20.4	-	-	-	251.5	40.8	-	-	-
246.4	118.4	-	-	-	259.1	-	7.90E+03	3.61E+02	-	256.5	42.4	-	-	-
251.5	87.4	-	-	-	261.6	73.7	-	-	-	261.6	45.9	-	-	-
256.5	67.3	-	-	-	266.7	20.4	-	-	-	266.7	42.6	-	-	-

Table 1-(Continued). Soil Depth, Apparent Resistivity, Heterotrophic and Oil Degrading Microorganism Population Numbers, Volatile Organic Acids, and Specific Groundwater Conductance Measurements.

VRP 9					VRP 5					VRP 4				
Depth (cm)	Resistivity Ohm. m	Heterotrophs (MPN/g soil)	Oil Degraders (MPN/g soil)	Conductance	Depth (cm)	Resistivity Ohm. m	Heterotrophs (MPN/g soil)	Oil Degraders (MPN/g soil)	Conductance	Depth (cm)	Resistivity Ohm. m	Heterotrophs (MPN/g soil)	Oil Degraders (MPN/g soil)	Conductance
259.1	-	3.77E+05	2.09E+03	-	271.8	44.1	-	-	-	269.2	-	-	-	1014
261.6	59.1	-	-	-	274.3	-	2.36E+02	3.07E+01	-	271.8	51.9	-	-	-
271.8	55.6	-	-	-	276.9	37.6	-	-	-	276.9	45.0	-	-	-
274.3	-		6.98E+01	-	278.0	-	-	-	?	281.9	50.7	-	-	-
276.9	57.5	-	-	-	281.9	54.6	-	-	-	287.0	47.3	-	-	-
281.3	-	-	-	877	287.0	32.8	-	-	-	297.2	48.9	-	-	-
281.9	60.8	-	-	-	292.1	65.0	-	-	-	297.8	-	-	-	1003
287.0	63.7	-	-	-	297.2	40.4	-	-	-	302.3	55.3	-	-	-
289.6	-		3.55E+02	-	302.3	48.3	-	-	-	307.3	67.3	-	-	-
292.1	70.1	-	-	-	304.8	-	1.53E+04	2.16E+03	-	312.4	55.2	-	-	-
297.2	71.4	-	-	-	307.3	52.0	-	-	-	317.5	53.0	-	-	-
302.3	69.8	-	-	-	312.4	42.1	-	-	-					
304.8	-	2.39E+02	1.85E+02	-	317.5	59.0	-	-	-					
307.3	75.2	-	-	-	320.0	-	3.86E+03	4.44E+02	-					
312.4	64.0	-	-	-	322.6	43.7	-	-	-					
317.5	74.5	-	-	-	324.0	-	-	-	842					
322.6	65.5	-	-	-	327.7	64.3	-	-	-					
327.0	-	-	-	-	332.7	67.4	-	-	-					
327.7	66.7	-	-	764	335.3	-	4.00E+02	3.20E+02	-					
332.7	64.8	-	-	-	337.8	50.0	-	-	-					
357.5	-	-	-	?	342.9	76.8	-	-	-					
					348.0	44.9	-	-	-					
					353.1	61.6	-	-	-					
					358.1	50.1	-	-	-					
					363.2	50.0	-	-	-					
					368.3	49.1	-	-	-					
					369.3	-	-	-	904					
					373.4	67.1	-	-	-					
					378.5	47.4	-	-	-					
					383.5	65.6	-	-	-					
					388.6	57.1	-	-	-					
					393.7	70.3	-	-	-					
					398.8	51.6	-	-	893					
					416.9	-	-	-	?					

Notes: BDL = below detectable levels; NR = no recovery from lysimeters.

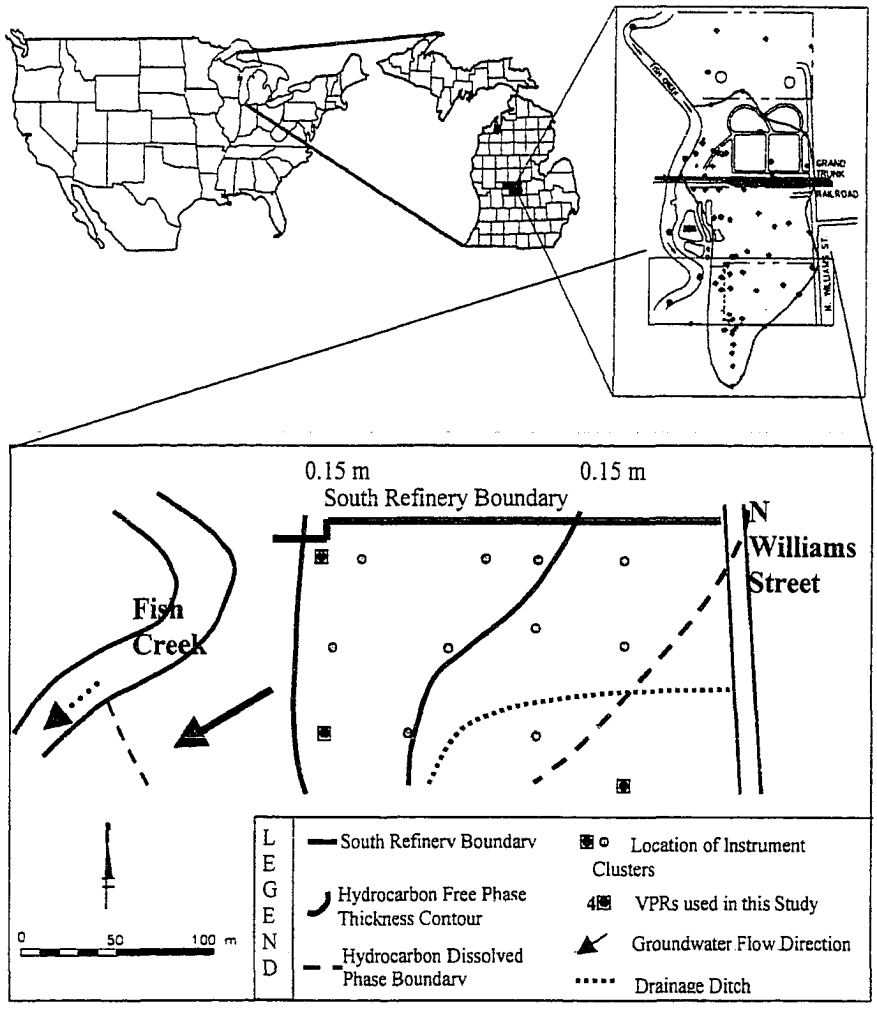

Figure 1. Former Crystal Refinery, Carson City, Michigan, Vertical Resistivity Probe and Instrument Clusters Locations.

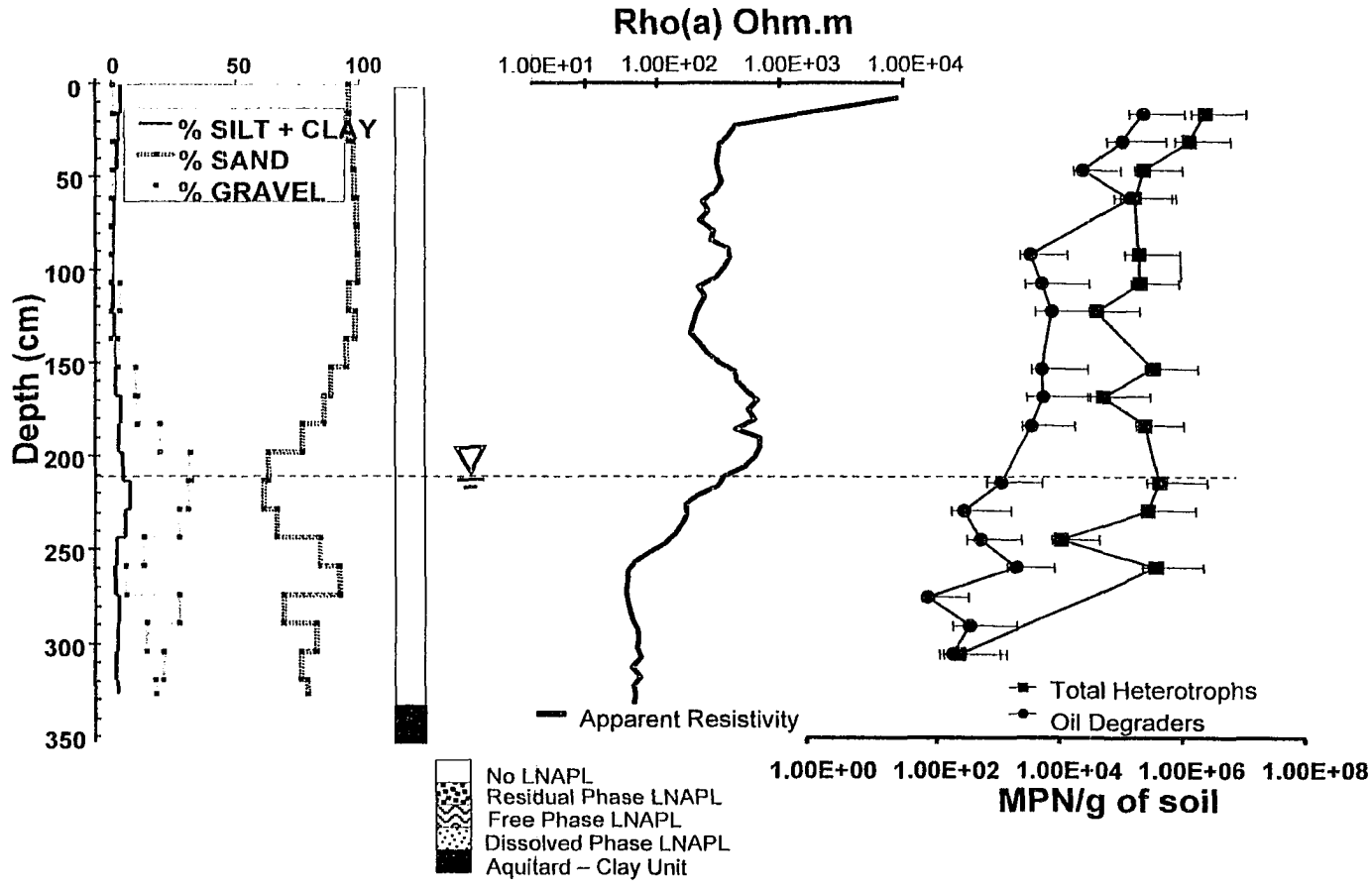

Figure 2. *In Situ* Resistivity, Microbial and Grain Size Distribution from VRP 9, the Background Location.

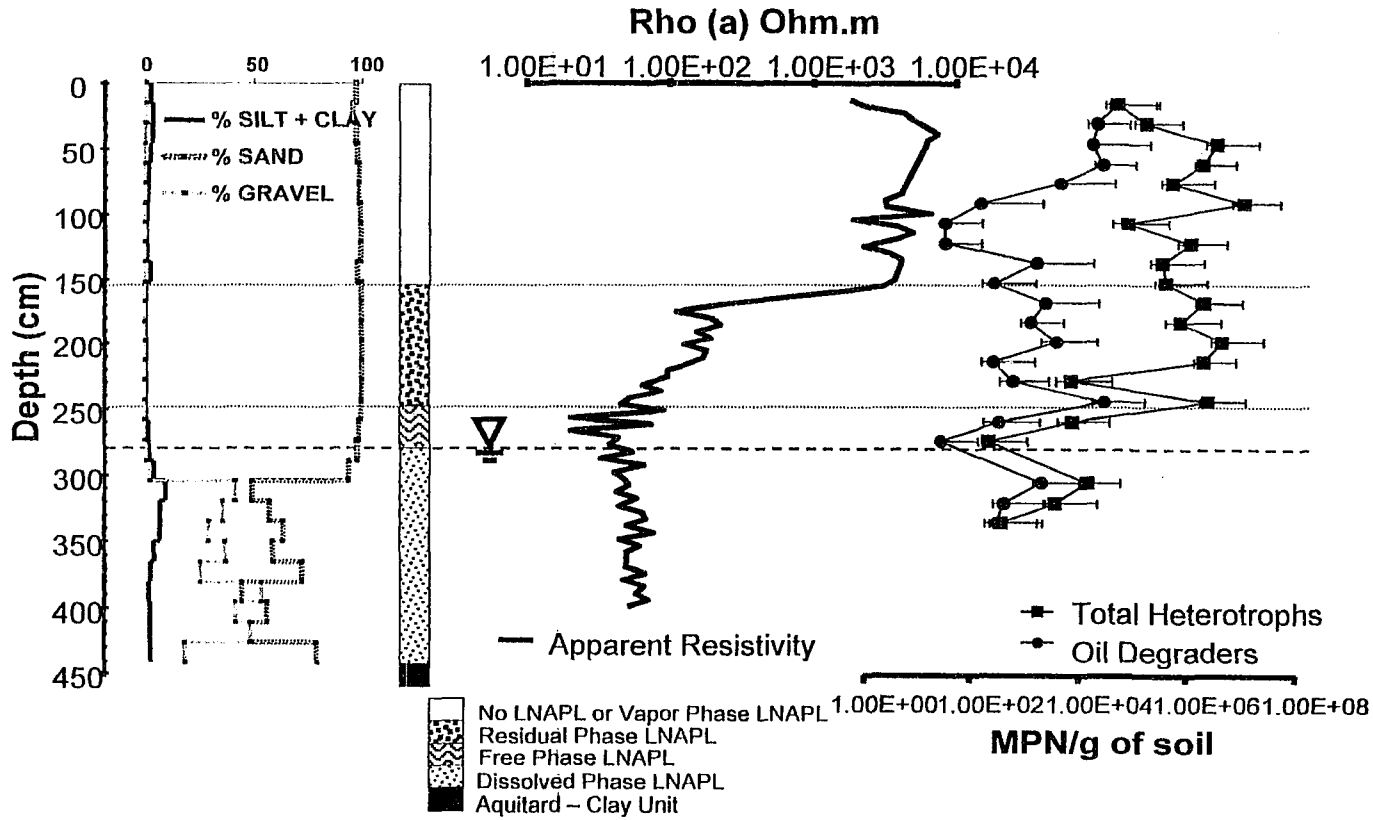

Figure 3. *In Situ* Resistivity, Microbial and Grain Size Distribution from VRP 5, a LNAPL-Contaminated Location.

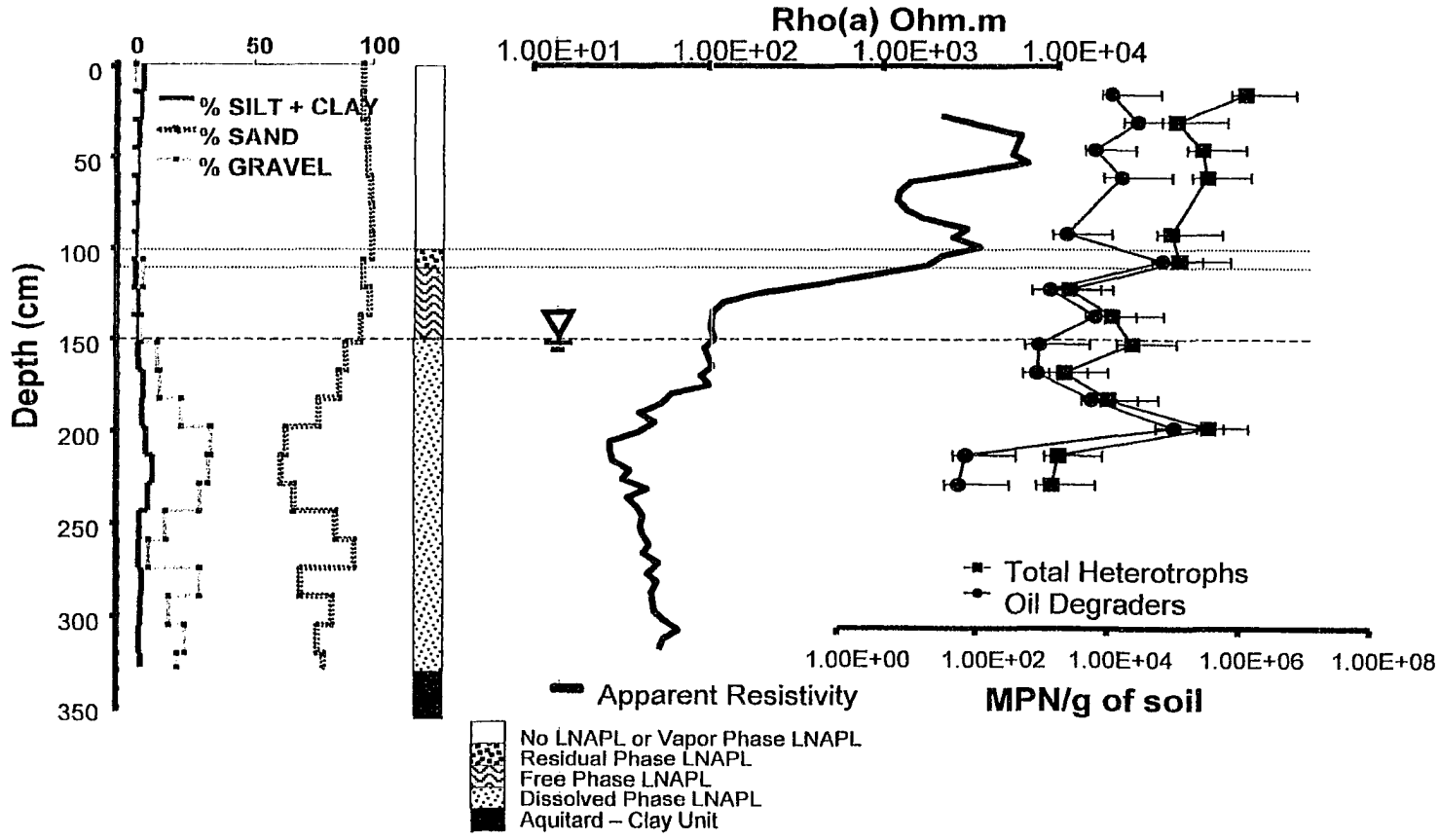

Figure 4. *In Situ* Resistivity, Microbial and Grain Size Distribution from VRP 4, a LNAPL-Contaminated Location.

CHAPTER 3

ARCHIE'S LAW ANALYSIS OF A SHALLOW HYDROCARBON CONTAMINATED AQUIFER: IMPLICATIONS FOR THE CONDUCTIVE MODEL FOR LNAPL IMPACTED SITES.

3.0 Introduction

It is generally accepted that geophysical methods are able to detect freshly released Light Non-Aqueous Phase Liquids (LNAPLs) in part due to their higher electrical resistivity (lower conductivity) that readily distinguishes them from the less resistive (more conductive) background groundwater. This hypothesis is supported by modeling, controlled spill, and laboratory experiments (De Ryck et al., 1993; Redman et al., 1994; Campbell et al., 1996; Kelly, 1996; Endres and Redman, 1996; Osiensky, 1997; Blacic and Arulanandan, 1999). This scenario forms the basis for the insulating layer model (Mazác et al., 1990) and is commonly used in the assessment of geophysical measurements from LNAPL impacted sites. However, electrical surveys at many old or aged LNAPL spill sites reveal low resistivity anomalies and not the expected highs predicted by the insulating layer model (Benson and Stubben, 1995; Gajdos and Král, 1995; Sauck et al., 1998; Atekwana et al., 1998; Atekwana et al., 2000). Further, some studies have observed the attenuation or "washing out" of GPR reflections, an indication of increased conductivity coincident with zones of LNAPL contamination (Olhoeft, 1986; Daniels et al., 1992; Benson and Stubben, 1995; Maxwell and Schmok, 1995; Benson et al., 1997; Sauck et al., 1998; Benson and Mustoe, 1998; King, 2000). Thus,

the results of these investigations call into question the validity or applicability of the insulating layer model in the characterization of older LNAPL impacted sites.

To explain these results several hypotheses have been suggested including imbibition and NAPL wetting phase effects (Swanson, 1980; Monier-Williams, 1995). However, more recent findings relate the lowered resistivity and attenuated GPR reflections to higher conductivities resulting from biologically mediated redox reactions associated with the microbial degradation of LNAPLs (Bermejo et al., 1997; Sauck et al., 1998; Werkema et al., 1998; Atekwana et al., 1998; Atekwana et al., 2000; Sauck, 2000; Lucius, 2000). In fact, this fascinating new area of research could be called "biogeophysics" (Knight, 2001). Indeed, numerous geochemical and microbial studies of LNAPL-contaminated aquifers show that highly conductive groundwater exists below some LNAPL plumes (Baedecker et al., 1987; Cozzarelli et al., 1990; Baedecker et al., 1993; Bennett et al., 1993; Eganhouse et al., 1993). Further, increased pore water conductance from enhanced mineral dissolution is possible via the production of carbonic and organic acids due to hydrocarbon degradation by bacterial activity in soil and groundwater (McMahon et al., 1995). This process leads to the production of a high total dissolved solids (TDS) leachate plume. The existence of this plume is reflected in the increased groundwater conductance observed in and around the zones of active biodegradation. Such changes can significantly influence the electrical properties of impacted media but have remained relatively unrecognized and/or unappreciated by previous geophysical investigations (Sauck et al., 1998). Consequently, the composition and physical properties of the free and/or residual product contamination and surrounding zone will evolve with time due to these biogeochemical alterations of the impacted area.

The apparent contradiction between field results and the insulating layer model is attributed to the fact that the existing "insulating layer" geophysical model does not take into account the dynamic biogeochemical changes that modify the subsurface to a different physical and chemical state, resulting in an alteration of the physical properties of the subsurface impacted media. It is on the basis of these biogeochemcial alterations that Sauck et al. (1998) and Sauck (2000) have proposed that microbial LNAPL degradation induces time dependent changes in the geoelectrical properties of LNAPL impacted soils in natural environments from resistive to conductive. It follows that sites impacted with LNAPL initially behave with high apparent resistivities (low conductivities) consistent with the insulating layer model assumption, but change to low apparent resistivities as the TDS concentrations increase due to enhanced mineral weathering.

Therefore, this project is driven by the need to evaluate the conductive plume model and to advance the understanding of the spatial and temporal nature of the conductive response at a site impacted with LNAPL contamination.

3.1 Study Site

The Crystal Refinery located in Carson City, Michigan (Figure 1) has had petroleum releases since 1945 from storage tanks and pipelines resulting in the seepage of hydrocarbons into the subsurface. This leakage has impacted soils and groundwater beneath the site, a cemetery to the north and the city park to the south. This study presents results of investigations focusing on the southern hydrocarbon contamination which extends southwesterly into the Carson City Park. In 1994, this contaminated zone

was approximately 229 m long and 82 m wide with a free phase LNAPL thickness between 0.3 m to 0.6 m and an estimated volume of 167,200 liters (Snell Environmental Group, 1994). Residual phase hydrocarbons are found at the fringes of the free phase area with high concentrations of benzene, toluene, ethyl benzene and xylene (BTEX) (Dell Engineering, 1992). Figure 1 shows the present distribution of LNAPL contamination with reference to the location of free phase LNAPL thickness and the residual phase LNAPL boundary.

Geologically, the site is characterized by approximately 4.6 m to 6.1 m of fine to medium sands, coarsening at and below the water table to gravel; this unit is underlain by a 0.6 m to 3 m thick clay aquitard unit (Dell Engineering, 1991; Dell Engineering, 1992). Due to topography, the depth to the water table varies from 0.6 m to 0.9 m in the west of the site to 4.6 m to 5.8 m in the east. Groundwater flows west-southwest toward a nearby creek with a hydraulic gradient of 0.0015 and a flow velocity of 1.7 m/day (Snell Environmental Group, 1994).

3.1.1 Site-Specific Research History

Previous work investigating the LNAPL contamination present at this site (Sauck et al., 1998; Atekwana et al., 2000; Sauck, 2000; Werkema et al., 2000) have demonstrated the presence of anomalously low resistivity (high conductivity) coincident with areas of LNAPL contamination. Furthermore, Cassidy et al., (2001) and Werkema et al. (2000) have presented additional evidence of high oil-degrading bacteria populations in zones coincident with the observed low apparent resistivity. These studies show a correlation between the biodegradation of the LNAPL-impacted zone and the

geoelectrically low resistivities observed. Furthermore, a study on the presence of biosurfactants has shown high concentrations produced at the LNAPL-impacted locations (Hudak, 2001) and coincident with the anomalous geoelectrical zones. These biosurfactants emulsify the hydrocarbon and play an important role in the geoelectrical response by allowing through-going water paths to develop within the free-product LNAPL zone. Finally, biological studies have found maximum oil-degrading bacteria populations within the LNAPL impacted zone while microscopic examination of sediment grains show etching and pitted surfaces suggestive of dissolution (Duris et al., 2000; Duris et al., 2001). These results show the mechanism by which the anomalous geoelectrical zone develops through enhanced mineral dissolution as a result of biological activity within zones of LNAPL impaction. These studies have provided evidence supporting the conductive model for LNAPL impacted unconsolidated sands and gravels (Sauck, 2000).

3.2 Field Methods – Vertical Resistivity Probes

Apparent resistivity measurements were collected using vertical resistivity probes (VRP). The VRPs consist of a 3.81 cm ID PVC dry well with 1.27 cm #10-24 pan-head stainless steel screws separated vertically every 2.54 cm. The screw heads serve as the electrode contact to the formation and the threaded ends allow contact inside the dry PVC well enabling 4-electrode apparent resistivity readings. Ten VRPs are currently installed at the Carson City Park (Figure 1). Installation of these probes includes a small bentonite slurry annulus, which allows installation below the saturated zone and decreases the contact resistance with the surrounding formation sediment in the unsaturated zone.

VRP measurements were made using a Syscal R2 resistivity meter with a automated/semi-automated switching system (Werkema et al., 1998). Apparent resistivity data were collected in the semi-automated mode using a 5.08 cm Wenner array. Data for each VRP were collected every month for at least 12 month period. Table 1 summarizes the VRP time range throughout which monthly measurements were collected. The VRP data required about a year to stabilize due to the bentonite (Groncki, 1999), thus the measurements shown here are at least a year or more after installation of the VRPs.

Precipitation data were from a weather station located at Greenville, MI., which is west of Carson City, in the prevailing upwind direction. The water table elevation and LNAPL thickness data were measured from a 2.54 cm monitoring well located within a 1 m radius of each VRP. Water level elevations were calculated from a detailed topographic survey (Figure 1) and corrected for the thickness of LNAPL measured (Fetter, 1993). These data are used for groundwater table elevation considerations in the analysis of the VRP data.

In order to investigate the VRP data for the influence of clay and silt content, a grain size analysis was completed, which included a description of the degree of LNAPL contamination. Continuous soil logs from either direct push using a small all-terrain drill rig (VRPs 1, 2, & 3), hand augering (VRPs 4, 5, 6, 7, & 8) or Geoprobe® sampling (VRPs 9 & 10) were used for the grain size analysis and descriptions of LNAPL contamination. Grains sizes were determined by sieving samples at 15.24 cm intervals. The grain sizes were divided as follows: silt & clay < 0.075 mm; 0.075mm < sand < 4.75 mm; 4.75 mm < gravel.

Levels of LNAPL contamination were determined from field observation as either free phase LNAPL, residual phase LNAPL, or dissolved phase LNAPL. The dissolved phase LNAPL were determined through chemical analysis (Legall, 2002). Based on these data, the VRP data are grouped into three categories representing three degrees of LNAPL contamination: free phase LNAPL contamination, residual phase LNAPL contamination, and no LNAPL contamination (i.e. control location).

3.3 Results – Vertical Resistivity Probes

Figure 2 presents the water table and precipitation data versus time during a complete hydrologic year. The monitoring well response is interpreted as the recharge response to the precipitation events. The relationship between precipitation and monitoring well response is very good, with a slight time lag in the response from the precipitation events to the monitoring wells. This behavior is due to the groundwater recharge and the resulting monitoring well response. These data show a precipitation and monitoring well groundwater level low occurring during November 1999, a high occurring in June of 2000 and another low during November 2000. These data also provide the necessary groundwater table elevations for the VRP Archie's Law analysis.

Figures 3 through 8 present the VRP data for each day the resistivity readings were taken, with the elevation above mean sea level along the vertical axis and the VRP data converted to conductivity and reported in milliSiemens per meter (mS/m) on the horizontal axis. Also indicated on Figures 3 through 8 are the grain size distribution per elevation and the relative LNAPL contamination.

3.3.1 Locations with Free Product LNAPL Contamination

A total of five VRPs are installed in locations where variable levels of free phase LNAPL are observed (see Figure 1). Amounts of free product observed in the monitoring wells range from a few centimeters up to 61 cm during the dates indicated in Table 1. The data from three of these locations, VRP 1, 4 and 5 (see Figure 1 for VRP locations) are included in Figures 3, 4 and 5.

Figure 3 shows the data for VRP 1. The grain size data show predominantly sand with a coarsening to gravel at and below the water table. The largest percentage of silt and clay was 5.9% at the highest elevation. Below this elevation the silt and clay never exceeded 2.7%. Overall, the grain size distribution indicates relatively uniform unconsolidated sand. At the elevations corresponding to the residual phase LNAPL layer and the groundwater table, the percent gravel increases and the sand content decreases. The contamination levels show a residual phase LNAPL layer occurring from 225 m to 226 m elevation. Below this point is a free phase layer continuing to 224.5 m. Underlying these LNAPL phases a dissolved phase was observed extending throughout the saturated zone. The VRP results show a variability of readings through the vadose zone to 226 m. This variability is attributed to moisture content variations and/or seasonal temperature fluctuations in the higher elevations, as the sediment profile does not change. This variability is common to all the VRPs included in this study. At 226 m elevation, a conductivity increase begins; its value is approximately 10 mS/m and grows to over 40 mS/m at approximately 225.2 meters. This elevation zone corresponds to the residual phase LNAPL zone. From 225.2 m to 224.6 m is a high conductivity bulge exhibiting the highest conductivities observed throughout the profile over the dates of

measurement. This bulge shows a maximum of approximately 50 mS/m and correlates with the free phase LNAPL zone; it occurs at an elevation at and below the lowest groundwater table elevation. The relationship of this conductivity maximum to the groundwater table is also common to most of the VRPs. Below this maximum, the conductivity profile decreases slightly, remaining relatively uniform and repeatable throughout the date range shown within the saturated zone.

Figure 4 displays the results from VRP4, another free phase LNAPL location. These data are presented in similar format to Figure 3. The grain size distribution shows sand-dominated sediment (~90 – 100 %) down to 224.5 m. At lower elevations, the grain size is approximately 50% sand and 50% gravel. The highest percent silt & clay size particles, representing 8% of the sample volume, occurs at the 224.7 m elevation. The LNAPL distribution consists of residual phase LNAPL from 225.8 m to 225.2 m, overlying a free phase LNAPL layer occurring from 225.2 m to 224.85 m. The dissolved phase LNAPL zone occurs from 224.85 m to 223.9 m, where the clay aquitard is encountered at the bottom 0.2 meters of the VRP. The conductivity profile again shows variability in the vadose zone above the high groundwater table elevation mark and the upper elevation of the residual phase LNAPL layer. At this elevation (~225.8 m), the profile displays an abrupt increase in conductivity from approximately 0.3 mS/m to about 10 mS/m over a 0.2 meter elevation change. The profiles from most dates measured follow this trend with the exception of 6/7/2000; this date is the only outlier and occurs during the largest precipitation event on record (see Figure 2). Continuing lower in elevation, the conductivity profile progressively increases until a maximum of approximately 50 mS/m is reached at 224.95 m, which correlates with the free phase

LNAPL layer and again occurs at and slightly below the lowest water level elevation. Below this conductivity maximum, the conductivity profile decreases uniformly through the saturated zone (dissolved phase LNAPL zone). The basal clay aquitard is not distinguished as a separate lithologic unit by the conductivity profile.

Figure 5 presents the results from another free phase LNAPL location, VRP5. The grain size distribution is similar to VRP 4 in that a predominant sand layer is present until 224.6 m and then a 50/50 mix of sand and gravel is encountered that continues with depth. The silt and clay fractions are very low (~0 to 10%) with the maximum occurring at 224.5 m. The conductivity profile shows a low and variable range from 0.01 to 1 mS/m throughout the vadose zone down to an elevation of 226.1 m. From 226.1 m to 225.8 m the conductivity increases linearly to around 10 mS/m. This increase occurs at the boundary between the residual phase LNAPL and the clean sediment above. Below the 225.8 m elevation and continuing to 225.1 m, the conductivity profile continues to increase to 37 mS/m through this residual LNAPL zone. Occurring at 225 m to 224.8 m is an alternating polarity conductivity high of 58 mS/m which is coincident with the free phase LNAPL – water interface. The alternating polarity response is typical of the Wenner array across a sharp geoelectric boundary (Telford et al., 1990). Below this high the conductivity profile gradually decreases to approximately 18 mS/m, over the dates measured, to the maximum depth of the VRP at an elevation of 223.5 m.

In summary, these three locations (VRPs 1, 4, and 5) represent different amounts of free phase LNAPL in topographically different locations. The conductivity results from within the free phase LNAPL-contaminated zones all reveal high conductivities. Of course, this is directly contrary to the insulating layer model. Specifically, the

conductivities range from 40 – 50 mS/m within the elevation zones impacted with free phase LNAPL.

3.3.2 Locations with only Residual LNAPL Contamination

Three VRPs are installed in the residual portion of the LNAPL plume (VRPs 2, 3, and 10). The data from VRP 3 and VRP 10 are included here as Figures 6 and 7, respectively. The grain size distribution plot for VRP 3 (Figure 6) shows 90 to 100 % sand from the surface elevation of 230.4 m to 225.2 m where the grain size becomes more heterogeneous, containing larger portions of gravel and silt-clay. The LNAPL distribution at this location contains no free phase LNAPL, but does exhibit residual phase LNAPL occurring from 226.2 m to 225.05 m elevation. Below 225.05 m is the saturated zone containing dissolved phase LNAPL. The conductivity profile shows a variable response in the vadose zone ranging from 0.1 to approximately 10 mS/m until 226.6 m elevation. At this point an abrupt decrease occurs to approximately 1 mS/m then the profile uniformly increases to 25 mS/m at approximately 225 m elevation. The reason for the abrupt decrease at 226.6 m is unknown. The remaining trend of the conductivity profile with decreasing elevation shows a conductivity maximum of 25 mS/m correlating with the residual phase LNAPL – dissolved phase LNAPL interface and at the lower elevation of the water table fluctuation as in the free phase locations. Below the residual phase zone, the conductivity profile decreases with depth in the saturated dissolved phase; there is no variability observable between dates in this region. In the zone showing the water table fluctuations and corresponding to the residual phase LNAPL (i.e., 226.2 m to 225.05 m elevation), temporal variations of conductivity profile

vs. elevation are evident through the dates of measurement. These variations are interpreted as groundwater level changes from recharge events.

Figure 7 includes the results from VRP 10, another residual phase LNAPL location. Again the grain size distribution shows 90 to 100 % sand from the surface elevation of 229.2 m to 224 m elevation. Below 224 m the grain size becomes predominantly a 50/50 mix of sand and gravel with some silt and clay. The LNAPL distribution contains a layer of residual phase LNAPL located from 225.7 m to 224.5 m. Below is the dissolved phase LNAPL and saturated zone continuing to the clay aquitard layer at 222.4 meters. As with the other VRPs, the conductivity profile is highly variable from the surface to an elevation of 225.7 m. Below 225.6 m the conductivity profile increases and shows a vertically-extensive conductivity bulge (or peak) with a maximum of 31 mS/m. This high conductivity bulge correlates with the elevation zone of the residual LNAPL phase and also lies within the lower elevations of the water table range. Below approximately 224.2 m the conductivity profile is generally repeatable with a consistent value of around 10 mS/m and a slight decrease in conductivity at the lower elevations to 8 or 9 mS/m.

Summarizing the results shown in Figure 6 and Figure 7, we observe a slight VRP response to fluctuating water table levels as observed through small conductivity profile variability or profile shifts to higher or lower elevations due to changes in pore water saturation. More importantly, these figures present conductivity maxima of approximately 30 mS/m occurring at and within the elevation zones of residual phase LNAPL contamination and in the lower elevations of the water table fluctuation. This behavior is in direct contradiction to the insulating layer model, which predicts a

conductivity minimum in these zones. Furthermore, the lithology logs indicate that this is not due to changing lithology (i.e. increasing clay or silt content). Therefore, these conductivity anomalies are attributed to pore fluid processes associated with the residual LNAPL impacted zones.

3.3.3 No Contamination (Control Locations)

Two VRP locations (VRP 7 and VRP 9) contain no evidence of LNAPL contamination and are considered the control locations at this site. Figure 8 shows the results from VRP 9. The grain size, as shown consistently throughout the site, is predominantly sand (~90-100%) from the surface until the distribution changes to include more gravel size particles with some silt and clay at approximately 224.75 m elevation. The conductivity results show some variability in the vadose zone, although not as much as at previous locations. The results also show a slight increase above the water table and then a gradual decrease through the transition zone and convergence of the values below the water table and into the saturated zone. These profiles reveal no conductivity maximum, as observed at the contaminated locations. Further, the uncontaminated VRP exhibits a gradual increase in conductivity through the transition zone as opposed to the sharp/abrupt boundaries observed at the contaminated locations. The conductivity profile stabilized below the range of water table variability to approximately 10 – 15 mS/m as compared to 15 – 27 mS/m and 25 – 40 mS/m for the residual and free product locations. Additionally, these VRP data reveal changes in the conductivity within the water table fluctuation zone, which is likely due to pore water saturation changes over time and

hysteresis as the transition zones alternates between imbibition and drainage (Knight, 1991).

3.4 Analysis and Discussion

3.4.1 Comparison of Free Phase, Residual Phase Contamination, and Uncontaminated Profiles

To further evaluate the existence of a conductivity anomaly coincident with different degrees of LNAPL contamination a detailed comparison between VRPs 1, 3, and 9 (i.e., free product, residual and uncontaminated, respectively) is presented for the December 1999 data set. Figure 9 presents the conductivity versus elevation for each of the three VRPs at a detailed elevation scale centered about the water table. Evident from this comparison is the gradual increase in conductivity through the transition zone and the relatively constant value of 15 mS/m within the saturated zone for the uncontaminated VRP 9. In contrast to this profile are the profiles for both the free product case at VRP 1 and the residual contamination at VRP 3 that show a zone of conductivity maximum from approximately 30 cm above to 30 cm below the water table. This zone corresponds to the presence of free phase and/or residual phase LNAPL. These two profiles then decrease in conductivity below the water table to average saturated zone values of 25 mS/m for VRP 3 and 35 mS/m for VRP 1. Figure 9 clearly shows that the profiles for both VRP 1 and VRP 3 display enhanced conductivity relative to the uncontaminated VRP 9. The values of maximum bulk conductivity in the zone at and above the water table for free phase LNAPL (VRP1) are 45 – 50 mS/m. The residual phase LNAPL location (VRP 3) shows a range from 25 – 30 mS/m and the clean location (VRP 9) reveals conductivity

values of 1 to 9 mS/m in the elevations corresponding to the water table and above. This observation is contrary to the insulating layer model for the geoelectric response, which would predict the profiles for VRP 1 and VRP 3 to be of lowered conductivity relative to VRP9 due to lower water saturation resulting from the displacement of conductive groundwater by an insulative LNAPL. Clearly these results show an enhancement of the conductivity at the locations impacted by LNAPL. In fact, the location with the free phase LNAPL showed a higher conductivity than the residual phase LNAPL, which was higher still than the clean site. This gradation suggests a relative increase in conductivity corresponding to higher degrees of LNAPL saturation.

3.4.2 Estimated Water Saturation and Estimated Pore Water Conductivity Enhancement

To further evaluate these conductivity anomalies, the VRP data were analyzed using some simple comparative calculations based on the empirical Archie's Law (Archie, 1942). According to Archie's law the electrical conductivity of clean geologic material (in the absence of clays) can be described by:

$$\sigma_e = \frac{\sigma_w}{\left(a\phi^{-m}S_w^{-n}\right)} \qquad (1)$$

where σ_e is the effective conductivity of the medium that is measured,

ϕ is the fractional pore volume (porosity),

S_w is the fraction of the pores containing water (i.e., water saturation)

σ_w is the pore water conductivity,

m is the cementation exponent,

n is the saturation exponent and

a is an empirical factor.

The cementation and saturation exponents implicitly incorporate information about pore structure and fluid distribution, respectively, into Archie's Law. As the grain size distribution data show, this site contains no appreciable amounts of silt or clay; hence, this form of Archie's Law is applicable to the aquifer material at this site.

A number of factors could contribute to the temporal and spatial conductivity variations observed in the VRP profiles, such as changes in lithology, temperature, water saturation, water conductivity, and/or porosity. The grain size distribution data do not show significant lithogical heterogeneities that correlate with the conductivity anomalies. Since sorting, porosity and pore structure are functions of grain size in unconsolidated aquifers, we have assumed that these factors are not a significant factor influencing the conductivity anomalies. Temperature variations undoubtedly occur in the near subsurface; however the conductivity profiles are fairly repeatable throughout a full hydrologic year, suggesting that significant conductivity variation is not due to seasonal temperature changes. Temperature variations may occur due to chemical or biologic reactions with depth; however, we have no data to evaluate this effect and have assumed it is not a large contributing factor. This process of elimination leaves water saturation (S_w) and pore water conductivity (σ_w) as the possible causes responsible for the temporal and spatial conductivity variations observed in the VRP profiles.

First, we assumed the changes in apparent conductivity above the top of water saturation were due entirely to variations in water saturation S_w; the pore water conductivity σ_w was taken as being a constant value. This approach would be consistent

with the insulating layer model for LNAPL pools as the insulating LNAPL displaces the conductive water from the pore space decreasing the water saturation. The unchanged pore water conductivity reflects the absence of biodegradation processes in this model.

The apparent water saturation was estimated for each VRP profile using Archie's Law. For this calculation, we have assumed that the porosity and pore structure are consistent through the aquifer. We will consider an effective conductivity at elevation z along the VRP profile. Suppose that σ_e^{sat} is the effective conductivity in the uncontaminated saturated zone of this aquifer. It can be shown from equation (1) that apparent water saturation $S_w(z)$ required to account for the effective conductivity $\sigma_e(z)$ is given by

$$S_w(z) = \sqrt[n]{\sigma_e(z)/\sigma_e^{sat}} \qquad (2)$$

While the observed values of n range between 1.1 and 2.6, it is commonly assumed to be 2 when there is no independent information; we have taken this approach (Schön, 1996). Based on the VRP profiles, we have used σ_e^{sat}=16 mS/m, the average effective conductivity of the uncontaminated saturated zone.

Figures 10 through 14 show the results from these estimations of water saturation for VRPs 1, 4, 5, 3, 10, and 9. The estimates were calculated for three dates selected as representative of precipitation maximum and minimum during the time of this study. November 1999, June 2000, and November 2000 were chosen. Additionally, the figures include the LNAPL description and the grain size distribution as in figures 3 through 8 in order to provide comparisons to these results.

3.4.2.1 Water Saturation Estimate – Free Phase LNAPL Locations

The S_w estimate for VRP 1 is shown in Figure 10. Inspection of figure 10 shows low water saturation in the vadose zone above an elevation of 226 m. Continuing to lower elevations reveals that from 225.4 m to 224.6 m an excess water saturation of up to 130% (1.3) is required to yield the conductivity profile observed for the three dates indicated. Further, the elevation zone of maximum estimated S_w is from 225 m to 224.4 m and is coincident with the zone of free phase LNAPL contamination. These elevations are within the maximum and minimum elevations of the groundwater table (i.e. the water fluctuation zone) and the saturation zone. In this zone, we should expect a maximum 100% saturation. Moreover, free phase LNAPL contamination is occupying some of the pores and lowering the water saturation. The estimates greatly in excess of 100% water saturation indicate that an alternative mechanism must be accounting for the enhanced conductivities observed. Additionally, the profiles from November 1999 and November 2000 are very similar with the exception of November 1999 requiring more water saturation at the anomalous zone. The June 2000 profile does show an excess of water saturation in the shallower elevations relative to the November dates. This is expected due to the excess precipitation at that date and shows that the excess S_w in the contaminated zone persist with time.

Figure 11 displays the results for VRP 4, another free phase LNAPL location. Again we see an excess calculated water saturation of up to 140% (1.4) coincident with the zone of free phase LNAPL and occurring at the base of the water table fluctuation zone (~225 m). The November 1999 data show the largest water saturation, while June

2000, the least. Although not directly related to this analysis an interesting observation is made in the June 2000 data. A wetting front due to the large precipitation event is clearly resolved by the VRP data, thereby showing the resolution of VRPs to observe hydrologic events.

Finally, the results of the estimated water saturation for the last free phase LNAPL location, VRP 5, are shown in Figure 12. These data also show an excess calculated water saturation of over 160% (1.6) required to achieve the conductivity profile observed. This excess occurs coincident with the free phase LNAPL location. Furthermore, the June 2000 results show at an elevation of approximately 225.6 m a lens of increased water saturation relative to the other dates. This is interpreted as the large recharge event inferred from the precipitation maximum in June 2000 as is evident from the VRP 4 (figure 11) analysis.

3.4.2.2 Water Saturation Estimate – Residual Phase LNAPL Locations

Figures 13 and 14 display the S_w estimate results for residual phase LNAPL locations. These data give maximum S_w estimates from 120% to 130% in the region containing the residual phase LNAPL zone – dissolved phase LNAPL interface. For comparison, recall the free phase LNAPL locations where estimates were between 130% and 160%. Notable from Figure 13 and 14 is the maximum S_w estimate occurs at the residual phase – dissolved phase interface and then decreases back to approximately 100% S_w in the saturated zone containing dissolved phase LNAPL and leachate from the active zone.

3.4.2.3 Water Saturation Estimate – No LNAPL Contamination Location

Figure 15, the S_w estimate for the uncontaminated location at VRP 9, shows no zone of excess water saturation when the Archie analysis is applied to the VRP data. The estimated water saturation profile increases to about 100% at the water table and remains near 100% into the saturated zone. Given the assumption in this analysis that conductivity changes are solely due to saturation variations with depth, these results can be used to determine the presence of enhanced water saturation zones associated with LNAPL contamination that are necessary to produce the observed conductivity profile.

In summary, according to the insulating layer model for LNAPL-impacted sites, impossibly large water saturation would have to occur to account for the VRP results observed. This result is obviously in conflict with the fact that the LNAPL should be displacing the pore water and lowering water saturation. As a result, another mechanism that is not incorporated into the standard insulating layer model is causing the anomalously high conductivity in the impacted zone.

3.4.3 Estimated Pore Water Conductivity

Since it is obvious that water saturations approaching 130%, and up to 160% are impossible, we have investigated whether changing pore water conductivity σ_w could produce the observed VRP results. In particular, the question we have posed is what increase in pore water conductivity is necessary to account for the VRP conductivity profiles at LNAPL-impacted locations. To answer this question, we again used Archie's Law to analyze the anomalous high conductivity responses observed at the free phase

LNAPL locations (VRPs 1, 4 & 5) and the residual phase LNAPL locations (VRPs 3 & 10).

To estimate pore water conductivity for each VRP profile, it was assumed that the water saturation profile $S_w(z)$ at the LNAPL impacted locations are the same as for the uncontaminated section at VRP 9. To compensate for the spatial variability of the water table at this site, the VRP profiles were shifted vertically such that their water table levels were coincident with that of VRP 9.

Let us consider an effective conductivity $\sigma_e^c(z)$ at elevation z along the shifted VRP profile at a contaminated location. Using equation (1), it can be shown that the pore water conductivity $\sigma_w^c(z)$ at elevation z along the shifted VRP profile at a contaminated location is given by

$$\sigma_w^c(z) = \frac{\sigma_e^c(z)}{\sigma_e^{uc}(z)} \sigma_w^{uc}(z) \qquad (3)$$

where $\sigma_e^{uc}(z)$ is the uncontaminated location apparent conductivity at elevation z along VRP 9 and $\sigma_w^{uc}(z)$ is the uncontaminated pore water conductivity at elevation z along VRP 9. Based on field measurements of pore water conductivity from a nearby uncontaminated monitoring well (Atekwana, 2002), we have used a constant value of $\sigma_w^{uc}(z) = 16$ mS/m (160 μS/cm) in our analysis.

As in the estimated pore water saturation analysis, the estimated pore water conductivity enhancement is performed for the three dates (November 1999, June 2000, and November 2000) representative of minimum and maximum water levels throughout

the hydrologic year. The resulting profiles for the contaminated locations are plotted in their vertical position relative to the groundwater table at the VRP 9 location per the measurement date. The estimated pore water conductivity profiles for each date are given in Figures 16, 17 and 18, respectively.

Comparison of the three figures reveals an elevated estimated pore water conductivity within approximately 0.75 meters of the groundwater table. The November 1999 results show the pore water conductivity estimate of up to 200 mS/m above the water table (2000 μS/cm). These data reveal the highest estimated conductivities associated with the locations of the greatest amount of free phase LNAPL. The June 2000 data reveal the greatest estimate for the free phase locations. The results from this date also show the high estimated conductivities to occur at and below the water table. Perhaps this stratification is due to the large precipitation event and the corresponding recharge. Finally, the November 2000 data also reveal the greatest estimates at the free phase LNAPL locations. However, these data show the high estimated conductivities to approach 1 meter in thickness and occur above and below the water table. Overall, these results show that estimated pore water conductivities of over 200 mS/m, are necessary to account for the VRP results observed at the contaminated locations (i.e. VRPs 1, 4, 5, 3, & 10). The zone of the predicted large pore water conductivity is coincident with the zones impacted with LNAPL.

Changes in the groundwater table elevations due to seasonal precipitation events appear to be related to the thickness of the high conductivity zone and its location relative to the groundwater table. Below the depth of the high pore water conductivities and into the saturation zone, no significant difference is observed. The depth regions of the high

estimated pore water conductivity may represent the smear zone as the LNAPL is repeatedly raised and lowered, smearing contamination along the vertical profile. Further, it is anticipated that water is displaced by the LNAPL in the smear zone; hence, the actual water saturation along the contaminated profiles would be lower than the water saturation at the equivalent depth along VRP 9. Therefore, the conductivity estimates calculated in this analysis are the minimum predicted value required to account for the field measurements.

The mechanism of this conductivity enhancement by microbially mediated processes of hydrocarbon degradation may explain the conductivity enhancement necessary. This result is contradictory to the insulating layer model and further explains the anomalous conductivities observed at this site and others in Michigan (Atekwana et al., 2002b; Sauck et al., 1998; Sauck, 2000).

3.5 Discussion and Conclusions

The results presented in this paper document over one year of VRP readings in six locations at a site impacted with LNAPL contamination. The conductivity versus elevation profiles at locations impacted with free phase LNAPL and residual phase LNAPL clearly show an electrical conductivity high coincident with the impacted sediment, contradicting the expected conductivity low predicted by the "insulating layer" model for LNAPL contamination. In fact, we observe the largest conductivities associated with free phase LNAPL, lesser conductivities at the residual phase LNAPL location, and the lowest conductivities at the location with no LNAPL contamination.

A simple analysis using Archie's Law reveals that the insulating layer model would require a large water saturation of over 130% at the contaminated locations to yield the conductivity profiles measured. This result is inconsistent with the expected displacement of water by LNAPL. Further analysis based on Archie's Law shows that increased pore water conductivity is necessary to produce the VRP field results from contaminated locations. Now the question remains, how is this conductivity enhancement occurring?

Previous studies at this site (Atekwana et al., 2002b; Sauck et al., 1998; Atekwana et al., 2000; Werkema et al., 2000) attribute the increased conductivity observed in the VRP profiles to the biogeochemical reactions occurring in the LNAPL-impacted zone. Specifically, an enhancement of the pore water total dissolved solids is the result of the biologically mediated degradation of the hydrocarbon source. Earlier studies have reported maximum oil degrading bacteria populations at the elevations coincident with the LNAPL contamination and the conductivity enhancements (Werkema et al., 2000; Duris et al., 2000; Duris et al., 2001). In particular, specific oil-degrading bacteria showed several orders of magnitude greater abundance at LNAPL impacted zones than the uncontaminated locations(Atekwana et al., 2002b). The production of acids as the microbes metabolize the hydrocarbon source and subsequent etching of the sediment grains would increase the total dissolved solids (TDS) in the pore water (Sauck, 2000; Werkema et al., 2000; Duris et al., 2000; Cassidy et al., 2001; Duris et al., 2001). Recent field measurements at the Carson City Park show average TDS values for the uncontaminated location to be 287.9 mg/L versus 698 mg/L for the contaminated locations (Atekwana et al., 2002a). Such an increase in the pore water conductivity due

to the increased TDS could easily increase the bulk conductivity measured geophysically in the field. Additionally this study(Atekwana et al., 2002a) also showed that the TDS could not account for all the observed conductivity, which supports the results shown in Figure 16, 17 and 18.

Additionally, biosurfactant production has been reported at the site coincident with the LNAPL contamination (Cassidy et al., 2001; Hudak, 2001; Cassidy et al., 2002). Biosurfactants can add to the total ion concentration thereby increasing conductivity. Biosurfactants also emulsify the hydrocarbons in the subsurface, providing electrical continuity through the free product LNAPL layer along water paths which contain excess TDS. The enhanced conductivity would then affect electrical resistivity and ground penetrating radar measurements (Sauck, 2000; Cassidy et al., 2001; Hudak, 2001).

Moreover, recent laboratory slurry reactor experiments provide evidence suggesting that LNAPL biodegradation under aerobic and anaerobic conditions can substantially change pore water biogeochemistry, producing dramatic increases in conductivity (Cassidy et al., 2001).

3.6 Implications

These results support that at a site of long term LNAPL contamination, in a predominately glacially derived sand and gravel geologic setting, the geoelectric response within the zone of LNAPL impaction is conductive rather than the traditionally accepted resistive layer. Specifically, this paper demonstrates that the zone of anomalously high conductivity occurs within and slightly above the water table fluctuation zone and not in the fully saturated zone. If this conductivity enhancement is the result of microbial

degradation of the LNAPL and the subsequent geochemical reactions, then the data indicate that the zone of most active degradation is within the fluctuating top of water saturation zone. These results are very significant in targeting the zone for remediation activities, sampling, and monitoring. Rather than focusing on the fully saturated zone, a more concerted effort should be made to sample within the zone of the fluctuating water table. It is in this zone where fresh recharged water is introduced into the system providing nutrients and oxygen for the microbial communities to flourish. The resulting physical changes, as observed in this study with simple DC resistivity, indicate an anomalous zone ripe for biogeochemical investigations.

Knight (2001) concedes that during laboratory experiments with organic contaminants, geophysicists have carefully controlled the physical and chemical conditions but completely neglected a control on or consideration of the biological conditions. It is through a more holistic approach including the contributions of the biological, chemical, and physical sciences that a comprehensive understanding of LNAPL-impacted sites and their long-term behavior will be possible.

Geochemists and/or hydrogeologists typically do not sample the fluctuating water table zone. Yet, this study clearly demonstrates that this is a geoelectrically active zone. The results presented here clearly point to this zone as the most active zone of degradation, assuming that the enhancement in conductivity is due entirely to degradation in the active zone of chemical weathering. Also, the flushing of this conductive zone through recharge events has significant implications for geochemical studies in the saturated zone, as the addition of ions from the water table fluctuating zone to the saturated zone below will influence geochemical measurements. The detection,

understanding, and monitoring of this anomalous conductive zone holds the key to understanding the dynamics at a site with unconsolidated sands and gravels impacted with LNAPL.

3.7 Acknowledgements

This work was funded in part by the AAPG Grants-In-Aid, NASA through the Michigan Space Grant Consortium, Western Michigan University Faculty Research and Creative Activities Support Fund, the Doctoral Dissertation Fellowship through the Graduate College at Western Michigan University, and the American Chemical Society-Petroleum Research Fund Grant (PRF No. 31594-AC2). Geophysical equipment used during this study was funded through a NSF Grant DUE-9550974. We also thank Joe Duris, Tyler Knoll, Andy Nichols and Jeff Locey for excellent technical assistance.

3.8 References

Archie, G. E. The Electrical Resistivity Log as an Aid in Determining Some Reservoir Characteristics. Transactions of the American institute of Mining, Metallurgical and Petroleum Engineers, 146, 54-62. 1942.

Atekwana, E., Rowe, R. S., Atekwana, E. A, Werkema, D. D., and Legall, F. D. Total Dissolved Solids in Groundwater and its Relationship to Bulk Conductivity of Soils Contaminated with Hydrocarbon. Journal of Environmental and Engineering Geophysics, in review. 2002a.

Atekwana, E. A. unpublished data, personal communication. 2002.

Atekwana, E. A, Sauck, W. A., and Werkema, D. D. Investigations of geoelectrical signatures at a hydrocarbon contaminated site. Journal of Applied Geophysics, 44, 167-180. 2000.

Atekwana, E. A, Werkema, D. D., Duris J.D., Rossbach S., Atekwana, E. A, Sauck, W. A., and Cassidy, D. P. *In situ* Apparent Resistivity measurements and Microbial

population distribution at a Hydrocarbon Contaminated Site: Implications for Assessing Natural Attenuation. Geophysics, In review. 2002b.

Atekwana, E. A., Sauck, W. A., and Werkema, D. D. Characterization of a Complex Refinery Groundwater Contaminant Plume using Multiple Geoelectric Methods. Proceedings of the Symposium on the Application of Geophysics to Engineering and Environmental Problems (SAGEEP '98), 427-436. 1998.

Baedecker, M. J., Cozarelli, I. M, and Eganhouse, R. P. The composition and fate of hydrocarbons in a shallow glaical-outwash aquifer. United States Geological Survey Open File Report, 87-109. 1987.

Baedecker, M. J., Cozarelli, I. M, Eganhouse, R. P., Siegel, D. I., and Bennett, P. C. Crude oil in a shallow sand and gravel aquifer: III. Biogeochemical reactions and mass balance modeling in anoxic groundwater. Applied Geochemistry, 8, 569-586. 1993.

Bennett, P. C., Siegel, D. I., Baedecker, M. J., and Hult, M. F. Crude oil in a shallow sand and gravel aquifer: I. Hydrogeology and inorganic geochemistry. Applied Geochemistry, 8, 529-549. 1993.

Benson, A. K. and Mustoe, N. B. Integration of Electrical Resistivity, Ground-Penetrating Radar, and Very Low-Frequency Electromagnetic Induction Surveys to Help Map Groundwater Contamination Produced by Hydrocarbons Leaking from Underground Storage Tanks. Environmental Geosciences, 5, 61-67. 1998.

Benson, A. K., Payne, K. L., and Stubben, M. A. Mapping Groundwater Contamination using DC Resistivity and VLF Geophysical Methods - A Case Study. Geophysics, 62[1], 80-86. 1997.

Benson, A. K. and Stubben, M. A. Interval resistivities and very low frequency electromagnetic induction - an aid to detecting groundwater contamination in space and time: a case study. 0. Environmental Geosciences, 2, 74-84. 1995.

Bermejo, J. L, Sauck, W. A., and , Atekwana E. A. Geophysical Discovery of a New LNAPL Plume at the Former Wurtsmith AFB, Oscoda, Michigan. Ground Water Monitoring & Remediation, XVII[4], 131-137. 1997.

Blacic and Arulanandan, K. Identification of Contaminated Soils by Dielectric Constant and Electrical Conductivity. Journal of Environmental Engineering, 103-105. 1999.

Campbell, D. L., Lucius, J. E., Ellefson, K. J., and Desczcs-Pan, M. D. Monitoring of a Controlled LNAPL Spill Using Ground Penetrating Radar. Proceedings of the Symposium on the Application of Geophysics to Engineering and Environmental Problems (SAGEEP '96), Keystone, Colorado, 511-517. 1996.

Cassidy, D. P., Hudak, A., Werkema, D. D., Atekwana, E., Rossbach S., Duris, J. W., Atekwana, E. A, and Sauck, W. A. *In Situ* Rhamnolipid Production At An Abandoned Petroleum Refinery. Soil and Sediment Contamination: an International Journal, In press. 2002.

Cassidy, D. P., Werkema, D. D., Sauck, W. A., Atekwana, E. A., Rossbach, S., and Duris, J. The effects of LNAPL biodegradation products on electrical conductivity measurements. Journal of Environmental and Engineering Geophysics, 6, 47-52. 2001.

Cozzarelli, I. M, Eganhouse, R. P., and Baedecker, M. J. Transformation of monoaromatic hydrocarbons to organic acids in anoxic groundwater environment. Environmental Geology and Water Science, 16[2], 135-141. 1990.

Daniels, J. J., Roberts, D., and Vendl, M. Site Studies of Ground Penetrating Radar for Monitoring Petroleum Product Contaminants. Proceedings of the Symposium on the Application of Geophysics to Engineering and Environmental Problems (SAGEEP '92), Oak Brook IL., 597-609. 1992.

De Ryck, S. M., Redman, J. D., and Annan, A. P. Geophysical Monitoring of a Controlled Kerosene Spill. Proceedings of the Symposium on the Application of Geophysics to Engineering and Environmental Problems (SAGEEP'93), San Diego, CA, 5-20. 1993.

Dell Engineering. Recovery System Performance Evaluation at the Refinery Site, Crystal Refining Company, Carson City, Michigan. Dell Engineering, Inc., September, 1991, Project No.90200. 1991.

Dell Engineering. Remedial Action Plan for Crystal Refining Company, 801 North Williams Street, Carson City, MI. Report DEI No.921660, Holland, Michigan. 1992.

Duris, J. W., Werkema, D. D., Atekwana A., Eversole, R., Beuving, L., and Rossbach S. Microbial Communities and Their Effects on Silica Structure & Geophysical Properties in Hydrocarbon Impacted Sediments. Geological Society of America Annual Meeting Abstracts, Reno, NV, A190. 2000.

Duris, J. W., Werkema, D. D., Davis, J., Eversole, R., Beuving, L., Atekwana A., and Rossbach S. Shifts in Microbial Community Structure in Hydrocarbon Impacted Sediments Associated with Alterations in Physical Parameters of Soil. Abstracts: American Society for Microbiology 101st General Meeting.ASM Press, Washington D.C., 655. 2001.

Eganhouse, R. P., Baedecker, M. J., Cozarelli, I. M, Aiken, G. R., Thorn, K. A., and Dorsey, T. F. Crude oil in a shallow sand and gravel aquifer: II. Organic geochemistry. Applied Geochemistry, 8, 551-567. 1993.

Endres, A. L. and Redman, J. D. Modelling the Electrical Properties of Porous Rocks and Soils Containing Immiscible Contaminants. Journal of Environmental and Engineering Geophysics, 0, 105-112. 1996.

Fetter, C. W. Contaminant Hydrogeology. 1, 225-231. 1993.

Gajdos, V. and Král, V. Influence of hydrocarbon pollution to soil conductivity. Proceedings of the Symposium on the Application of Geophysics to Engineering and Environmental Problems (SAGEEP '95), 785-789. 1995.

Groncki, J. M. Calibration, installation techniques, and initial measurements for vertical resistivity probes in hydrogeologic investigations. M.S.Thesis, -122. 1999.

Hudak, A. In situ biosurfactant production at Carson City Park, MI. M.S.Thesis, Western Michigan University. 2001.

Kelly, B. F. J. Electrical Properties of Sediments and the Geophysical Detection of Ground-Water Contamination. abstract of Ph.D.thesis, Department of Water Engineering, School of Civil Engineering, The University of New South Wales, Sydney, Australia, published in Ground Water, 43. 1996.

King, M. L. Locating a subsurface oil leak using ground penetrating radar. 8th International Conference on Ground Penetrating Radar, Bellingham, WA., 346-350. 2000.

Knight, R. Hysteresis in the electrical resistivity of partially saturated sandstones. Geophysics, 56[12], 2139-2147. 1991.

Knight, R. Ground Penetrating Radar for Environmental Applications. Annual Review Earth and Planetary Science, 29, 229-255. 2001.

Legall, F. D. unpublished data, personel communication. 2002.

Lucius, J. E. Detectability of Crude Oil in the Subsurface near Bemedji, Minnesota, using Ground Penetrating Radar. Proceedings of the Symposium on the Application of Geophysics to Engineering and Environmental Problems (SAGEEP'00), Arlington, Virginia, 311-319. 2000.

Maxwell, M and Schmok, J. Detection and Mapping of an LNAPL Plume using GPR: A Case Study. Proceedings of the Symposium on the Application of Geophysics to Engineering and Environmental Problems (SAGEEP '95), 15-23. 1995.

Mazác, O., Benes, L., Landa, I., and Maskova, A. Determination of the extent of oil contamination in groundwater by geoelectrical methods. Geotechnical and Environmental Geophysics, vol II, S.H.Ward editor, 107-112. 1990. Tulsa, OK, Society of Exploration Geophysicists.

McMahon, P. B., Vroblesky, D. A., Bradely, P. M., Chapelle, F. H., and Gullet, C. D. Evidence for enhanced mineral dissolution in organic acid-rich shallow ground water. Ground Water, 33[2], 207-216. 1995.

Monier-Williams, M. Properties of light non-aqueous phase liquids and detection using commonly applied shallow sensing geophysical techniques. Proceedings of the Symposium on the Application of Geophysics to Engineering and Environmental Problems (SAGEEP '95).Orlando, FL, 1-13. 1995.

Olhoeft, G. R. Direct Detection of Hydrocarbon and Organic Chemicals with Ground Penetrating Radar and Complex Resistivity. Proceedings of the NWWA/API Conference on Petroleum Hydrocarbons and Organic Chemicals in Ground Water-Prevention Detection and Restoration. 1986.

Osiensky, J. L. Ground Water Modeling of mise-a-la-masse Delineation of Contaminated Ground Water Plumes. Journal of Hydrology, 146-165. 1997.

Redman, J. D., De Ryck, S. M, and Annan, A. P. Detection of LNAPL Pools with GPR: Theoretical Modelling and Surveys of a Controlled Spill. Proceedings of the Fifth International Conference on Ground Penetrating Radar (GPR'94), Kitchener, Ontario, 1283-1294. 1994.

Sauck, W. A. A model for the resistivity structure of LNAPL plumes and their environs in sandy sediments. Journal of Applied Geophysics, 44/2-3, 151-165. 2000.

Sauck, W. A., Atekwana, E. A., and Nash, M. S. High Conductivities Associated with an LNAPL Plume Imaged by Integrated Geophysical Techniques. Journal of Environmental and Engineering Geophysics, Vol. 2, No. 3, 203-212. 1998.

Schön, J. H. Physical Properties of Rocks: Fundamentals and Principles of Petrophysics. 1996. Tarrytown: Pergamon.

Snell Environmental Group. Technical Memorandum Task 1B-IRAP Evaluation, Crystal Refinery, Carson City, Michigan, MERA ID #59003. 1994. Michigan Department of Natural Resources, Grand Rapids District Office.

Swanson, B. F. Rationalizing the Influence of Crude Wetting on Reservoir Fluid Flow with Electrical Resistivity Behavior. Journal of Petroleum Technology, 1459-1464. 1980.

Telford, W. M., Geldart, L. P., and Sheriff, R. E. Applied Geophysics . Second, 558. 1990. Cambridge University Press.

Werkema, D. D., Atekwana, E.A., Sauck W. A., and Asumadu, J. A Versatile Windows Based Multi-Electrode Acquisition System for DC Electrical Methods Surveys. Environmental Geosciences, 5[4], 196-206. 1998.

Werkema, D. D., Atekwana A., Sauck, W., Rossbach.S., and Duris J. Vertical Distribution of Microbial Abundances and Apparent Resistivity at an LNAPL Spill Site. Proceedings of the Symposium on the Application of Geophysics to Engineering and Environmental Problems (SAGEEP 2000). 2000.

Table 1. Date Ranges of VRP Measurements for This Study.

VRP #	*Dates*	*Days*
1	10/19/97 – 11/6/00	1 – 1104
2	2/15/98 – 10/16/00	120 – 1083
3	3/27/99 – 10/16/00	518 – 1083
4	3/20/99 – 10/16/00	511 – 1083
5	4/17/99 – 11/06/00	539 – 1104
6	3/20/99 – 10/16/00	511 – 1083
7	4/17/99 – 10/16/00	539 – 1083
8	3/27/99 – 10/16/00	518 – 1083
9	8/18/99 – 11/06/00	658 – 1104
10	8/18/99 – 11/06/00	658 – 1104

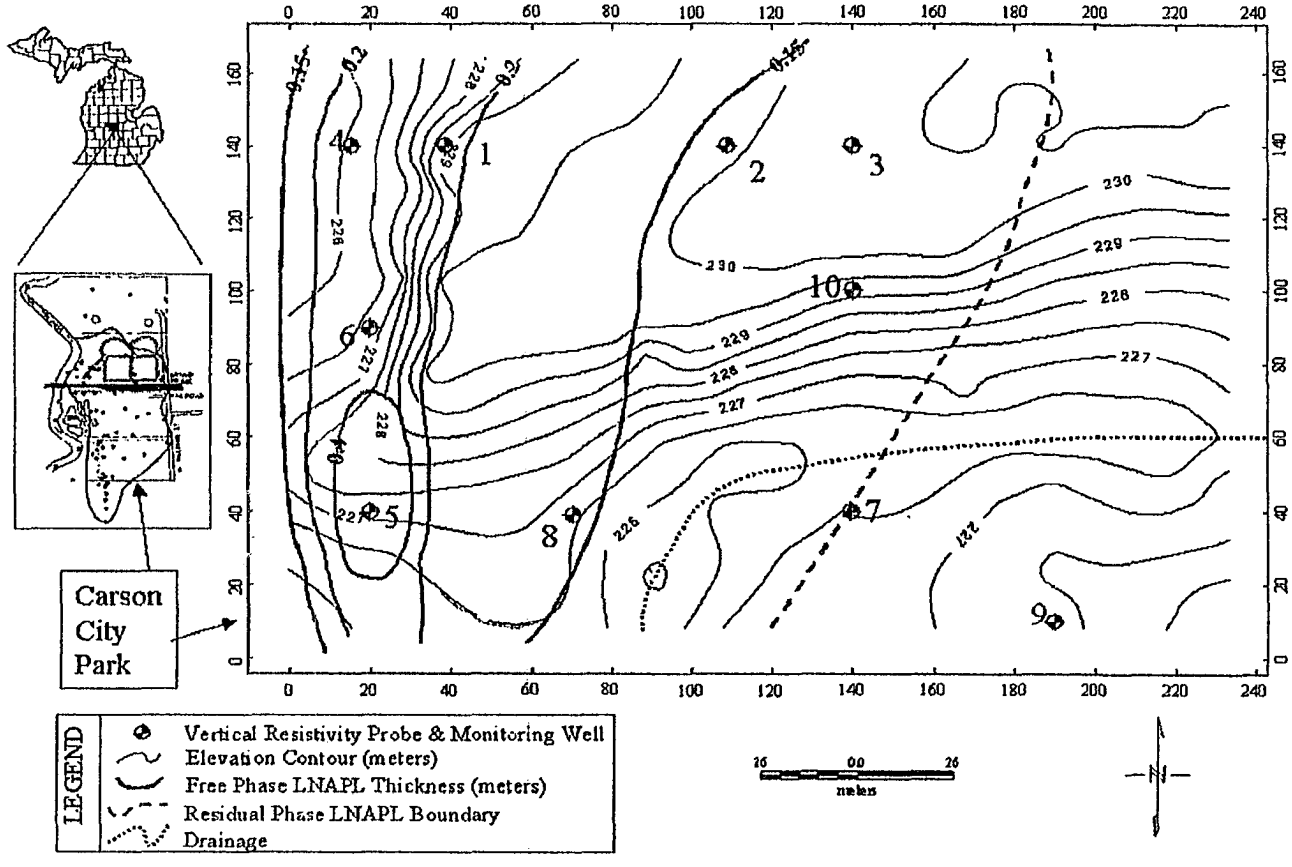

Figure 1. Site Map – Carson City Park, Carson City, Michigan USA. (43°07'11" N Latitude, 84°51'15" W Longitude). Site map includes regional setting, topography, LNAPL contamination levels and relevant surface features.

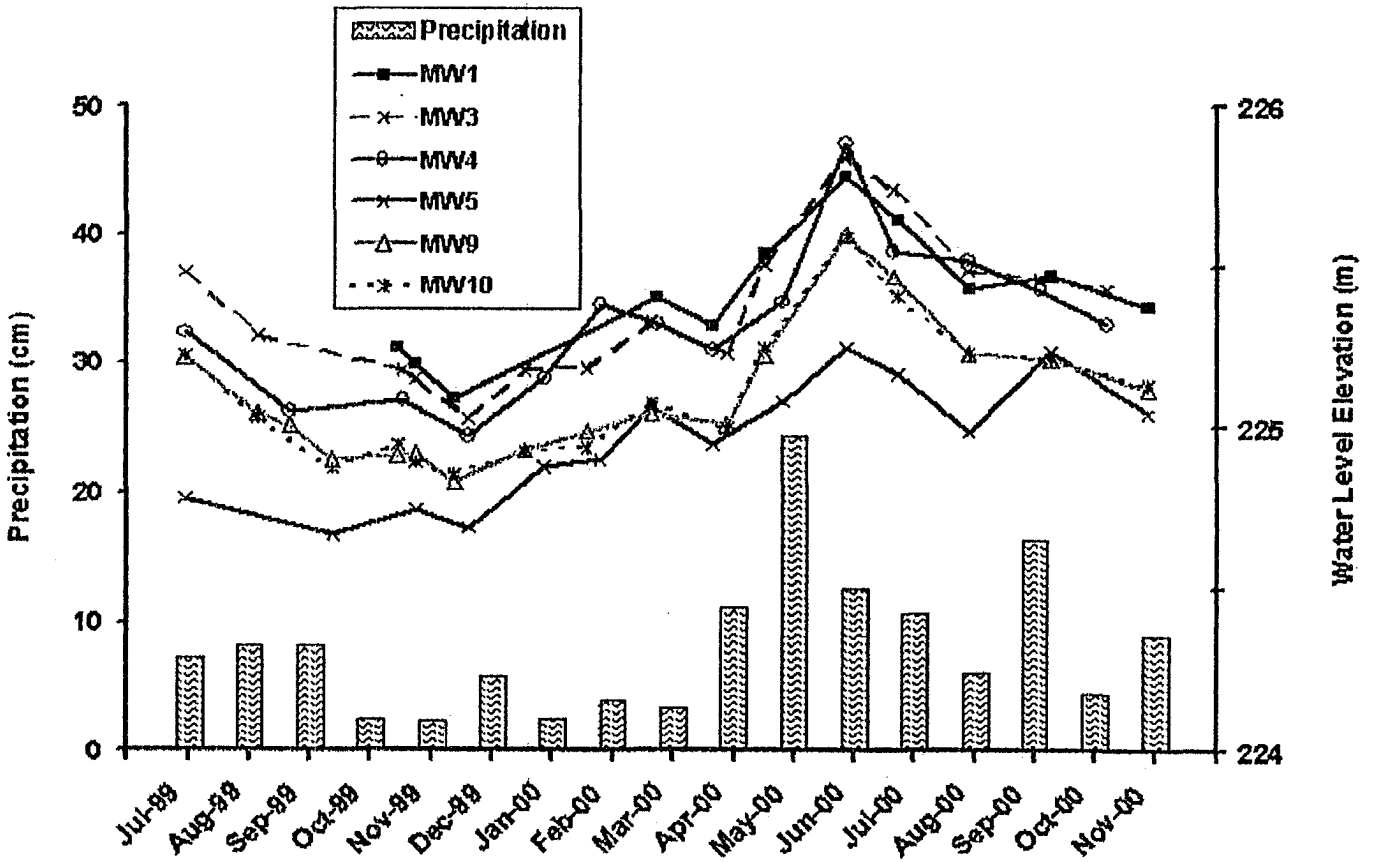

Figure 2. Static Water Level as Measured from 1" Monitoring Wells and Precipitation from July 1999 to November 2000.

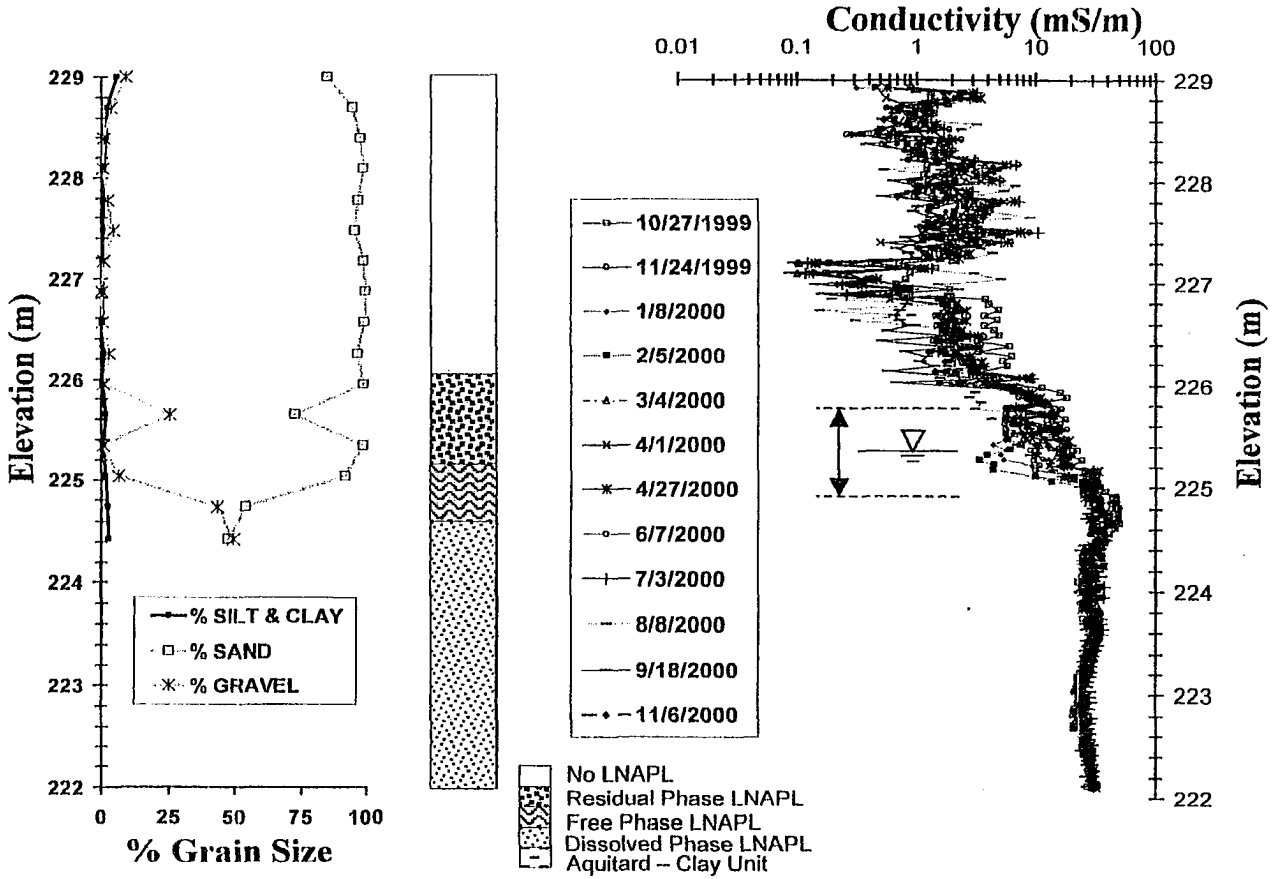

Figure 3. VRP 1, Free Phase LNAPL Location, Grain Size, LNAPL Distribution with Elevation and VRP Measurements Converted to Conductivity.

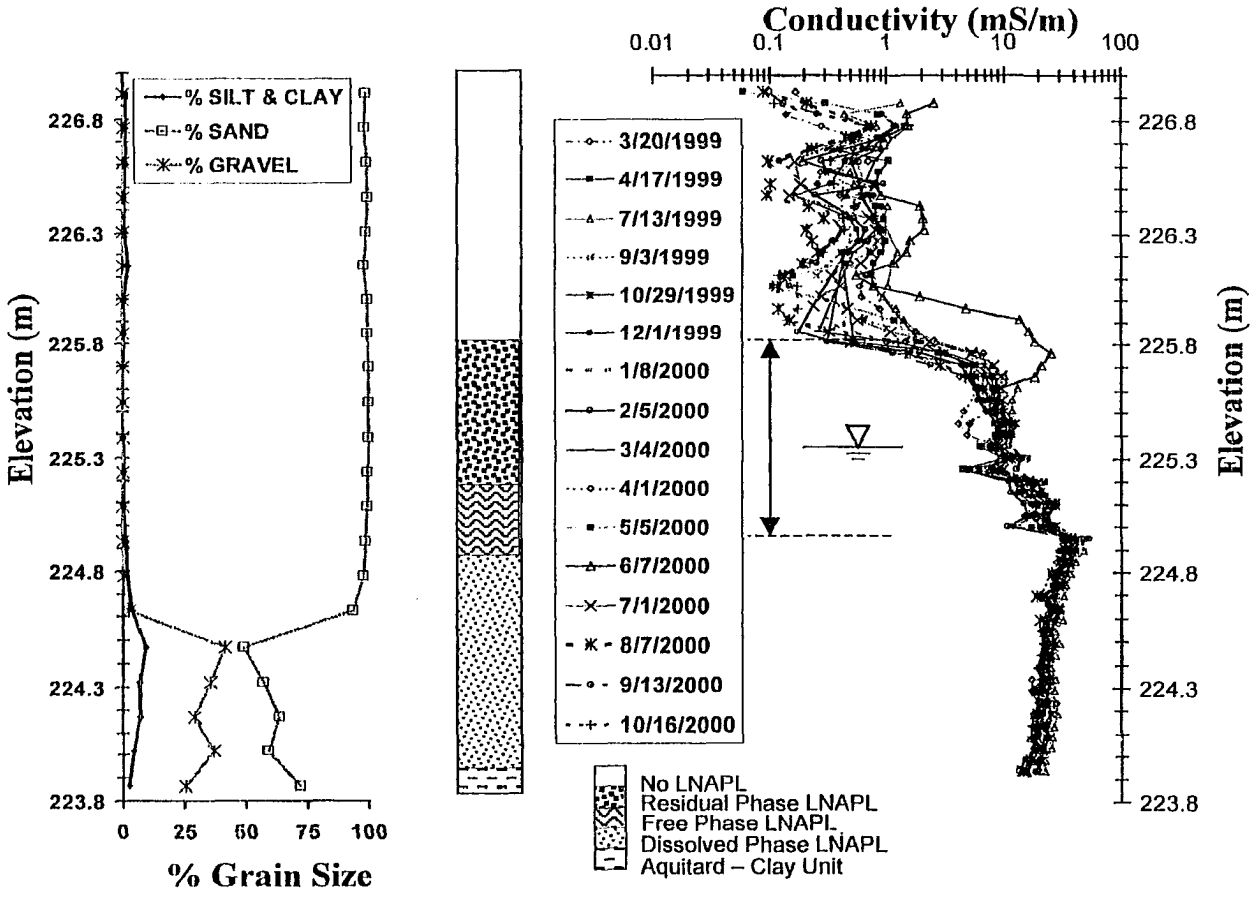

Figure 4. VRP 4, Free Phase LNAPL Location, Grain Size, LNAPL Distribution with Elevation and VRP Measurements Converted to Conductivity.

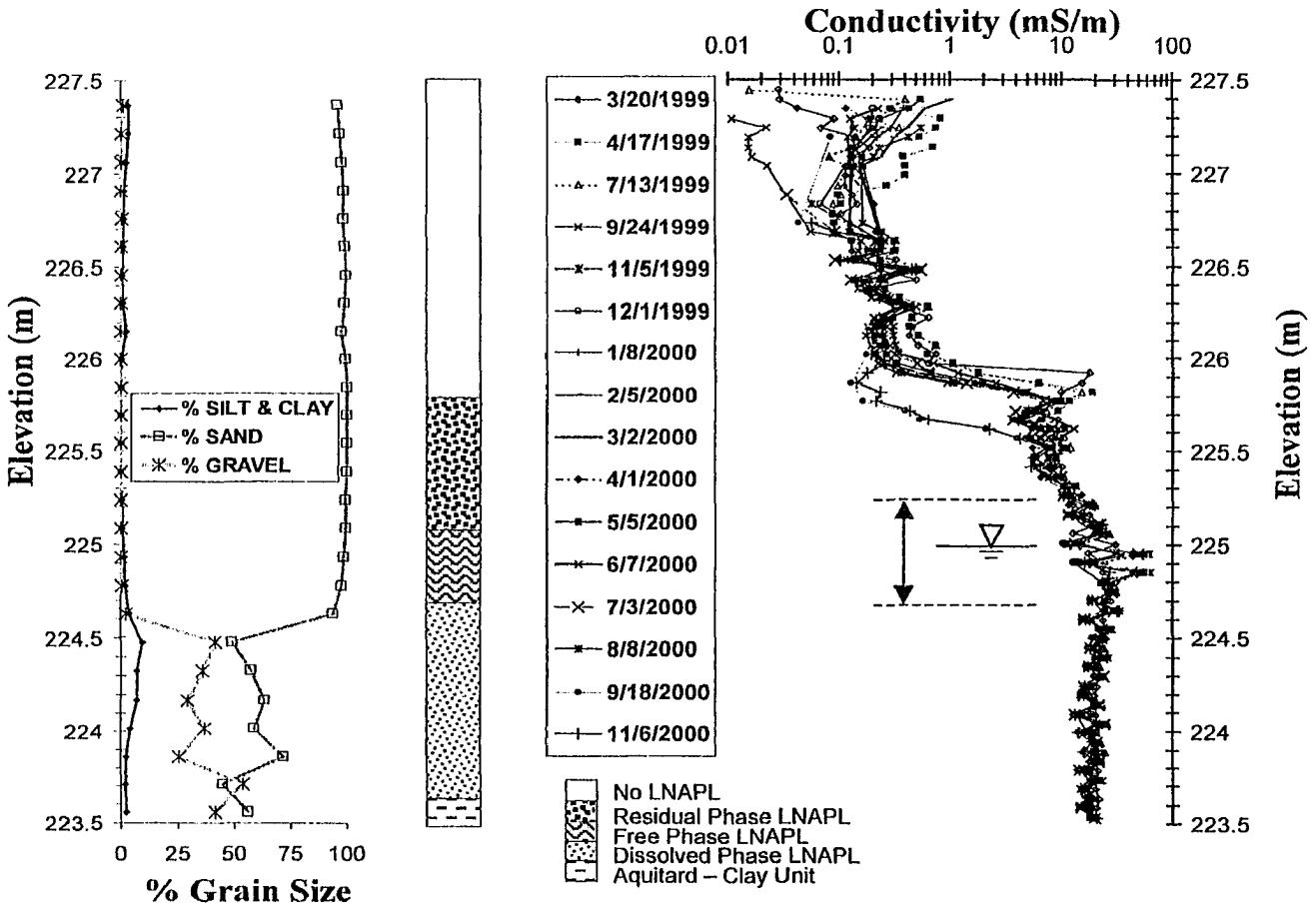

Figure 5. VRP 5, Free Phase LNAPL Location, Grain Size, LNAPL Distribution with Elevation and VRP Measurements Converted to Conductivity.

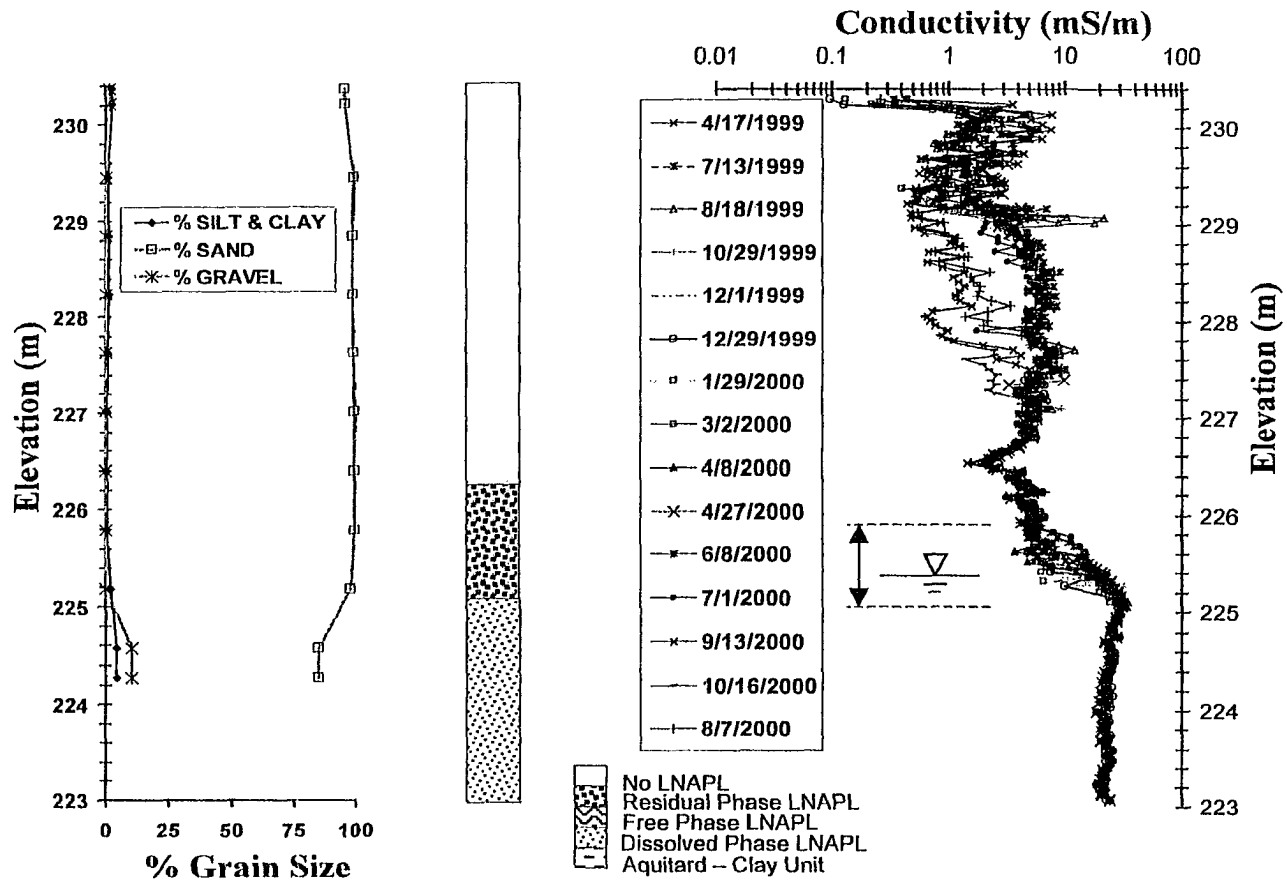

Figure 6. VRP 3 Residual Phase LNAPL Location, Grain Size, LNAPL Distribution with Elevation and VRP Measurements Converted to Conductivity.

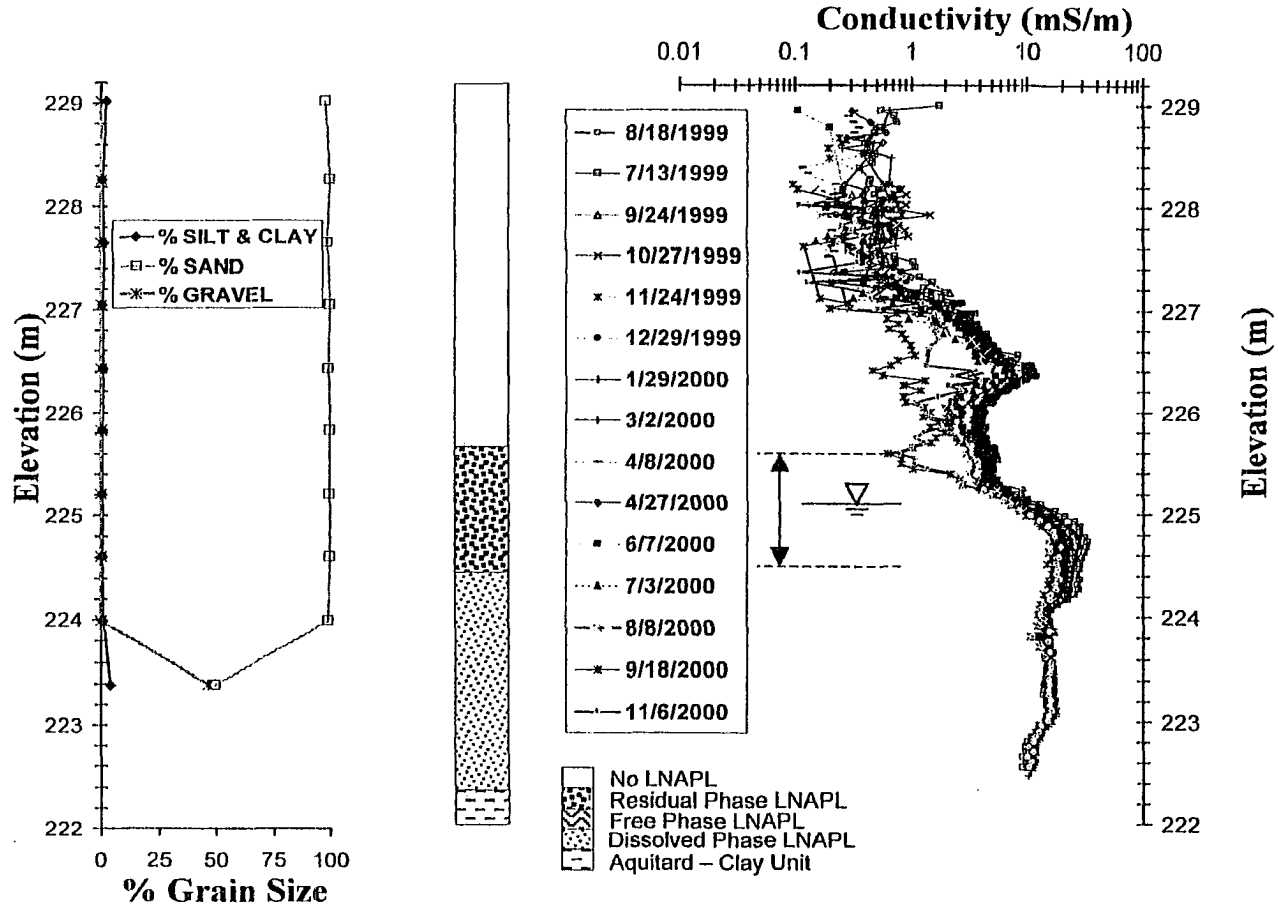

Figure 7. VRP 10, Residual Phase LNAPL Location, Grain Size, LNAPL Distribution with Elevation and VRP Measurements Converted to Conductivity.

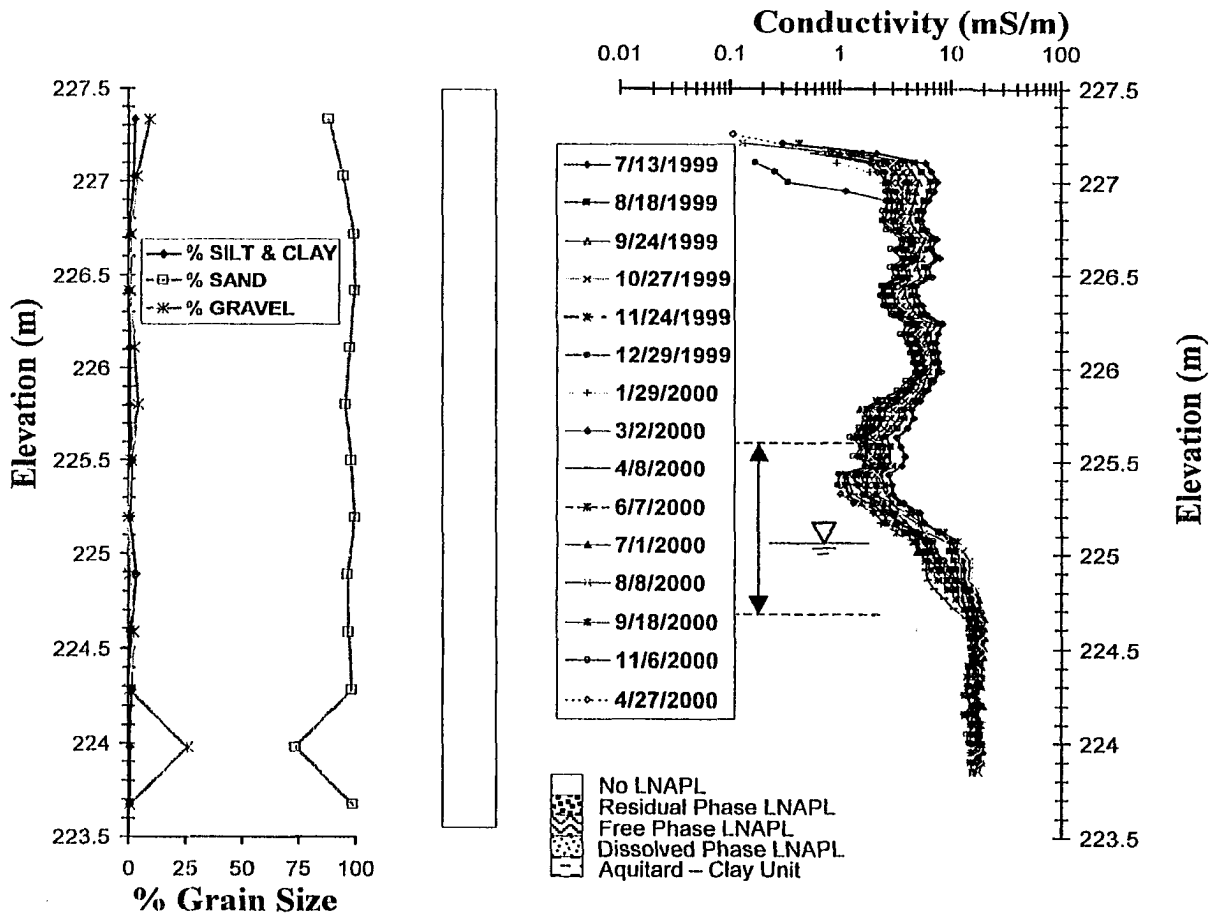

Figure 8. VRP 9, No LNAPL Contamination, Grain Size, and VRP Measurements Converted to Conductivity.

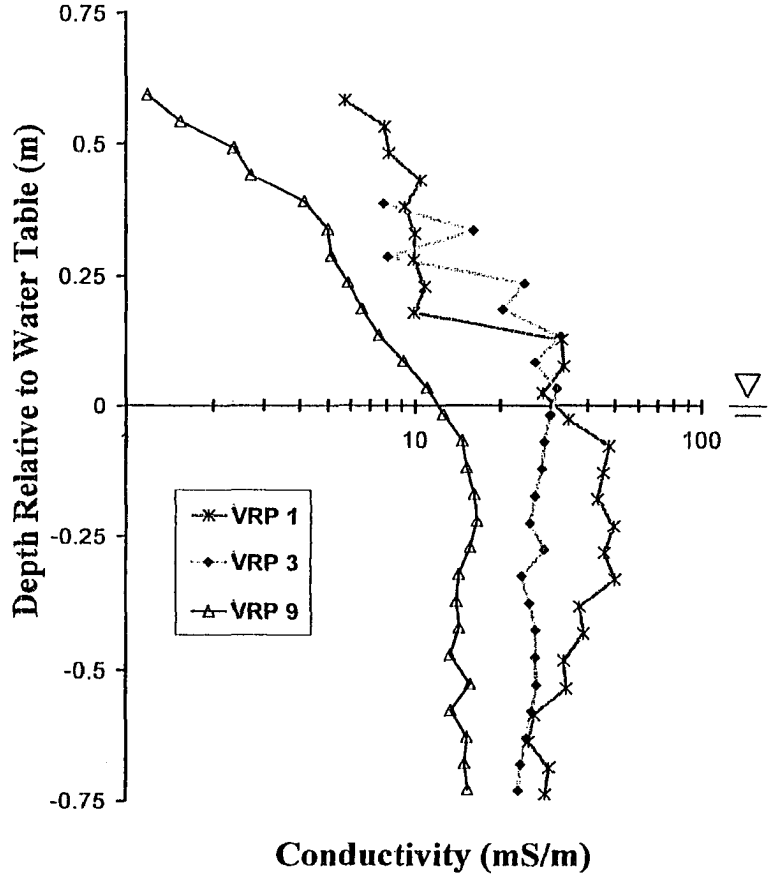

Figure 9. Comparison of the Conductivities for the Three LNAPL Cases (Free-product, Residual Product, and Uncontaminated) on December 1, 1999. (Vertical scales have been referenced to the water table.)

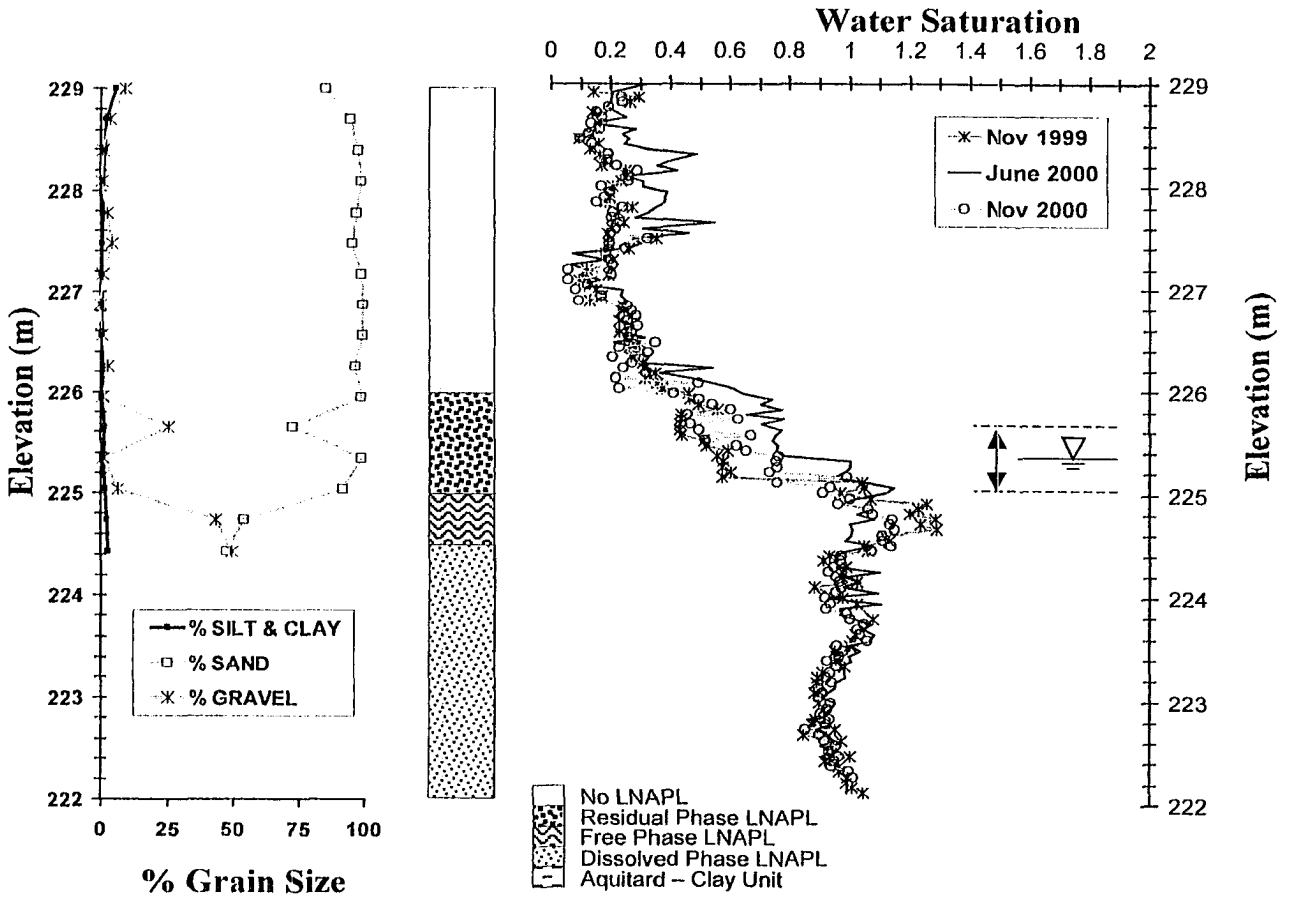

Figure 10. VRP 1, Free Phase LNAPL Location. Estimated Water Saturation (Sw) from Archie's Law to Explain the Anomalous Conductivity.

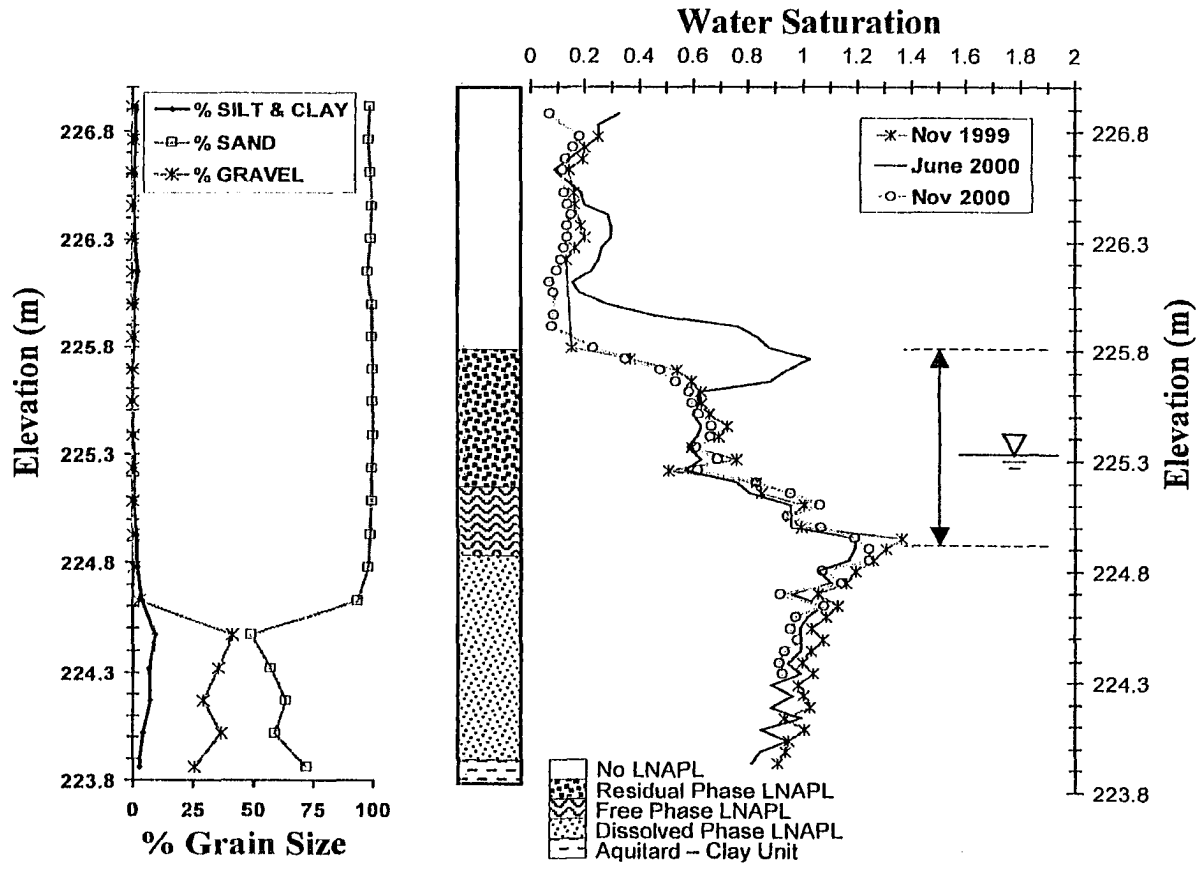

Figure 11. VRP 4, Free Phase LNAPL Location. (Estimated Water Saturation (Sw).)

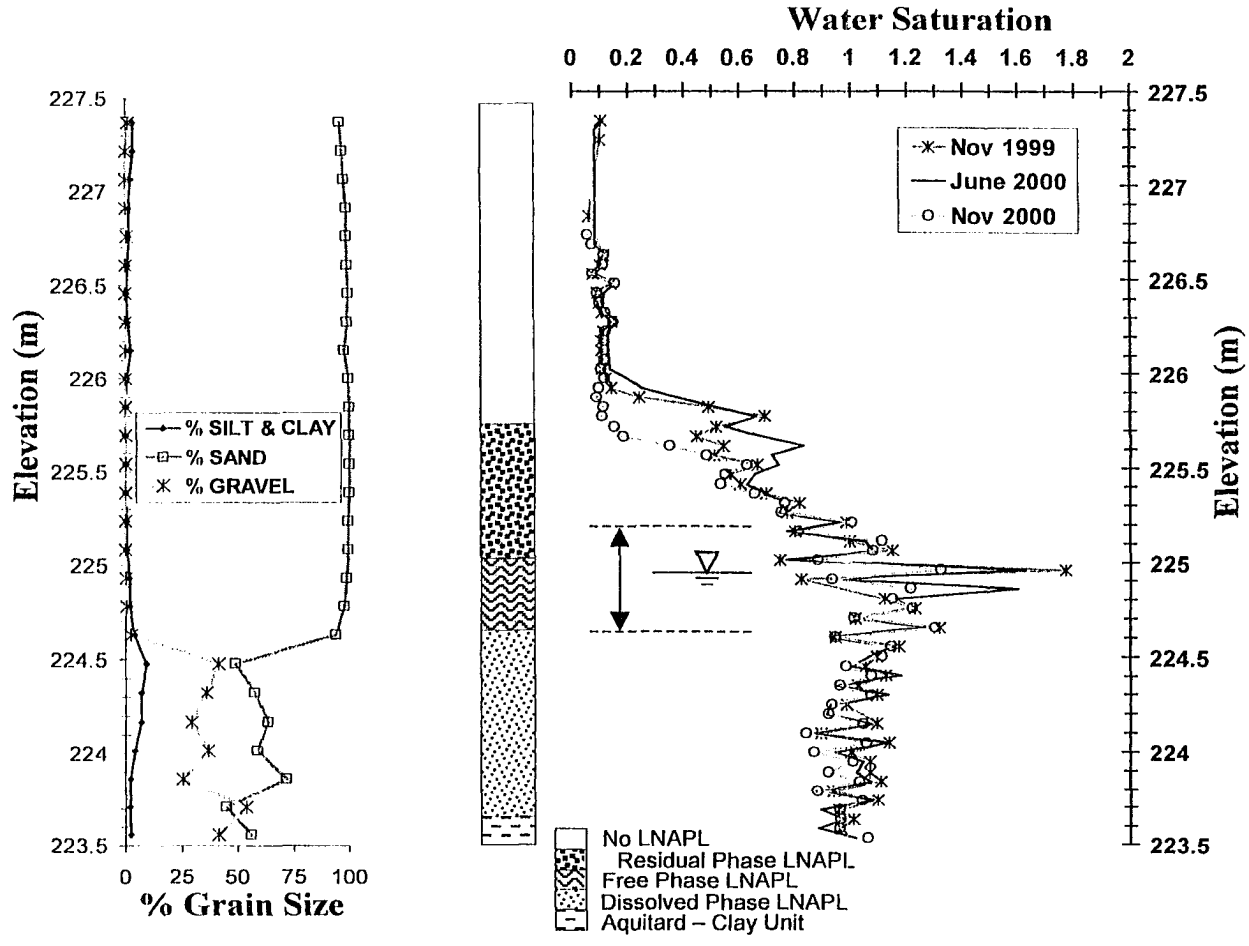

Figure 12. VRP 5, Free Phase LNAPL Location. (Estimated Water Saturation (Sw).)

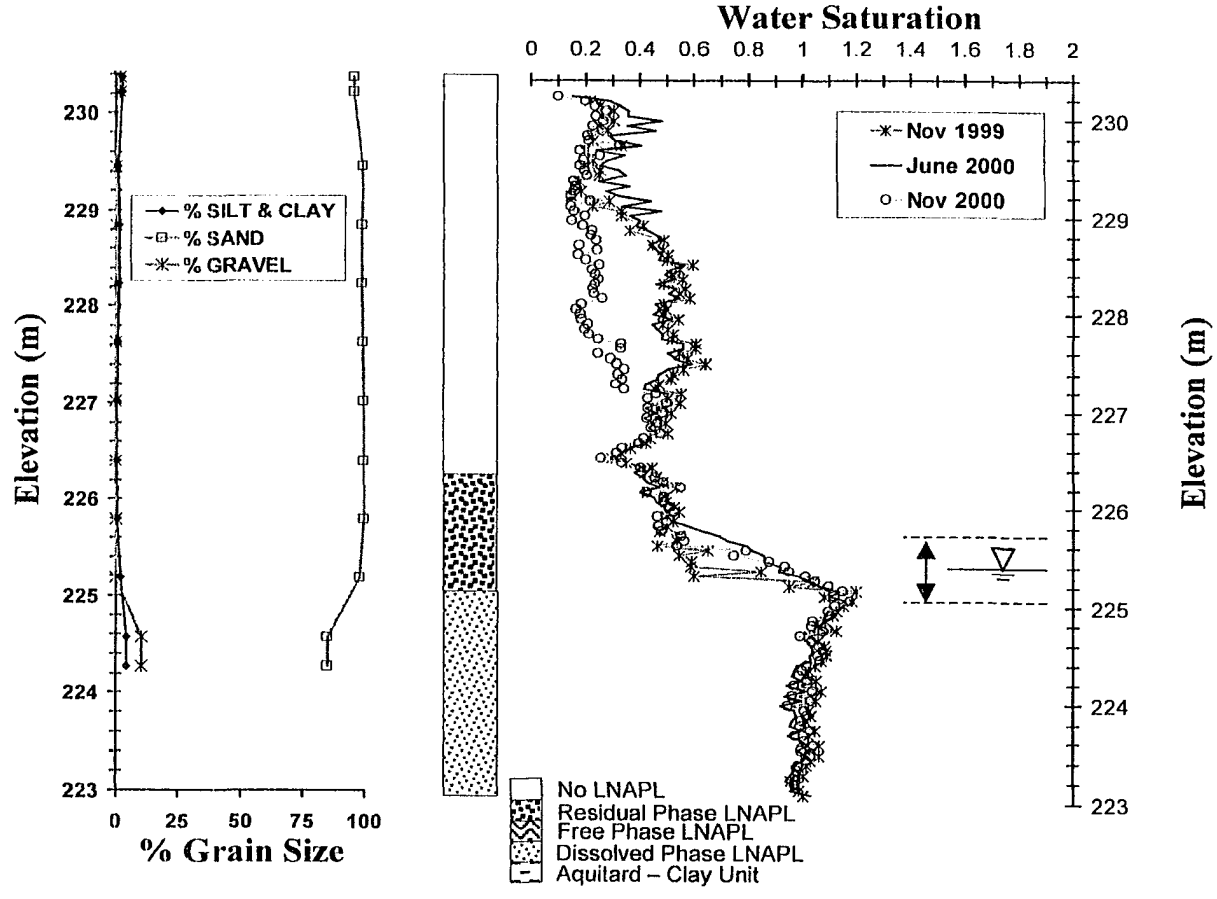

Figure 13. VRP 3, Residual Phase LNAPL Location. (Estimated Water Saturation (Sw).)

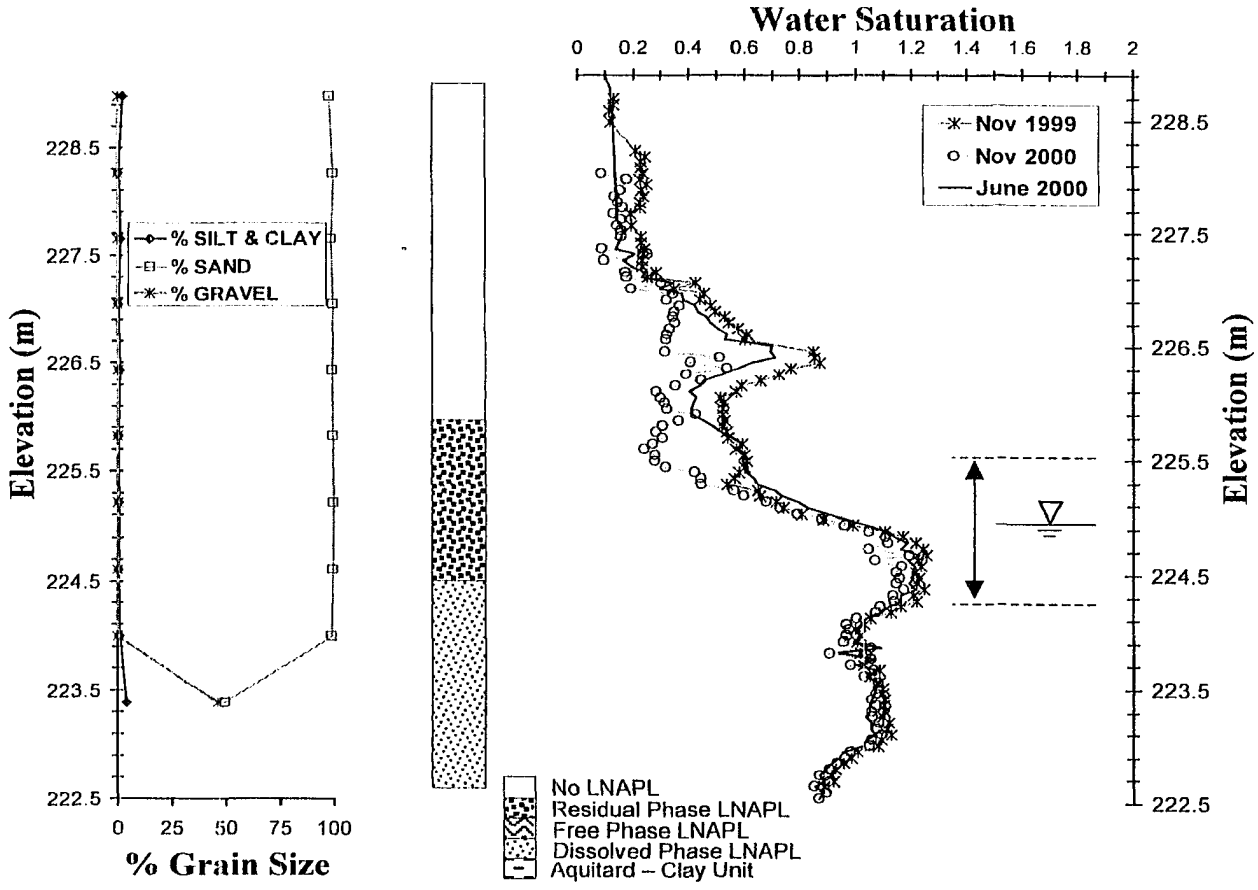

Figure 14. VRP 10, Residual Phase LNAPL Location. (Estimated Water Saturation (Sw).)

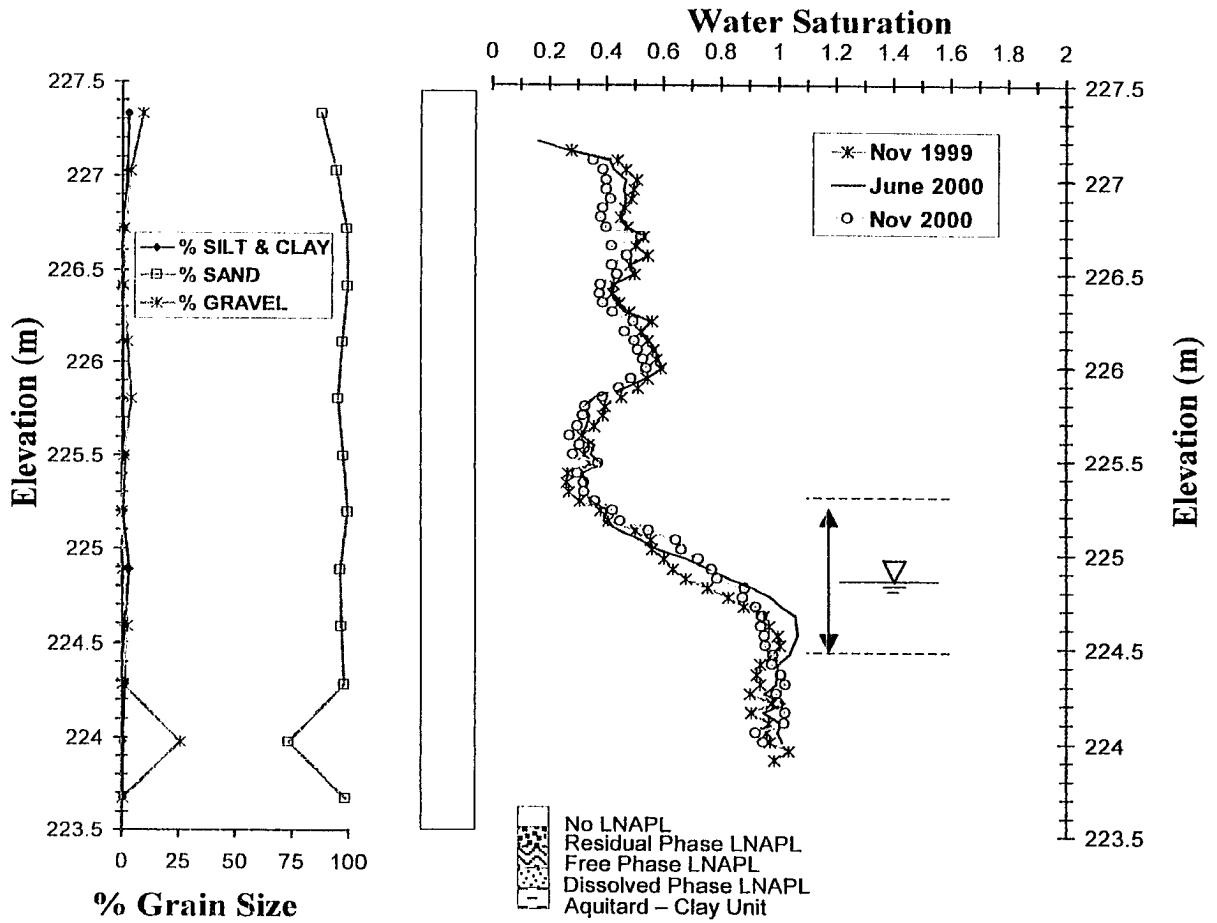

Figure 15. VRP 9, No LNAPL Location. (Estimated Water Saturation (Sw).)

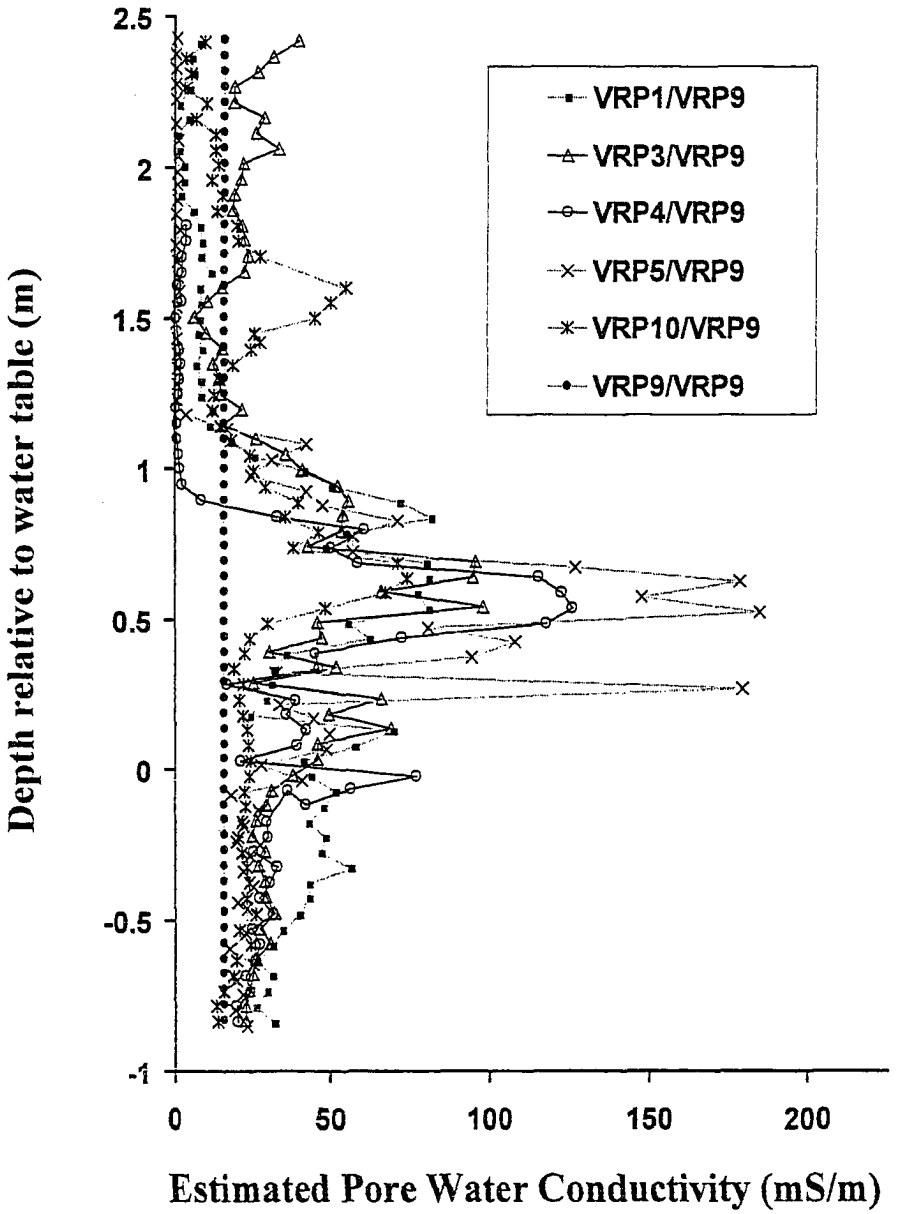

Figure 16. November 1999 Estimated Pore Water Conductivity Enhancement to Explain the Anomalous Conductivity.

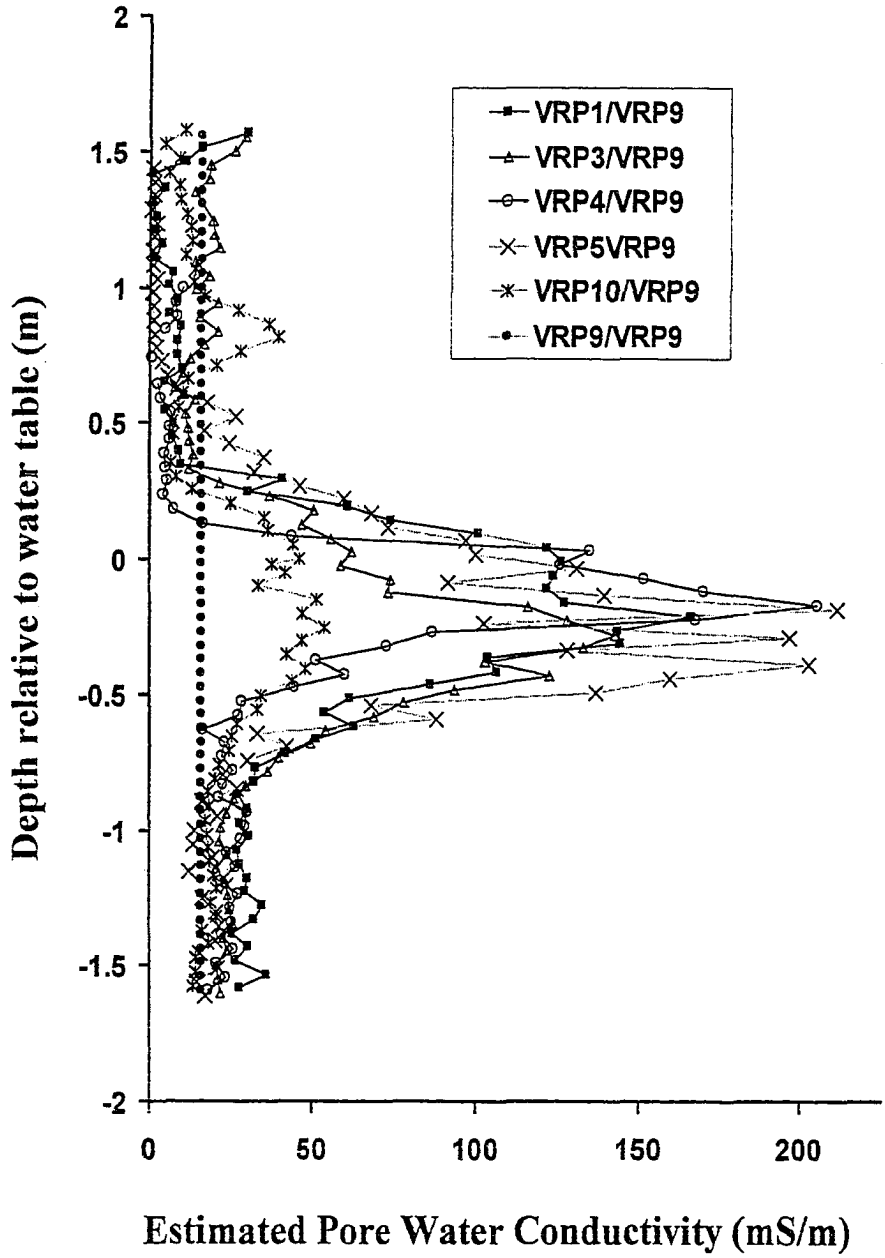

Figure 17. June 2000 Estimated Pore Water Conductivity Enhancement.

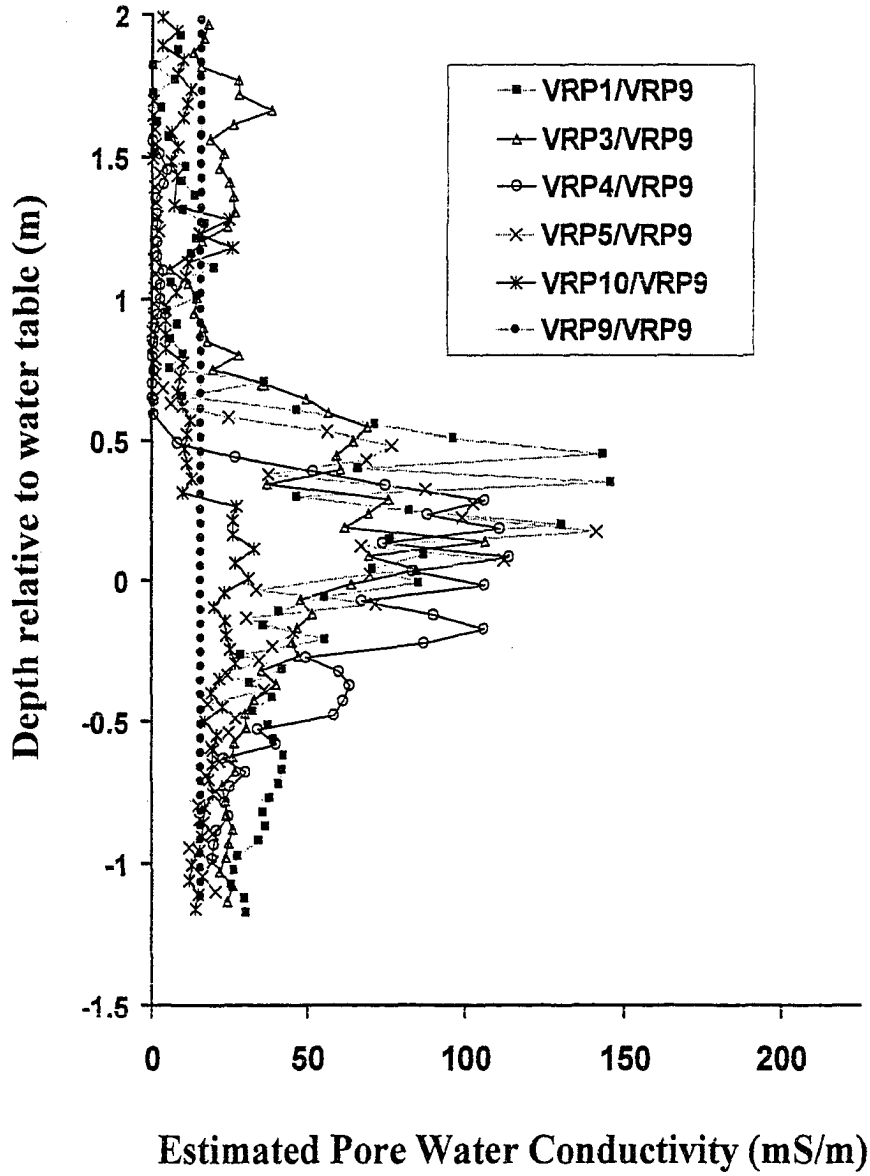

Figure 18. November 2000 Estimated Pore Water Conductivity Enhancement.

CHAPTER 4

SPATIAL AND TEMPORAL VARIATIONS IN THE GEOELECTRICAL RESPONSE AT A HYDROCARBON CONTAMINATED SITE

4.1 Introduction

Groundwater contamination by light non-aqueous phase liquids (LNAPLs) remains a major problem in the United States of America today. Over the past several years, natural attenuation (microbial mediated degradation) has become increasingly accepted as a remedial alternative for many sites contaminated with LNAPLs, partly because of the relatively lower costs.

Since 1995, the number of sites using natural attenuation for contamination with benzene, toluene, ethylbenzene, and xylene (BTEX) has grown significantly. Nonetheless, the documentation and success of natural attenuation often requires a substantial degree of understanding of the subsurface processes. As a result, the main expense at contaminated sites will shift from the design and operation of active remediation systems to detailed investigations and monitoring of the site-specific contamination and geologic setting. The main goal is to understand the natural dynamic groundwater flow and the biogeochemical processes controlling the fate of contaminants. Additionally, the cause and effect relationship between the loss of contaminant and the mechanism responsible for the natural degradation is critical to establish (Bekins et al., 2001). All of these processes occur within dynamic systems where the geochemical and hydrogeological conditions are changing with time and location in the subsurface. For

example, it is well documented that hydrocarbon compounds (BTEX) can partition in the subsurface into vapor, residual, free product and dissolved phases. Dynamic hydrologic processes such as fluctuations in the water table can affect the concentrations of these contaminant phases and their vertical positions; in turn, these factors affect the degradation of the contaminant (Mercer and Cohen, 1990). These dynamic changes challenge traditional means of studying LNAPL natural attenuation in field settings which rely heavily on invasive sampling methodologies (e.g. soil, fluid and gas samples from drilled boreholes and monitoring wells). Also, the zone that is most impacted by the dynamic hydrologic changes (i.e. the smear zone) is often the least understood region because of difficulties encountered by traditional techniques. In particular, monitoring wells can only sample from the saturated zone; multi-level lysimeters, which can sample the soil moisture, are rarely used. Therefore, biogeochemical processes occurring within this smear zone are only partially understood. Furthermore, the effects of changing water levels on contaminant degradational activities and the physical properties of the contaminant are fundamentally not properly or well understood (Strachan and Wolfe, 2001). Such difficulties necessitate the development of alternative, more cost effective methodologies to properly address this problem.

4.1.1 The Role of Geophysics

Geophysical techniques have commonly been applied at remediation sites mostly for site characterization and determination of contaminant distribution (Daniels et al., 1992; Maxwell and Schmok, 1995; Benson et al., 1997; Bermejo et al., 1997; Vanhala, 1997). In some cases, they have been used to monitor active remediation programs such

as air sparging (Schima et al., 1996) and steam injection (Newmark, 1994; LaBrecque et al., 1998). However, their use in the assessment of intrinsic bioremediation and or biogeochemical changes has not been realized. However, recent geophysical investigations are beginning to demonstrate the important influence that biodegradational processes have on the geoelectrical properties at such sites (Atekwana et al., 2002; Sauck, 2000; Werkema et al., 2000; Duris et al., 2000; Cassidy et al., 2001). These studies show high anomalous conductivity zones coincident with zones of contamination, suggesting a relationship between the high conductivities and processes of biodegradation. Such relationships have been given much credence by the discovery of high oil-degrading microbial populations coincident with zones of both LNAPL contamination and high conductivities (Atekwana et al., 2002; Werkema et al., 2000; Duris et al., 2000). These studies further show significant etching and pitting of soil grains within these conductive zones (e.g., Duris et al., 2000). This phenomenon indicates significant dissolution of mineral grains due to acid leaching resulting from the degradational activities and is consistent with similar findings at other sites (McMahon et al., 1995). These dissolved minerals would contribute to the high conductivities.

More recently, analysis of data from in situ resistivity probes installed within the contaminated zones showed that a very high pore water conductivity is required to yield the anomalous conductivity profiles (Werkema et al., 2002). This same study showed that the highest conductivity enhancement occurred within the zone most influenced by water table fluctuations. Such high conductivities may be indicative of active degradation within the smear zone. Geochemical findings show natural attenuation of petroleum hydrocarbons within the zone of water table fluctuations (Lee et al., 2001). These results

point to an important role for geophysical techniques in the assessment of both biodegradational and hydrologic processes within this dynamic zone. Although geophysical studies have been used to investigate hydrologic processes such as infiltration fronts (Chan et al., 2001; Binley et al., 2001) and water table fluctuations (Ernston and Schere, 1986; Hincapie et al., 2001), there are no studies that assess the influence of hydrologic processes on geoelectrical properties as they relate to biodegradational activities or a LNAPL contaminated system. Such studies are critical and should form the foundation of petrophysical models needed to model these systems and the eventual development of geophysical methodologies for the assessment of intrinsic bioremediation or natural attenuation at these sites. Therefore, the specific objectives of this study are to (a) investigate the spatial and temporal variations in conductivity within a hydrocarbon-contaminated zone, and (b) assess the role of water level fluctuations on the measured soil conductivity.

4.2 Study Site

This study was conducted adjacent to a former refinery (Crystal Refinery) located in Carson City, Michigan (Figure 1). Petroleum releases since 1945 from storage tanks and pipelines resulted in seepage of hydrocarbons into the subsurface, impacting soils and groundwater beneath the site, a cemetery to the north and a city park to the south (Figure 1). Investigations in this study were limited to the southern LNAPL plume extending southwesterly into the Carson City Park (site). Preliminary investigations have documented free product thickness between 0.3 m to 0.6 m (Snell Environmental Group, 1994). Residual phase hydrocarbons were found at the fringes of the free product zone

with high concentrations of benzene, toluene, ethyl benzene and xylene (BTEX) (Dell Engineering, 1992). Also shown in Figure 1 is the present distribution and thickness of free phase LNAPL and the residual phase LNAPL boundary. Levels of LNAPL contamination were determined from field observations and through chemical analysis (Legall, 2002) and categorized as either free phase LNAPL, residual LNAPL, or dissolved LNAPL. A biofeasibility study showed active biodegradation occurring at the site (Snell Environmental Group, 1997)

The site is characterized by 4.6 m to 6.1 m surface aquifer composed of fine to medium sands, coarsening at and below the water table to gravel; there is no appreciable clay (Atekwana 2002, Werkema 2002). The sand and gravel is underlain by a 0.6 m to 3.1 m clay aquitard unit (Dell Engineering, 1991; Dell Engineering, 1992). Due to topographic variations at the site, depth to the water table varies from 0.6 m to 0.9 m in the west of the site to 4.6 m to 5.8 m in the east. Groundwater flows west-southwest towards a nearby creek with a hydraulic gradient of 0.0015 and a velocity of 1.7 m/day (Snell Environmental Group, 1994). From October 1999 through November 2000, the water table fluctuated through a depth range of 0.95 m to 0.56 m at different topographic locations. Soil borings have documented a LNAPL smear zone ranging in thickness from 0.9 m to 1.2 m throughout the site resulting from past water table fluctuations. Specific descriptions of the vertical distribution of LNAPL contamination have been previously reported (Atekwana et al., 2002; Atekwana et al., 2000; Werkema et al., 2000). Figure 1 also shows the locations of the free phase LNAPL distribution and the locations of the instrument clusters at the site. Relevant to this study are locations 1, 4, and 5, which are classified as free phase LNAPL locations and contain the largest smear zone thickness.

Location 1 contains a smear zone from 226.1 m to 224.5 m elevation. The smear zone at location 4 occurs from 225.85 m to 224.9 m and at location 5 from 225.85 m to 224.7 m. Residual phase LNAPL locations used in this study are 3 and 10. The smear zone at location 3 ranges from 226.35 m to 225.2 m and at location 10 from 225.7 to 224.4 m.

4.3 Field Methods – Vertical Resistivity Probes

Figure 1 shows the locations of instrument clusters, numbered from 1 to 10. Instrument cluster locations include vertical resistivity probes (VRPs) and 2.54 cm monitoring wells installed within a 92 cm radius of each other at every location. These installations are located within the free phase LNAPL contamination (1, 4, 5, 6 & 8), within the residual phase LNAPL contamination (2, 3, 7, & 10), and at the background location of no LNAPL contamination (9).

Apparent resistivity measurements were collected using the VRPs, which consist of a 3.8 cm ID PVC dry well with 1.3 cm #10-24 pan head stainless steel screws separated vertically at 2.54 cm intervals. The screw heads serve as the electrode contact with the formation and the threaded ends inside the PVC casing were used to make contact with the measurement equipment. Installation of these probes includes a small bentonite slurry annulus that facilitates installation below the saturated zone and decreases the contact resistance with the formation in the vadose zone.

VRP measurements were made using a Syscal R2 resistivity meter with an automated/semi-automated switching system (Werkema et al., 1998). Apparent resistivity measurements were collected, in the semi-automated mode using a mechanical switchbox. The electrodes were selected by the switching system to obtain a series of

5.08 cm Wenner arrays along the probe. The VRP installations required about a year to stabilize, probably because of the bentonite (Groncki, 1999); thus, the measurements shown here are at least a year or more after installation of the VRPs. The measurements used in this study were made monthly from October 1999 through November 2000.

Precipitation data were collected from a weather station located at Greenville, Michigan, which is about 15 km west of the Carson City Park. Water table elevations were determined from 2.54 cm monitoring wells located in each instrument cluster. Groundwater elevations for locations with free product were corrected for the thickness of LNAPL (Fetter, 1993).

4.4 Results – Vertical Resistivity Probes

The resistivity measurements were converted to apparent conductivity and are reported in milliSiemens per meter (mS/m). The results of apparent bulk conductivity are shown in Figures 2 through 7. Labeled on these figures are the water table elevations, during the time of data collection, and the zones and slices used for further analysis (see Section 4.5). These plots contain partial elevation sections taken from the full VRP data. Previous reports have shown the geoelectrical signature referenced to the surface elevation of each VRP, extending to the maximum depth of the VRP (Atekwana et al., 2002; Atekwana et al., 1998; Atekwana et al., 2000; Werkema et al., 2000; Werkema et al., 2002). For example, VRP 1 has a full elevation range from 229 m to 222 m; however, this study focuses on the elevations about the water table and the smear zone. As a result, the data included here from VRP 1 are restricted to these elevations which range from 226.25 m to 224 m. The elevation ranges reported for the remaining VRPs in

this study are from a similar elevation range within the water table fluctuation zone and the LNAPL smear zone. These regions are potentially those most influenced by the fluctuating water table.

4.4.1 Locations with Free Product LNAPL Contamination

Results of bulk conductivity for locations with free phase LNAPL are shown in Figures 2, 3 and 4.

Figure 2 shows the conductivity profile for VRP 1 from 226.25 m to 224 m elevation. The water table fluctuated from 225.78 m to 225.1 m. The first evidence of LNAPL contamination was observed from soil cores and occurred at 226.1 m. The conductivity measurements from the highest elevations, which includes portions of the vadose zone above the smear zone, shows the lowest values, less than 10 mS/m. Continuing with depth, a slight conductivity increase is observed below 226 m.

A more significant conductivity increase at 225 m begins starting from approximately 15-20 mS/m and increasing to over 40 mS/m at approximately 224.75 meters. The profile then decreases back to around 25 mS/m below 224.5 m. This conductivity bulge exhibits the highest conductivities, up to 50 mS/m, and correlates to the free phase LNAPL zone and portions of the dissolved phase LNAPL zone. Below this bulge, the conductivity profile decreases slightly and remains relatively uniform at approximately 25 mS/m throughout the range of dates shown. The conductivity bulge is most pronounced on 10/27/99, 11/24/99, and 1/08/00 when the water table was low; and its position showed only minimal changes through time. The bulge continues throughout

the rest of the dates, albeit less obvious, until another water table low on 11/6/00, when it becomes more evident.

During the spring and summer when water table elevations are the highest, there was a notable reduction in the overall conductivity of the pronounced conductivity bulge. During these seasons, the increase in conductivity with depth is more gradual. This gradual change may be due to dilution by new pore water from recharge events; however this is speculative, as no direct evidence is available. Conversely, the amplitude of the bulge is greatest in the fall when the recharge is at its lowest. The elevation zone of the conductivity bulge is relatively static and does not appear to change location when the groundwater elevation fluctuates.

Figure 3 displays the results from VRP4 from 226.5 m to 224.5 m elevation. At this location the water table fluctuated from 225.9 m to 224.9 m.

The conductivity profile shows relative uniformity of around 1 mS/m until 225.75 m where the profiles show a gradual increase to 10 mS/m. At this location, this corresponds with the maximum elevation of the smear zone at 225.85 m. Below 225.75 m the conductivity profile increases uniformly from 10 mS/m to 20 mS/m at 225.0 m. Below 225.0 m the profile abruptly increases from approximately 20 mS/m to over 40 mS/m at 224.9 m. This zone of highest conductivity correlates to the free phase LNAPL layer and occurs at and slightly below the lowest water level elevation observed during the experiment. Below this maximum, the conductivity profile decreases uniformly through the saturated zone to about 25-30 mS/m. Notable in these profiles is the secondary high conductivity bulge occurring at approximately 225.75 m on 6/7/00. This feature occurs one month after the highest precipitation event on record (see Figure 9 for

precipitation and conductivity profiles). This may represent the conductivity response of a wetting front that increases conductivity as water occupies more pore space and increases water saturation. The overall shape of the profile is consistent throughout the dates measured with the conductivity bulge most pronounced during stages/seasons of water table elevation lows.

The conductivity profiles for the elevation range from 226.25 m to 224.25 m of VRP5 are presented in Figure 4. At this location, the water table fluctuated from 225.25 m to 224.69 m. The profile shows a low range of conductivities from 0.01 to 1 mS/m throughout the vadose zone to an elevation of 225.75 m. From 225.8 m to 225.50 m the conductivity increases from 1 mS/m up to 20 mS/m. This increase occurs within the residual phase LNAPL zone corresponding to the smear zone.

An alternating polarity conductivity high occurs between 225 m to 224.8 m. This feature is coincident with the free phase LNAPL – water interface during some dates and its vertical position does not change with the water table fluctuations. This geoelectrical response is a typical alternating polarity response of the Wenner array across a sharp conductive boundary (Telford et al., 1990). Below this high, the conductivity profile gradually decreases to approximately 25 mS/m. Again, the water table changes are not clearly discernable in the conductivity profiles throughout the year.

In summary, the geoelectrical response at the free phase LNAPL locations show only minor changes in the conductivity structure due to recharge events. Specifically, the conductivity maximum does not shift vertically in response to recharge events. The only observable variability is the magnitude of the conductivity bulge through the dates

measured. Therefore, the presence of the free phase LNAPL appears to suppress the geoelectrical response to recharge events.

4.4.2 Locations with Residual LNAPL Contamination

Figure 5 shows the conductivity profiles from VRP 3 over the elevation range of 226.5 m to 224.25 m. At this location, the water table fluctuated from 225.9 m to 225.0 m. From 226.5 m to 225.5 m the conductivity is uniformly around 5 mS/m. Slightly below 225.5 m, there is an increase in the conductivity to approximately 30 mS/m that continues until 224.75 m. The profile then gradually decreases to about 20-25 mS/m at elevations within the saturated zone.

The broad maximum conductivity bulge to 30 mS/m corresponds to the location of the residual phase LNAPL contamination. This bulge exists throughout the experiment, but becomes slightly less defined at its upper boundary during times of high water table (i.e. spring and summer). In particular, the conductivity increase about 225.5 m elevation becomes less abrupt and more gradual from 6/8/00 to 9/13/00 when the abrupt increase returns. The geoelectrical response for these dates (i.e., 6/8/00, 7/1/00, and 8/7/00) could reflect a recharge event from the precipitation high in May 2000. These data do exhibit a dependence on water table changes as the conductivity bulge does move up or down in elevation with water table fluctuations. For example, the upper boundary of the conductivity bulge raises in elevation from 1/29/00 through 4/27/00 with the water table rise. Further, the conductivity bulge becomes less distinct after the large precipitation event in May 2000; this behavior could be due to higher water saturation above the residual LNAPL zone.

Figure 6 shows the conductivity profile at VRP 10 over the elevation range of 226.0 m to 223.5 m; water table ranges from 225.6 m to 224.8 m at this site. The conductivity profile averages approximately 5 mS/m down to 225.25 m. Below this elevation, the profile increases and shows a vertically broad conductivity bulge with a maximum amplitude of 31 mS/m. This high conductivity bulge correlates with the elevation of the residual LNAPL phase and is within the lower elevations of the water table range. Below approximately 224.1 m, the conductivity profile is a consistent value of around 18 mS/m throughout the experiment. Over the measurement dates, the conductivity bulge decreases in amplitude to slightly over 20 mS/m during water table highs. VRP10 behaves similarly as VRP 3 to water table changes. The conductivity profile shifts in elevation or becomes smoother as the water table rises. As the elevation of the water table drops, the elevation of the conductivity bulge drops. In addition, the slope of the conductivity profile is steepest above and below the bulge during water table elevation lows, as observed previously.

The geoelectrical response at the residual LNAPL locations is different than the free phase locations. In particular, the conductivity bulge at the residual locations changes its position and amplitude with seasons. This behavior suggests that events that cause water table fluctuations are accompanied by changes in the position and magnitude of the bulge.

4.4.3 Location with No LNAPL Contamination (Control Site)

Figure 7 shows the results at VRP 9 over an elevation section of 226.0 m to 224.25 m; the water table level ranged from 225.6 m to 224.8 m. These results show a

range of conductivities from 1 to 5 mS/m above the water table which represents the vadose zone with no LNAPL smearing. It is notable that these data do not show a large conductivity bulge of the type observed at the LNAPL-impacted locations. However, there is a steady, gradual increase in conductivity to a maximum value of approximately 20 mS/m. Then the conductivities remain relatively constant with increasing depth to around 17 mS/m. This increase occurs below the water table and is most pronounced during times of water table highs. During water table lows the conductivity profile is more gradual (i.e. 10/27/99, 8/08/00, 9/18/00, and 11/06/00.

4.5 VRP Depth Zones

Further work was done in an effort to quantify the temporal variations in the conductivity values and describe the influence of fluctuating water table elevations on the conductivity. This analysis was started by subdividing the profiles into three zones including: (1) the saturated zone average conductivity (SatZoneAve), which was determined as the average of the conductivity values below the water table elevation to the depths shown in Figures 2 through 7; (2) a slice through time at the maximum conductivity zone (MaxSlice): and (3) a slice at the maximum elevation of the hydrocarbon smear zone (MaxSZ), determined as the top of the residual phase LNAPL zone. These three discrete zones were chosen as potential locations where the conductivity is most sensitive to hydrologic changes (i.e., water table elevation changes and recharge events).

Figures 8 through 13 display the results for the analysis of the geoelectrical variability over time at the discrete elevation zones and slices. Each figure has four time series

labeled (a) through (d). Series (a) is the conductivity slice at the maximum elevation of the smear zone. This elevation was approximated as the highest elevation where residual phase LNAPL was observed. Series (b) is the conductivity slice at the elevation of the maximum conductivity. The maximum values were determined by visual inspection of the conductivity profiles. Series (c) is the saturated zone average conductivity within the elevations reported in this study. The error bars represent one standard deviation about the mean. The bottom-most series, (d), presents the precipitation and water table elevation data versus time, from October 1999 through November 2000.

Upon visual inspection, the relationship between precipitation and monitoring well response is very good, with an apparent 1-month time lag in the response from the monitoring wells to precipitation events. Several researchers (Viswanathan, 1984; Manglick and Rai, 2000) have established that this time lag is due to groundwater recharge; hence, the water table data can be used as a measure of groundwater recharge due to precipitation. These data show a precipitation and monitoring well water level low occurring during November 1999. This is followed by a precipitation high occurring in May of 2000 and its corresponding water level high in June 2000. Finally, another precipitation low occurs during October 2000 with a corresponding monitoring well low in November 2000.

To quantitatively evaluate the relationship between the geoelectrical response at the selected elevation intervals and hydrologic events, a simple linear regression analyses between water table elevation and conductivity were performed. The results from the linear fits for each VRP per each elevation zone is shown in Figure 14 with the computed slope (m), correlation coefficient (R), and p values summarized in Table 1. The R value

is the correlation coefficient where values closer to 1 indicate very good correlation between the independent factor (water table elevation) and the dependent factor (conductivity). The p-value is the probability that R is zero. If $p<0.01$, then there is a 95% confidence that R is not zero and the two data sets are related. A 99% confidence level is obtained when $p<0.001$. Figure 14 includes the best fit regression plots for each VRP.

4.5.1 Free Phase LNAPL Locations – Temporal Variability

Figure 8 shows the time series for VRP1; the results of the regression analysis are given in Figure 14a. The saturated zone average response (Figure 8c) ranges from 28 mS/m to 36 mS/m. This time series is generally an inverse form and suppressed amplitude relative to the monitoring well response. The precipitation high in May of 2000 was observed via the monitoring well elevation high in early June 2000, and a saturated zone average conductivity low in June of 2000. The other high precipitation event of September 2000 does not show a significant response in the saturated zone average conductivity. The regression analysis found $m=-13.95$, $R=-0.81$ and $p=0.0042$ which quantifies a relative strong inverse relationship between the saturated zone average response and recharge.

The values at the maximum conductivity elevation slice (Figure 8b) ranged from 30 mS/m to over 50 mS/m, showing low amplitude variations from February 2000 onward. The highest conductivities occur during the first three months of measurements, followed by an abrupt decrease. Beyond February 2000 the conductivity values remain low regardless of the large precipitation event in May 2000. Overall, the regression

analysis of these data (Figure 14b) suggest the existence of an inverse relationship to the recharge (m=-20.11, R=-0.633, p=0.049).

The conductivity values for the slice through the maximum elevation of the smear zone (Figure 8a) have a range from 0.5 mS/m to 4 mS/m. The response over time is much smoother than the monitoring well data and does not show the stepped fluctuations in precipitation that the precipitation record reveals. The regression analysis (Figure 14b) suggests an extremely weak correlation, if any, between the recharge events and the conductivity of this slice (m=0.051, R=0.011, p=0.976)

Figure 9 presents the time series for VRP 4, another free phase LNAPL location. The saturated zone average response (Figure 9c) ranges from 20 to 30 mS/m and shows an inverse relationship to the precipitation record and the monitoring well data. The regression analysis (Figure 14b) suggests a strong inverse relationship (m=-11.54, R=-0.834, p=0.00074) between the saturated zone average response and recharge.

The time series slice through the maximum conductivity zone (Figure 9b) indicates a range from 30 mS/m to 50 mS/m and a generally elevated set of readings from November 1999 to February of 2000. After this date, the data abruptly decrease to between 30 and 40 mS/m throughout the rest of the measurements and show very subtle fluctuations. The regression analysis (Figure 14b) shows an inverse relationship, but not as strong or confident as VRP1 (m=-17.90, R=-0.586, p=0.045).

The time series data through the maximum elevation of the smear zone (Figure 9a) reveals a response similar to the monitoring well elevation changes. In this elevation slice the values range from 0.4 mS/m to 18 mS/m and show a very large amplitude response. Notable is the conductivity high of 18 mS/m occurring in June 2000, one

month after the greatest precipitation on record. This data point may be considered a statistical outlier and not included in the regression analysis; however, since this data represents the VRP response to a real precipitation event, the data point was included in the regression analysis. The regression analysis (Figure 14b) suggests these data have a strong direct relationship with the water table (m=15.58, R=0.7376, p=0.00618).

The VRP 5 time series data, shown in Figure 10, is the last free phase LNAPL location presented. The time series at the saturated zone average conductivity (Figure 10c) shows a range from 24 mS/m to 27 mS/m. The regression analysis (Figure 14c) indicate m=-0.374, R=-0.0749 and a p=0.817, which is very strong evidence that there is no correlation between these conductivity data and recharge.

The time series slice through the maximum conductivity elevation (Figure 10b) shows a range from 30 mS/m to 60 mS/m with very little fluctuation. The trend over time reveals a gradual decrease in conductivity over the dates measured from the maximum of 60 mS/m to the low of 30 mS/m. The regression analysis (Figure 14c) reveals an indirect relationship (m=-24.11, R=-0.608,p=0.036) with recharge; however the correlation is relatively weak.

The time series data through the maximum elevation of the smear zone (Figure 10a) shows a range of conductivity from 0.5 mS/m to 5 mS/m. The form of these data up to September 2000 resemble and the monitoring well record. However, the last two data points show very low conductivities during a time when the water table was dropping. The regression analysis (Figure 14c) suggests a very weak indirect correlation, if any, to recharge (m=-3.44, R=-0.3679 and p=0.24354).

In summary, the conductivity profiles at the free phase LNAPL locations over time show that the saturated zone average conductivity has an inverse relationship to the precipitation and monitoring well response, with a very high level of confidence, p~0.004; with the exception of VRP5, which shows no correlation. The time series slice through the maximum conductivity zone revealed elevated conductivities, and an inverse relationship to hydrologic events, with less confidence (p~0.04) than the saturated zone time series data for VRPs 1 and 4. The regression analysis at the slice through time at the maximum elevation of the smear zone does not suggest an overall trend. However, the results from VRP4 do reveal a strong correlation to recharge, with a high level of confidence, as a result of the large precipitation event. If this event did not occur, VRP would most likely show a similar result as VRPs 1 and 5.

4.5.2 Residual Phase LNAPL Locations – Temporal Variability

Figure 11 shows the time series results for VRP3. The saturated zone average conductivity (Figure 11c) ranges from 22 mS/m to 27 mS/m, and shows an inverse relationship to the water table elevations. The regression analysis (Figure 14d) shows a very strong inverse relationship to the recharge with a slope of –6.57, coefficient of –0.94 and a p-value and less than 0.0001.

The time series slice at the maximum conductivity zone (Figure 11b) reveals a range from 25 mS/m to about 35 mS/m and very little fluctuation over time. The data before March 2000 do exhibit some oscillations; however, from March 2000 onward the conductivity data are relatively uniform and decrease slightly. The regression results

(Figure 14d) suggest these data are not correlated with the recharge (m=-0.234, R=-0.0336, p= 0.91739).

The time series slice at the maximum elevation of the smear zone (Figure 11a) shows a range from 4 to 5 mS/m. The regression results suggest that these data are inversely related to the monitoring well data (R=-0.737, p=0.00627); however the slope is very flat, m=-1.51, suggesting recharge is not a large contributor to the conductivity time series.

Figure 12 shows the time series data from VRP10. The time series data within the saturated zone average conductivity (Figure 12c) range from 15 to 20 mS/m. As with VRP3, the regression results (Figure 14e) from these data indicate a strong inverse relationship (m=-6.12, R=-0.826,p=0.0009) to recharge.

The maximum conductivity slice data (Figure 12b) show very little fluctuation over the dates measured and in fact a general decrease in conductivity over time is observed. These data show a range from 15 mS/m to 25 mS/m. The regression results (Figure 14e) indicate a slope of –3.85, a correlation coefficient of –0.377 and a p-value of 0.226. This suggests these data have very little correlation and/or relationship to recharge.

The slice through the elevation of the maximum smear zone (Figure 12a) reveals conductivities from 2 mS/m to slightly over 4 mS/m. The regression analysis (Figure 14e) suggest these data exhibit a strong inverse relationship to recharge (R=-0.734, p=0.0066). However, as at VRP3 the slope is very flat (m=-2.62) which indicates recharge is not a large factor in the conductivity time series.

In summary, the residual phase LNAPL locations exhibit a strong inverse relationship in the saturated zone average conductivity and the maximum elevation of the smear zone to recharge. Both elevation zones show correlation coefficients of an inverse sense with values from –0.73 to –0.94 and p-values indicating 99% confidence. However, the result from the maximum elevation of the smear zones show very flat slopes, indicating recharge is not greatly affecting the conductivity time series. The time series data at the elevation of the maximum conductivity show no relationship to the recharge.

4.5.3 No LNAPL Contamination – Temporal Variability

Lastly, the time series conductivity response from the uncontaminated location, VRP9, is presented in Figure 13. The saturated zone average conductivity series (Figure 13c) exhibits the lowest range from 10 mS/m to 15 mS/m. The regression analysis (Figure 14f) show a weakly direct relationship to recharge (m=2.38,R=0.434, p=0.105). The p-value does not indicate a high degree of confidence and the R–value suggests the relationship is weak. The slope is very flat indicating recharge is not greatly affecting the conductivity time series in this zone.

The time series conductivity slice through the estimated maximum conductivity (Figure 13b) shows a conductivity range from 13 mS/m to 20 mS/m. Even though VRP9 does not reveal a clear conductivity maximum, as in the LNAPL impacted locations, this elevation zone was picked for comparison purposes, and does in fact represent some of the highest conductivities measured at VRP9. Noteworthy is that this "high" conductivity zone is very close to within the range of conductivity values for the

saturated zone average conductivity. Regardless, the regression analysis (Figure 14f) through the maximum conductivity zone reveals a very strong direct relationship to the recharge (m=6.48,R=0.7525) with a 99% confidence (p=0.001).

Lastly, the time series data from the equivalent maximum elevation of the smear zone (Figure 13a) show conductivities from 4 mS/m to 7 mS/m. The regression results for these data (Figure 14f) provide very strong evidence that there is no correlation between this time series and recharge (m=0.121, R=0.0306, p=0.9139).

4.6 Discussion and Conclusions

The results reveal three major points: (1) the geoelectrical response differs with the category of LNAPL contamination, (2) the conductivity profiles vary with seasonal hydrologic changes, and (3) there are correlations between the geoelectrical character of discrete depth zones and water table levels that vary with the category of LNAPL contamination.

4.6.1 Conductivity and Varying Degrees of LNAPL Contamination

The relationship between the geoelectrical response and varying degrees of LNAPL contamination show a direct relationship between a highly conductive anomaly and high degrees of LNAPL impaction. The maximum conductivity values are found at the free phase LNAPL locations and reveal conductivities 2 to 3 times that of the background values (30 – 60 mS/m vs. 14 – 19 mS/m). In comparison, locations of residual contamination have conductivities up to twice that of the background values (15 – 30 mS/m vs. 14 – 19 mS/m). These results corroborate previous studies and provide

support to the conductive response at an aged LNAPL impacted site (Atekwana et al., 2002; Sauck, 2000; Werkema et al., 2002), and are summarized in Table 1.

4.6.2 Conductivity Profiles of Varying Degrees of LNAPL vs. Recharge

The conductivity profile variation due to fluctuating water table elevations is related to different degrees of LNAPL impaction. In the case of the free phase locations, the maximum conductivity bulge does not shift vertically in response to water table elevation changes. The only variability observed is the magnitude of the bulge. Perhaps the conduction at this location is not simply a function of the pore water chemistry (i.e., ionic concentration), as no vertical shifts occur. If conduction were mainly due to the pore water chemistry, recharge water would be expected to dilute the pore water and decrease the conductivity. Since this is not observed, perhaps another mechanism of conduction related to the aquifer sediment itself or the biogeochemical reactions with the free phase LNAPL and the aquifer sediment is affecting the conductivity. The geology at these locations and these elevations do not reveal the presence of a highly conductive lithology (i.e. clay lens) (Atekwana et al., 2002; Werkema et al., 2000). So the geology cannot be used to explain the conductivity bulge. The fact that the conductivity bulge does not respond to changing water table levels indicates that this zone is vertically fixed. This suggests that an alternative mechanism is perhaps responsible and may explain these results. This mechanism may be associated with biogeochemical reactions with the free phase LNAPL because this elevation zone has been shown to contain large populations of oil degrading bacteria (Atekwana et al., 2002).

On the other hand, the residual phase LNAPL location does shows slight changes in the shape, position and amplitude of the conductivity bulge throughout the seasons and inversely related to water table elevation changes. At this location the pore water chemistry may be a more important factor in the conductivity response observed. If there has been significant bioremediation of the LNAPL-impacted zone, the conductive model at LNAPL impacted sites suggests that a corresponding increase in the electrolyte conductance will follow (Sauck, 2000). Intrinsic or natural biodegradation has been reported to be occurring at this site (Snell Environmental Group, 1997). Therefore, the resulting change in pore water chemistry via increased ionic concentration is possible. The inverse relationship between the conductivity and recharge events may be due to dilution as the pore water becomes diluted and therefore the electrolytic properties more resistive. Of course, this mechanism to explain the results assumes the recharge is vertical and horizontal recharge does not affect the conductivity profile.

The response from the clean/control location, VRP9, shows that the water table changes affect the shape of the conductivity profile. The conductivity profile becomes smoother during water table elevation lows. At times of water table elevation highs the conductivity profile looks similar to a water saturation curve; however, the increase in conductivity does not occur at the water table but well below it. From these data it appears that small water table fluctuations are not revealed in changes in the conductivity profile, as it is assumed that the conductivity would change as the pore water saturation changes in the absence of LNAPL contamination. This is based on the direct relationship between the measured conductivity and the saturation as described by Archie's Law (Archie, 1942). The closest correlation to the water table is observed during the dates

after the large May 2000 rainfall. Assuming vertical recharge, perhaps the conductivity as measured from the VRP is most sensitive to large water table fluctuations, the resulting saturation change, and is insensitive to smaller water table changes.

4.6.3 Temporal Variations at Discrete Elevation Intervals

The results from the temporal variations at discrete elevation zones and slices are summarized in Table 1 and the best fit regression plots in Figure 14.

The saturated zone average conductivity for all the locations impacted with LNAPL (whether free or residual phase) shows an inverse relationship to the water table elevation. The clean location reveals a direct relationship with the water table elevation, although the slope indicates recharge does not greatly affect the conductivity. The relationship for VRPs 1, 4, 3 and 10 has higher correlation coefficients and greater confidence. The inverse relationship at the LNAPL locations may be attributed to electrolyte dilution as fresh vertically recharged water enters the system. The direct relationship at the location of no LNAPL-contamination may be attributed to increased pore water saturation and not to electrolytic chemistry related to biodegradation, as LNAPL is absent.

The relationship between the LNAPL locations and the non-contaminated location is also observed at the maximum conductivity slice. These results are interpreted in a similar manner; however, the slope for the non-contaminated location reveals there is more of a relationship between recharge and the conductivity.

Lastly, the relationship between the conductivity time series data at the maximum elevation of the smear zone and the water table elevation is explored. Within locations of

free phase LNAPL there is no overall trend in these relationships. VRP4 shows the best correlation verses VRP1 and VRP5. This may be due to the location of VRP4. It is in a topographically lower position than the others and has a much smaller vadose zone. Therefore, the correlation at this VRP to water table elevation changes may be reflective of the thin vadose zone because vertical recharge is probably the greatest. Specifically, the conductivity increase occurring after the May 2000 precipitation event (see Figure 3 6/7/00 and Figure 9a) may be due to increased pore water saturation pooling above a permeability barrier related to the residual LNAPL zone. The indirect relationship between the residual phase LNAPL and water table elevations within the maximum elevation of the smear zone may be attributed to diluting the ionic concentration of the pore water due to the biodegrdadation of the LNAPL. Finally, the relationship at the clean location yields very strong evidence that there is no correlation between the time series of this conductivity slice and recharge. Perhaps the VRP conductivity data at a location of no LNAPL contamination is not sensitive enough to reveal subtle changes in pore water saturation as a recharge wetting front progresses with depth. On the other hand, wetting fronts due to vertical recharge may have passed through the time between the monthly measurements were made and these data simply missed it.

4.7 Implications

The results from this study imply that the geoelectrical changes at locations of LNAPL contamination vary based on the degree of LNAPL impaction and hydrologic events. The important results from this study show that there are discrete elevation zones of different geoelectrical properties within a site impacted with LNAPL. Furthermore,

these zones respond differently to recharge events. The geoelectrical response characterizes physical changes occurring within these zones throughout a full hydrologic year. Geochemists now potentially have a tool (i.e. the VRP) to locate these physically active zones or elevation regions and then focus their investigations. Generally, geochemists focus on the fully saturated zone, while this study shows that physical changes are occurring above this zone. It is only through the high-resolution geophysical characterization at this site that VRPs can be utilized as a tool for future investigations into the biogeochemical dynamics at a site impacted with LNAPL.

The anomalous zones and regions identified by the VRP data require additional biogeochemical studies and subsequent analysis in order to provide insights into the mechanisms responsible for these conductivity responses. The achievement of the objectives from this study now allows geochemists to focus on these zones.

Ultimately, geoelectrical techniques may be used as a supplement for groundwater sampling and analysis and potentially achieve lower cleanup and monitoring costs thereby accomplishing the goals set forth by Bekins et al. (2001). Specifically, geoelectrical observations could be used to decrease the number and frequency of direct groundwater sampling, and guide the efficient design, implementation and monitoring of remediation systems by targeting subsurface contaminated zones resulting in significant increases in remediation effectiveness and cost savings.

This study represents some of the first steps taken to understand the subsurface geoelectrical signatures in the presence of LNAPL contamination and relate them to the natural hydrologic dynamics. These results show the application of geophysical techniques to monitor hydrologic events in the presence of LNAPL contamination.

4.8 Acknowledgements

This work was funded in part by the AAPG Grants-In-Aid, NASA through the Michigan Space Grant Consortium, Western Michigan University Faculty Research and Creative Activities Support Fund, the Doctoral Dissertation Fellowship through the Graduate College at Western Michigan University, and the American Chemical Society-Petroleum Research Fund Grant (PRF No. 31594-AC2). Geophysical equipment used during this study was funded through a NSF Grant DUE-9550974. We also thank Joe Duris, Tyler Knoll, Andy Nichols and Jeff Locey for excellent technical assistance.

4.9 References

Archie, G. E. The Electrical Resistivity Log as an Aid in Determining Some Reservoir Characteristics. Transactions of the American institute of Mining, Metallurgical and Petroleum Engineers, 146, 54-62. 1942.

Atekwana, E. A, Sauck, W. A., and Werkema, D. D. Investigations of geoelectrical signatures at a hydrocarbon contaminated site. Journal of Applied Geophysics, 44, 167-180. 2000.

Atekwana, E. A, Werkema, D. D., Duris J.D., Rossbach S., Atekwana, E. A, Sauck, W. A., and Cassidy, D. P. *In situ* Apparent Resistivity measurements and Microbial population distribution at a Hydrocarbon Contaminated Site: Implications for Assessing Natural Attenuation. Geophysics, In review. 2002.

Atekwana, E. A., Sauck, W. A., and Werkema, D. D. Characterization of a Complex Refinery Groundwater Contaminant Plume using Multiple Geoelectric Methods. Proceedings of the Symposium on the Application of Geophysics to Engineering and Environmental Problems (SAGEEP '98), 427-436. 1998.

Bekins, B, Rittmann, B. E., and MacDonald, J. A. Natural Attenuation Strategy for Groundwater Cleanup Focuses on Demonstrating Cause and Effect. EOS, Transactions, American Geophysical Union, 82[5], 53-58. 1-30-2001.

Benson, A. K., Payne, K. L., and Stubben, M. A. Mapping Groundwater Contamination using DC Resistivity and VLF Geophysical Methods - A Case Study. Geophysics, 62[1], 80-86. 1997.

Bermejo, J. L, Sauck, W. A., and , Atekwana E. A. Geophysical Discovery of a New LNAPL Plume at the Former Wurtsmith AFB, Oscoda, Michigan. Ground Water Monitoring & Remediation, XVII[4], 131-137. 1997.

Binley, A., Winship, P., Middleton, R., Pokar, M., and West, J. Observations of Seasonal Dynamics in the Vadose Zone Using Borehole Radar and Resistivity. Proceedings of the Symposium on the Application of Geophysics to Engineering and Environmental Problems (SAGEEP 2001), VZC-3. 2001.

Cassidy, D. P., Werkema, D. D., Sauck, W. A., Atekwana, E. A., Rossbach, S., and Duris, J. The effects of LNAPL biodegradation products on electrical conductivity measurements. Journal of Environmental and Engineering Geophysics, 6, 47-52. 2001.

Chan, C. Y., Kim, C., and Holt, J. J. Monitoring Saturatin in the Vadose Zone After Simulated Rainfall Using Ground Penetrating Radar. Proceedings of the Symposium on the Application of Geophysics to Engineering and Environmental Problems (SAGEEP 2001), VZC-5. 2001.

Daniels, J. J., Roberts, D., and Vendl, M. Site Studies of Ground Penetrating Radar for Monitoring Petroleum Product Contaminants. Proceedings of the Symposium on the Application of Geophysics to Engineering and Environmental Problems (SAGEEP '92), Oak Brook IL., 597-609. 1992.

Dell Engineering. Recovery System Performance Evaluation at the Refinery Site, Crystal Refining Company, Carson City, Michigan. Dell Engineering, Inc., September, 1991, Project No.90200. 1991.

Dell Engineering. Remedial Action Plan for Crystal Refining Company, 801 North Williams Street, Carson City, MI. Report DEI No.921660, Holland, Michigan. 1992.

Duris, J. W., Werkema, D. D., Atekwana A., Eversole, R., Beuving, L., and Rossbach S. Microbial Communities and Their Effects on Silica Structure & Geophysical Properties in Hydrocarbon Impacted Sediments. Geological Society of America Annual Meeting Abstracts, Reno, NV, A190. 2000.

Ernston, K. and Schere, H. U. Self-potential variations with time and their relation to hydrogeologic and meteorological parameters. 10. Geophysics, 51, 1967-1977. 1986.

Fetter, C. W. Contaminant Hydrogeology. 1, 225-231. 1993.

Groncki, J. M. Calibration, installation techniques, and initial measurements for vertical resistivity probes in hydrogeologic investigations. M.S.Thesis, -122. 1999.

Hincapie, J. O., Doser, D. I., Yuan, D., and Baker, M. R. Detection of Shallow Water Table Fluctuation Using the Spectral Analysis of Surface Waves (SASW)

Technique. Proceedings of the Symposium on the Application of Geophysics to Engineering and Environmental Problems (SAGEEP 2001). 2001.

LaBrecque, D., Bennett, J., Heath, G., Schima, S., and Sowers, H. Electrical Resistivity Tomography Monitoring for Process Control in Environmental Remediation. Proceedings of the Symposium on the Application of Geophysics to Engineering and Environmental Problems (SAGEEP '98), 613-622. 1998.

Lee, C. H., Lee, J. Y., Cheon, J. Y., and Lee, K. K. Attenuation of Petroleum Hydrocarbons in Smear Zones: A Case Study. Journal of Environmental Engineering, 639-645. 2001.

Legall, F. D. unpublished data, personel communication. 2002.

Manglick, A. and Rai, S. N. Modeling of Water Table Fluctuations in Response to Time-varying Recharge and Withdrawl. Water Resources Management, 14, 339-347. 2000.

Maxwell, M and Schmok, J. Detection and Mapping of an LNAPL Plume using GPR: A Case Study. Proceedings of the Symposium on the Application of Geophysics to Engineering and Environmental Problems (SAGEEP '95), 15-23. 1995.

McMahon, P. B., Vroblesky, D. A., Bradely, P. M., Chapelle, F. H., and Gullet, C. D. Evidence for enhanced mineral dissolution in organic acid-rich shallow ground water. Ground Water, 33[2], 207-216. 1995.

Mercer, J. W. and Cohen, R. M. A Review of Immiscible Fluids in the Subsurface. Journal of Contaminant Hydrogeology, 6, 107-163. 1990.

Newmark, R. L. Using Geophysical Techniques to Control In Situ Thermal Remediation. Proceedings of the Symposium on the Application of Geophysics to Engineering and Environmental Problems (SAGEEP'94), 196-211. 1994.

Sauck, W. A. A model for the resistivity structure of LNAPL plumes and their environs in sandy sediments. Journal of Applied Geophysics, 44/2-3, 151-165. 2000.

Schima, S., LaBrecque, D. J., and Lundegard, P. D. Monitoring Air Sparging Using Resistivity Tomography. Ground Water Monitoring & Remediation[Spring], 131-138. 1996.

Snell Environmental Group. Technical Memorandum Task 1B-IRAP Evaluation, Crystal Refinery, Carson City, Michigan, MERA ID #59003. 1994. Michigan Department of Natural Resources, Grand Rapids District Office.

Snell Environmental Group. Biofeasibility Study Report, Crystal Refinery, Carson City, Michigan, MERA ID #59003. SEG Project #9441-4848-03. 1997. Michigan Department of Environmental Quality Environmental Response Division, Grand Rapids District Office.

Strachan, E. and Wolfe, P. Seimoelectric Investigations at Clean and Contaminated Sites. Proceedings of the Symposium on the Application of Geophysics to Engineering and Environmental Problems (SAGEEP 2001). 2001.

Telford, W. M., Geldart, L. P., and Sheriff, R. E. Applied Geophysics . Second, 558. 1990. Cambridge University Press.

Vanhala, H. Mapping Oil-Contaminated Sand and Till with the Spectral Induced Polarization (SIP) Method. Geophysical Prospecting, 45, 303-326. 1997.

Viswanathan, M. N. Recharge characteristics of an unconfined aquifer from the rainfall-water table relationship. Journal of Hydrology, 70, 233-250. 1984.

Werkema, D. D., Atekwana, E.A., Sauck W. A., and Asumadu, J. A Versatile Windows Based Multi-Electrode Acquisition System for DC Electrical Methods Surveys. Environmental Geosciences, 5[4], 196-206. 1998.

Werkema, D. D., Atekwana A., Sauck, W., Rossbach.S., and Duris J. Vertical Distribution of Microbial Abundances and Apparent Resistivity at an LNAPL Spill Site. Proceedings of the Symposium on the Application of Geophysics to Engineering and Environmental Problems (SAGEEP 2000). 2000.

Werkema, D. D., Atekwana, E. A., Endres, A. L., Sauck, W. A., and Cassidy, D. P. Archie's Law Analysis of a Shallow Hydrocarbon Contaminated Aquifer: Implications for the Conductive Model for LNAPL Impacted Sites. In Review. 2002.

Table 1. Correlation Results Between Water Table Elevation and Conductivity for the Three Depth Slices.

VRP	*Sat Zone Ave σ*	*Hydro Correlation*	*Max σ Slice*	*Hydro Correlation*	*Max Smear Zone Slice*	*Hydro Correlation*
1 : free phase LNAPL	28-36 mS/m	m = -13.95 R = -0.81343 p = 0.0042	30-50 mS/m	m = -20.11 R = -0.63301 p = 0.04947	0.5-4 mS/m	m = 0.051 R=0.01091 p=0.97614
4: free phase LNAPL	20-30 mS/m	m = -11.54 R = -0.83418 p = 0.000742	30-50 mS/m	m = -17.90 R = -0.58609 p = 0.04521	0.4-18 mS/m	m = 15.58 R = 0.737692 p = 0.00618
5: free phase LNAPL	22-27mS/m	m = -0.374 R = -0.07492 p = 0.817	30-60 mS/m	m = -24.11 R = -0.608 p = 0.03596	0.5-5 mS/m	m = -3.44 R = -0.36488 p = 0.24354
3: residual phase LNAPL	22-27 mS/m	m = -6.57 R = -0.94202 p = <0.0001	25-35 mS/m	m = -0.234 R = -0.03362 p = 0.91739	4-5 mS/m	m = -1.51 R = -0.73681 p = 0.00627
10: residual phase LNAPL	15-20 mS/m	m = -6.12 R = -0.82607 p = 0.000927	15-30 mS/m	m = -3.85 R = -0.37742 p = 0.22647	2-4 mS/m	m = -2.62 R = -0.73404 p = 0.00657
9: No LNAPL	10-15 mS/m	m = 2.38 R = 0.43456 p = 0.10552	14-19 mS/m	m = 6.48 R = 0.7525 p = 0.00121	4-7 mS/m	m = 0.121 R = 0.03056 p = 0.9139

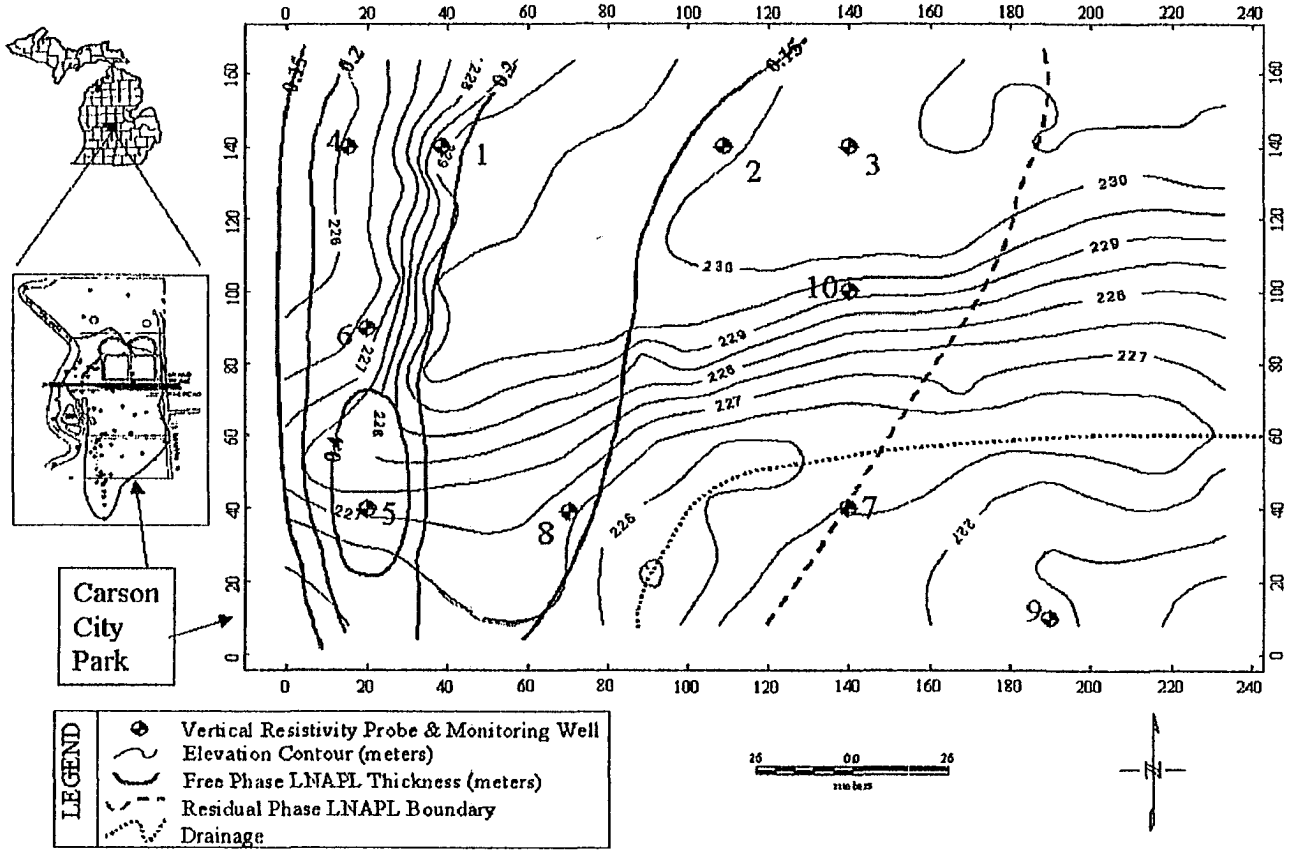

Figure 1. Site Map – Carson City Park, Carson City, Michigan USA. (43°07'11" N Latitude, 84°51'15" W Longitude). Site map includes regional setting, topography, LNAPL contamination levels and relevant surface features.

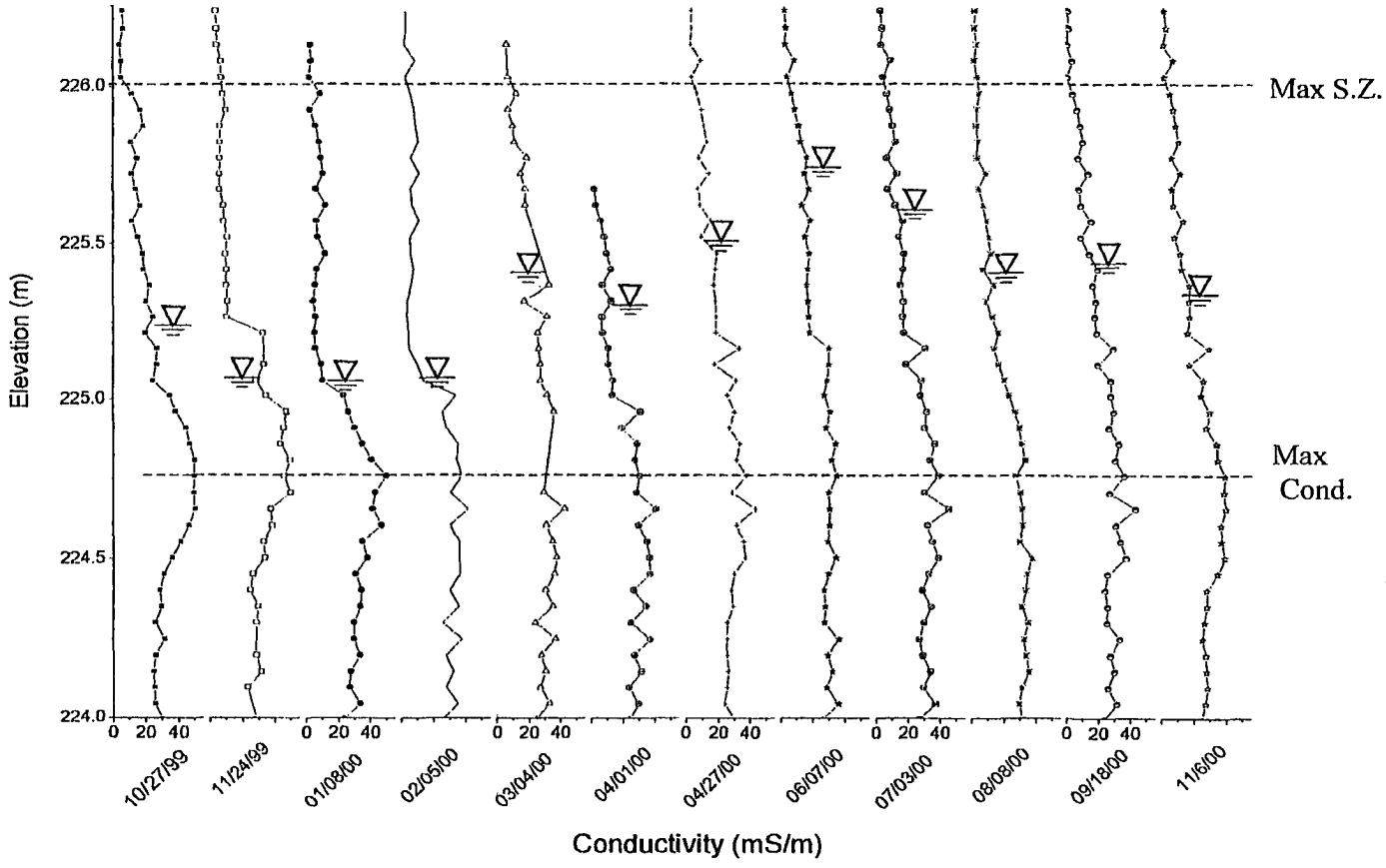

Figure 2. VRP 1, Free Phase LNAPL Location; Conductivity vs. Elevation Over Time. Maximum Elevation of Smear Zone (MaxSZ) and Elevation of Maximum Conductivity (Max Cond.) Shown for Reference to Figures 8-13.

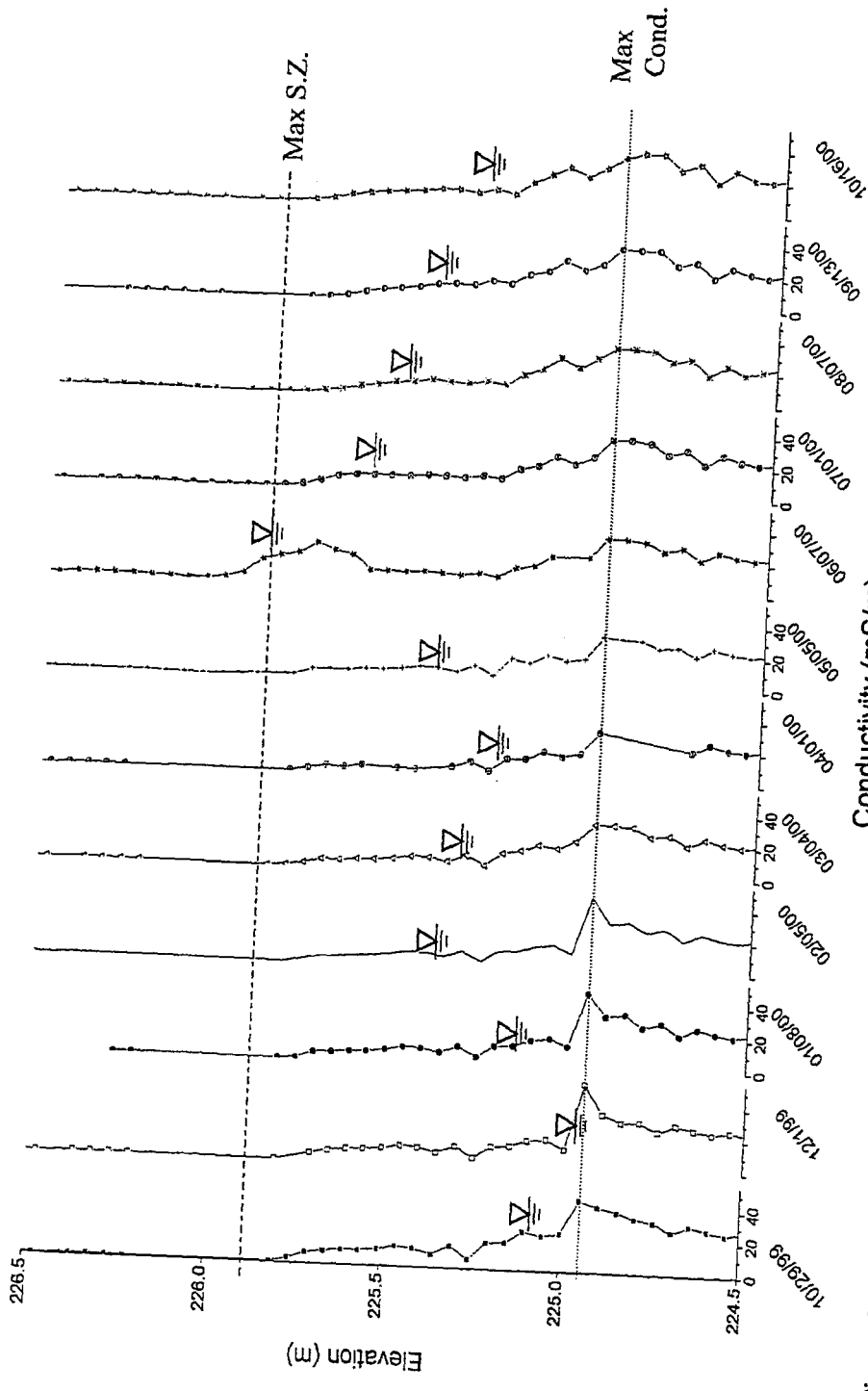

Figure 3. VRP 4, Free Phase LNAPL Location; Conductivity Vs. Elevation Over Time. Maximum Elevation of Smear Zone (MaxSZ) and Elevation of Maximum Conductivity (Max Cond.) Shown for Reference to Figures 8-13.

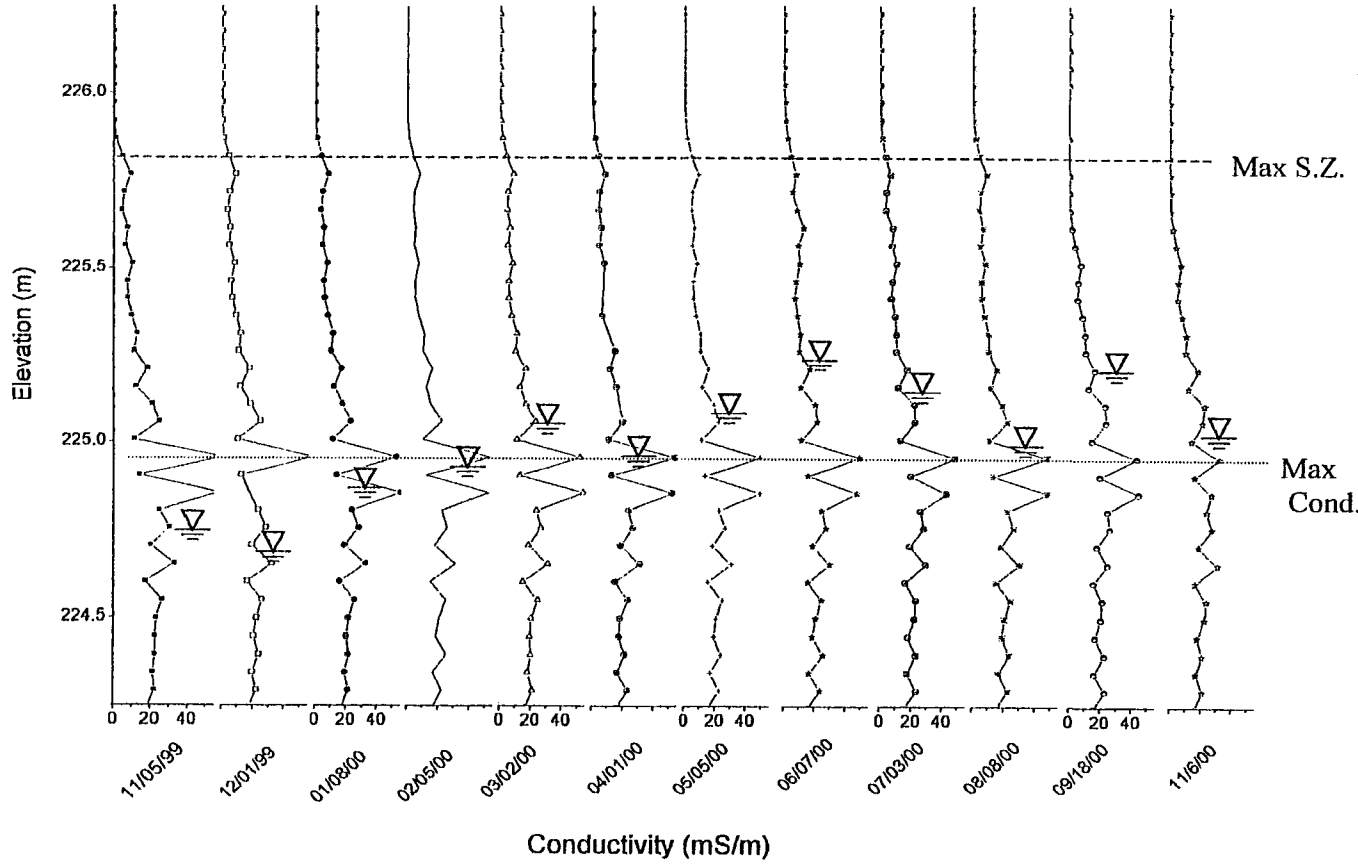

Figure 4. VRP 5, Free Phase LNAPL Location; Conductivity Vs. Elevation Over Time. Maximum Elevation of Smear Zone (MaxSZ) and Elevation of Maximum Conductivity (Max Cond.) Shown for Reference to Figures 8-13.

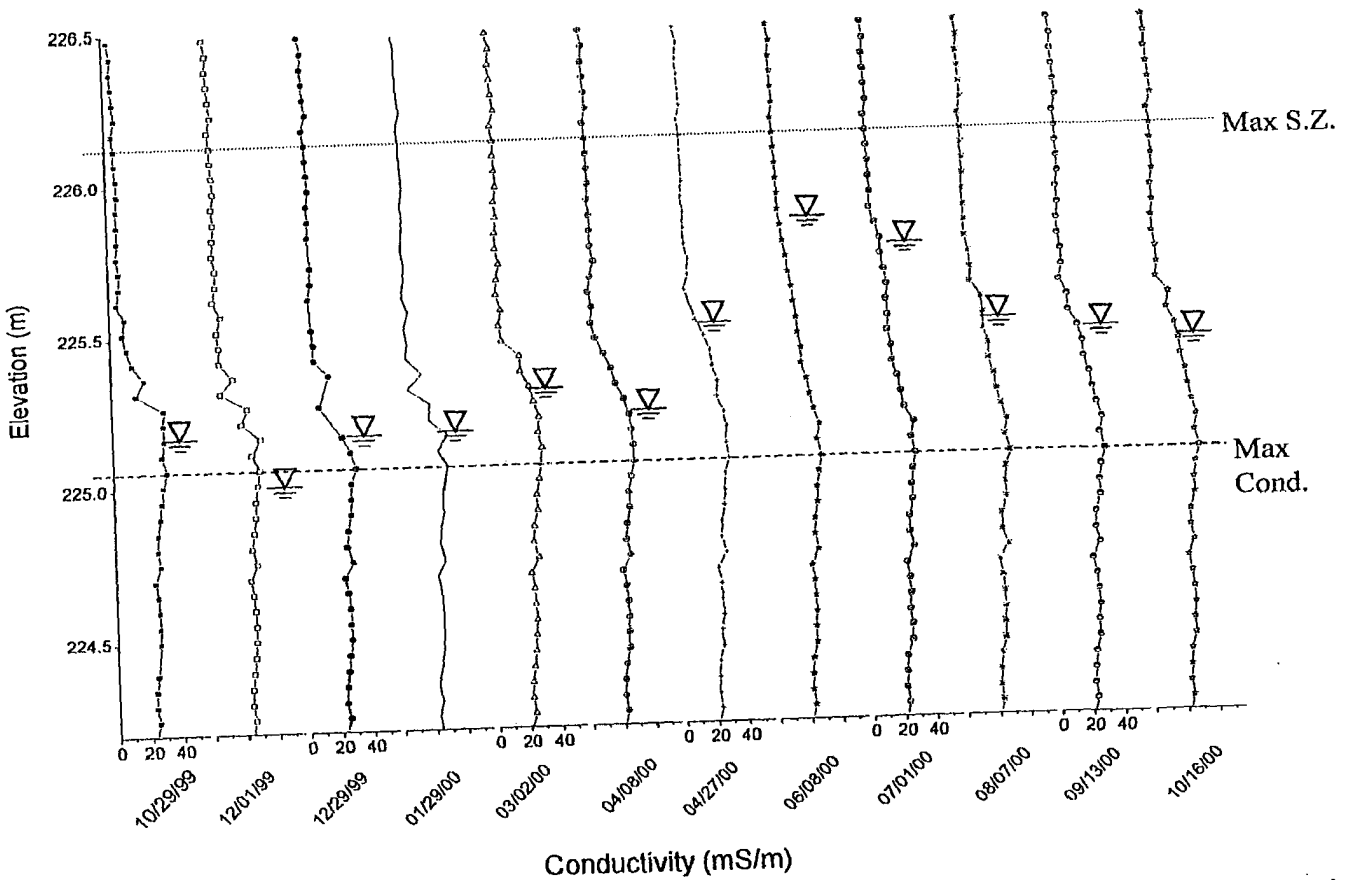

Figure 5. VRP 3, Residual Phase LNAPL Location; Conductivity Vs. Elevation Over Time. Maximum Elevation of Smear Zone (MaxSZ) and Elevation of Maximum Conductivity (Max Cond.) Shown for Reference to Figures 8-13.

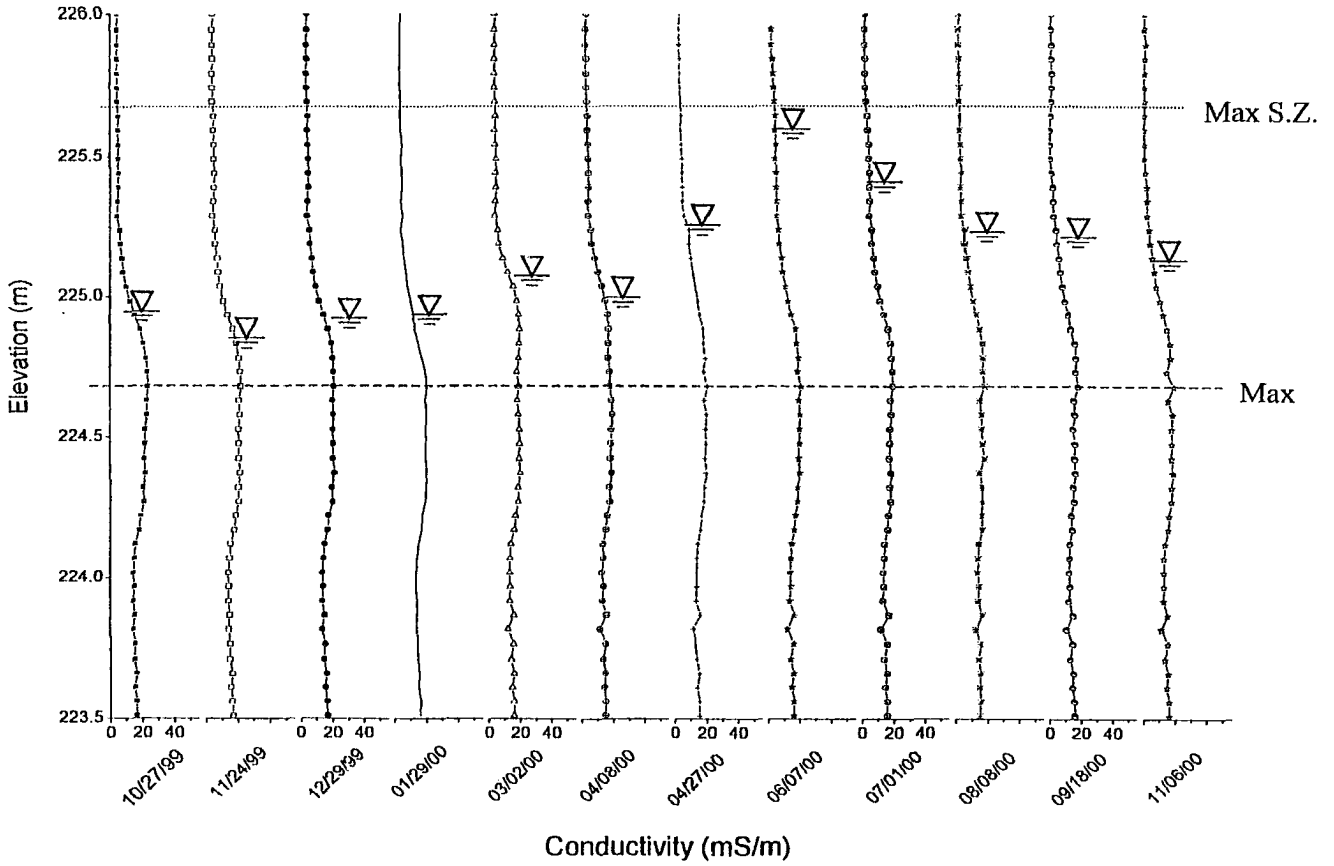

Figure 6. VRP 10, Residual Phase LNAPL Location; Conductivity Vs. Elevation Over Time. Maximum Elevation of Smear Zone (MaxSZ) and Elevation of Maximum Conductivity (Max Cond.) Shown for Reference to Figures 8-13.

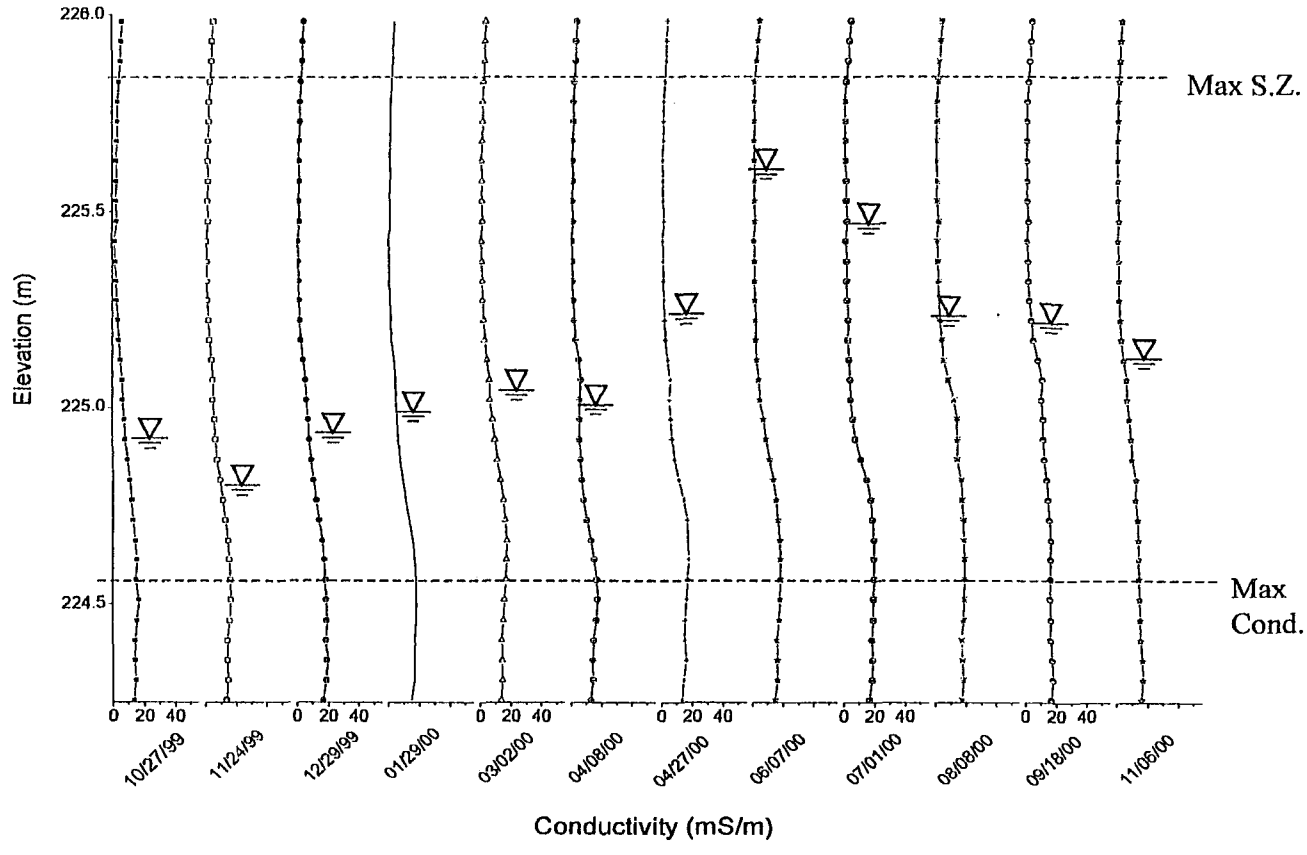

Figure 7. VRP 9, No LNAPL Location; Conductivity Vs. Elevation Over Time. Estimated Maximum Elevation of Smear Zone (MaxSZ) and Elevation of Similar Maximum Conductivity (Max Cond.) As at LNAPL Locations. Shown for Reference to Figures 8-13.

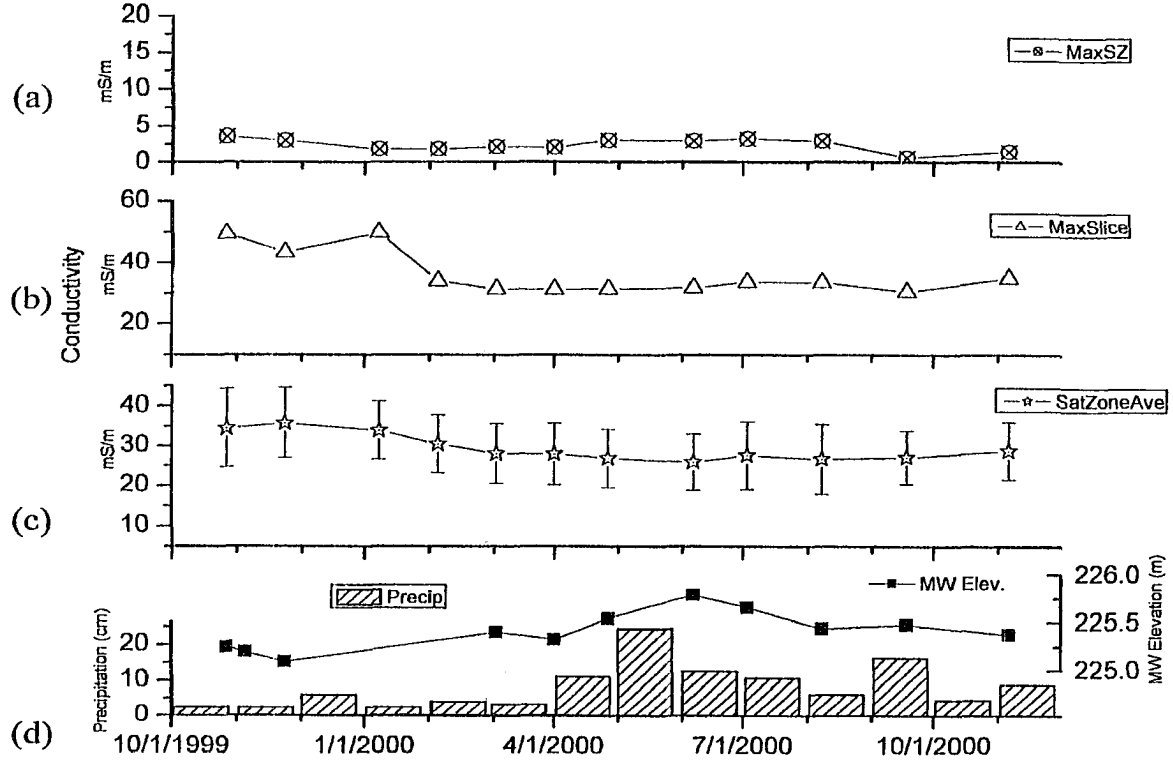

Figure 8. VRP 1, Free Phase LNAPL Location Conductivity Zones and Slices vs. Time. (a) Maximum Elevation of the LNAPL Smear Zone Conductivity Time Series. (B) Time Series Through the Maximum Conductivity Zone. (C) Time Series of the Saturated Zone Average Conductivity, Error Bars Indicate One Standard Deviation. (D) Precipitation and Monitoring Well Elevation Time Series.

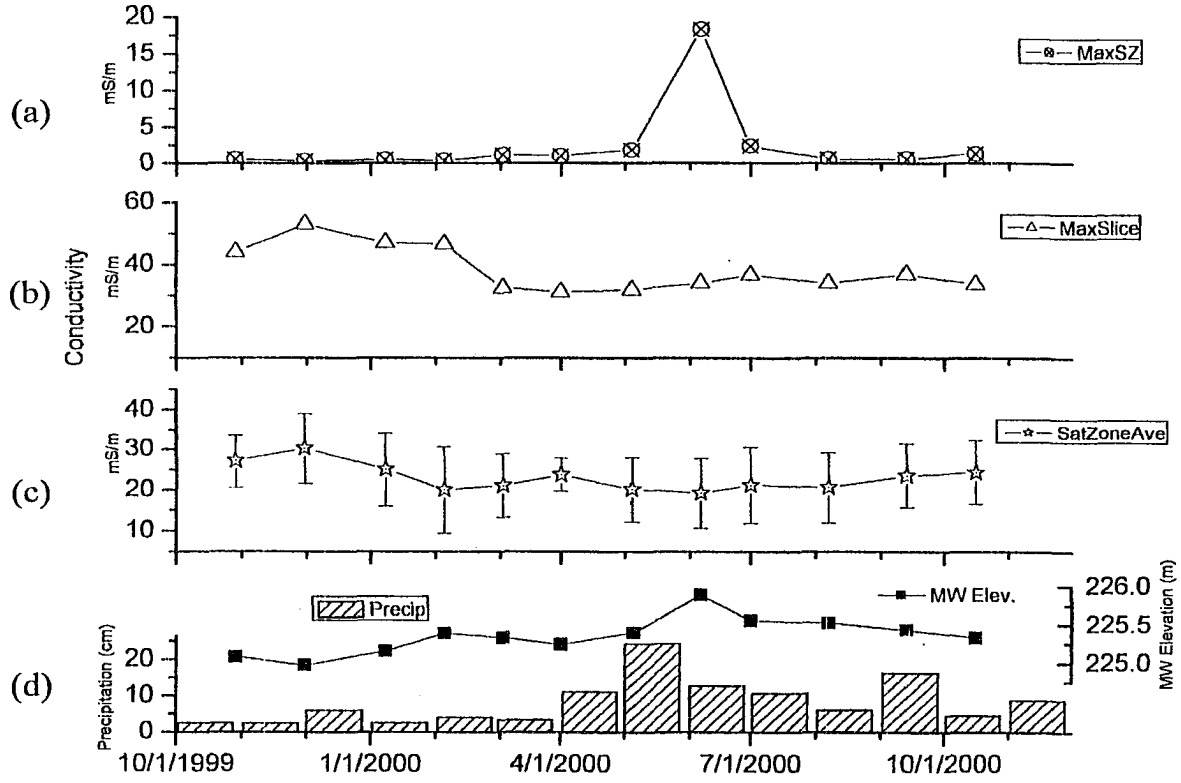

Figure 9. VRP 4, Free Phase LNAPL Location Conductivity Zones and Slices Vs. Time. (A) Maximum Elevation of the LNAPL Smear Zone Conductivity Time Series. (B) Time Series Through the Maximum Conductivity Zone. (C) Time Series of the Saturated Zone Average Conductivity, Error Bars Indicate One Standard Deviation. (D) Precipitation and Monitoring Well Elevation Time Series.

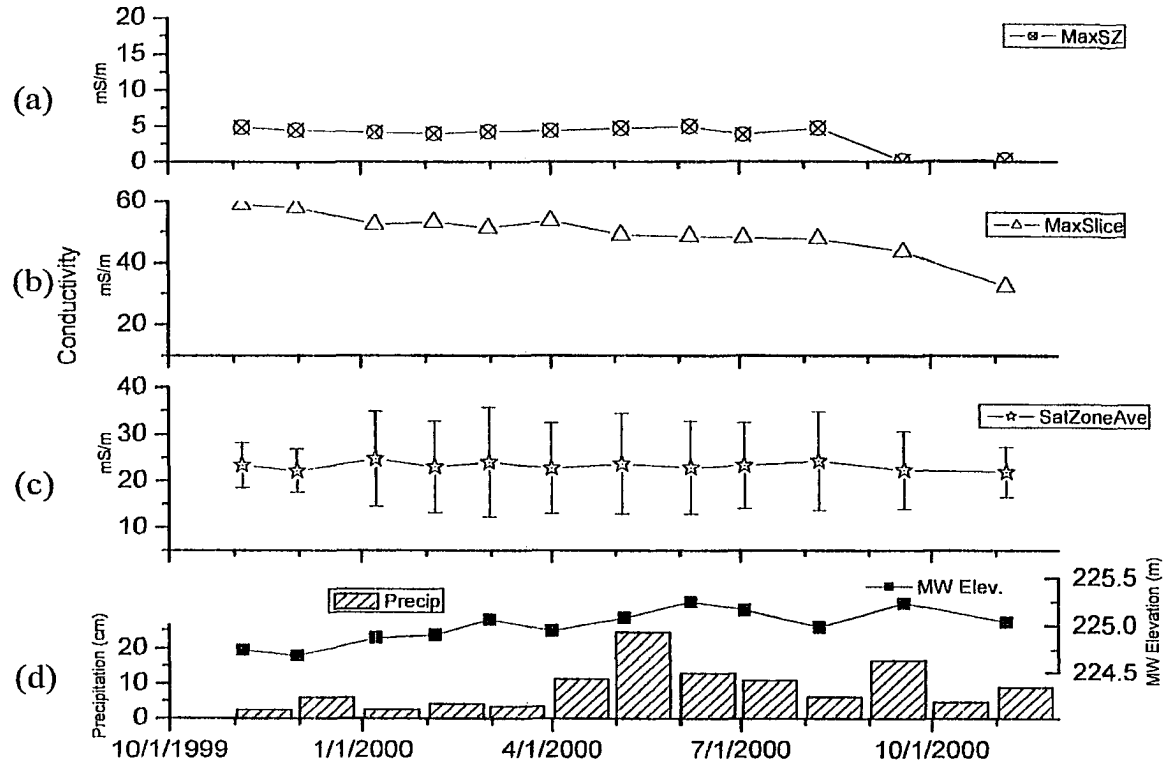

Figure 10. VRP 5, Free Phase LNAPL Location Conductivity Zones and Slices Vs. Time. (A) Maximum Elevation of the LNAPL Smear Zone Conductivity Time Series. (B) Time Series Through the Maximum Conductivity Zone. (C) Time Series of the Saturated Zone Average Conductivity, Error Bars Indicate One Standard Deviation. (D) Precipitation and Monitoring Well Elevation Time Series.

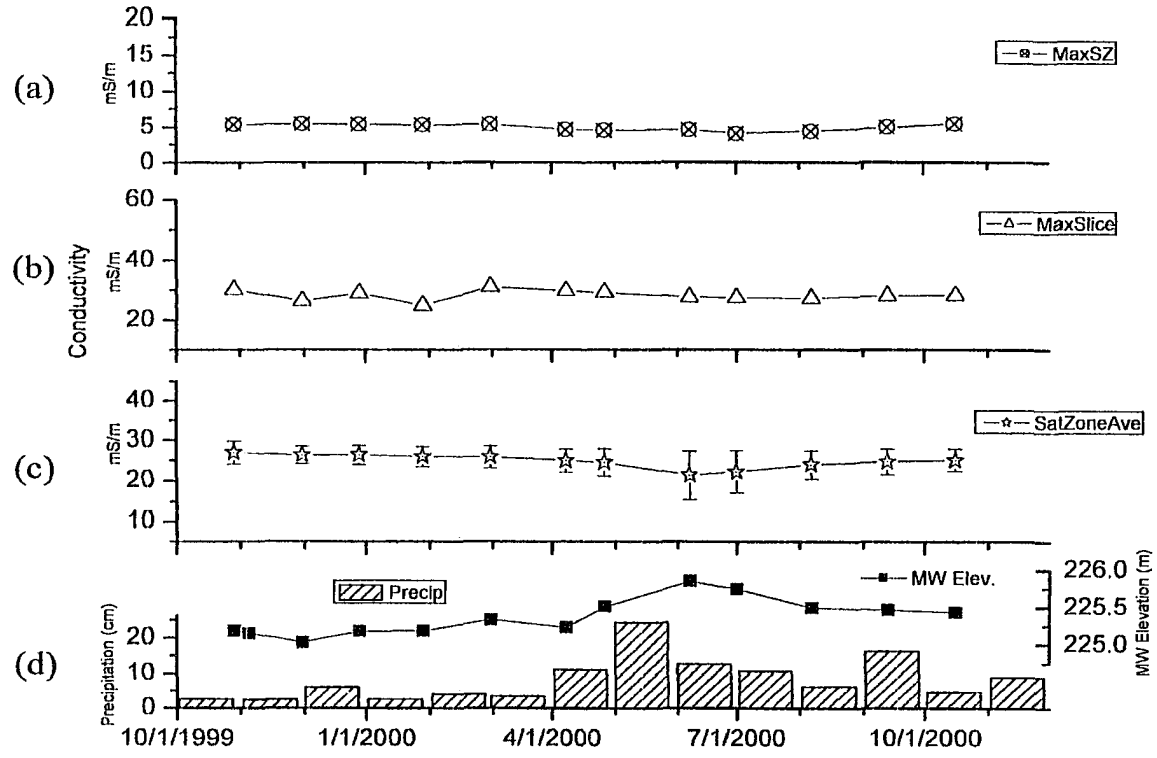

Figure 11. VRP 3, Residual Phase LNAPL Location Conductivity Zones and Slices Vs. Time. (A) Maximum Elevation of the LNAPL Smear Zone Conductivity Time Series. (B) Time Series Through the Maximum Conductivity Zone. (C) Time Series Of the Saturated Zone Average Conductivity, Error Bars Indicate One Standard Deviation. (D) Precipitation and Monitoring Well Elevation Time Series.

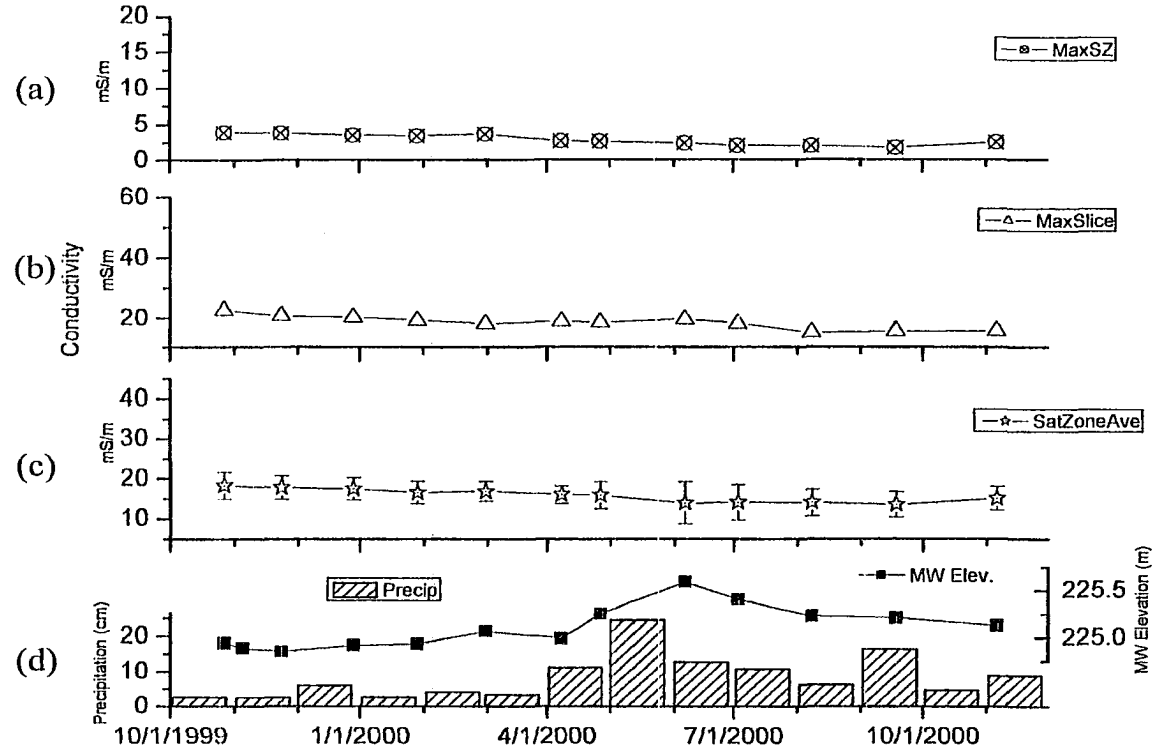

Figure 12. VRP 10, Residual Phase LNAPL Location Conductivity Zones and Slices Vs. Time. (A) Maximum Elevation of the LNAPL Smear Zone Conductivity Time Series. (B) Time Series Through the Maximum Conductivity Zone. (C) Time Series Of the Saturated Zone Average Conductivity, Error Bars Indicate One Standard Deviation. (D) Precipitation and Monitoring Well Elevation Time Series.

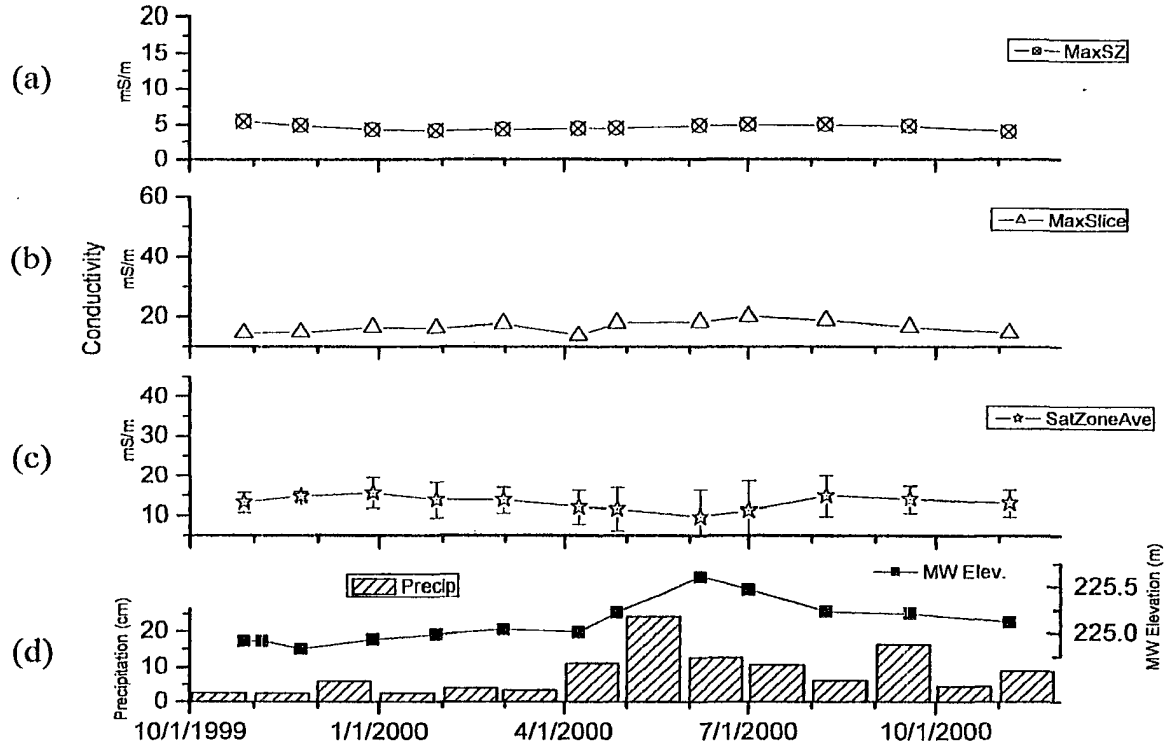

Figure 13. VRP 9, No LNAPL Location Conductivity Zones and Slices Vs. Time. (A) Estimated Maximum Elevation of the LNAPL Smear Zone Conductivity Time Series. (B) Time Series Through the Maximum Conductivity Zone. (C) Time Series Of the Saturated Zone Average Conductivity, Error Bars Indicate One Standard Deviation. (D) Precipitation and Monitoring Well Elevation Time Series.

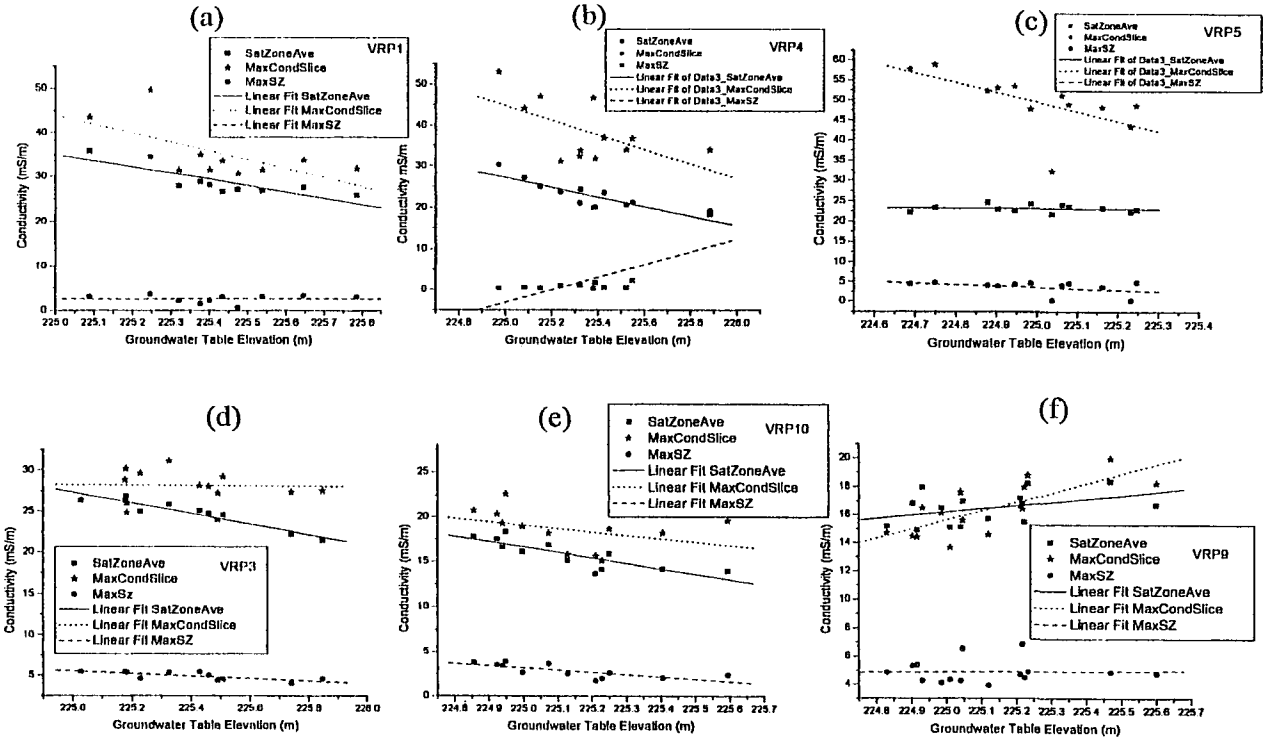

Figure 14. Results of Linear Regression Analysis of the Groundwater Table Elevation Vs. Conductivity Slices and Zones for Each VRP Location. (A) VRP1, (B) VRP4, (C) VRP5, (D) VRP3, (E) VRP10, (F) VRP9

CHAPTER 5

CONCLUSIONS

Past geoelectrical investigations of LNAPL contamination have yielded contradictory results, observed as both resistive and conductive. The resistive response is observed primarily from short-term laboratory or controlled spill experiments and the conductive response is associated with older in situ contamination. Additionally, this conductive response is apparently due to the products and byproducts from the natural biologically mediated metabolism of the LNAPL, which suggests that time is a critical factor controlling the geoelectrical response (Sauck, 2000). Therefore this project was performed to test the conductive plume model at a site of long term LNAPL contamination. Furthermore, this project included investigations into how the geoelectrical response changed both vertically and horizontally throughout the site and to investigate the influence of recharge on the geoelectrical response.

Results show corroborative evidence from biological studies linking the geoelectrically conductive zone to peak oil-degrading microbial populations. Further, geochemical evidence showed that the conductive response is dependent on the byproducts of microbial degradation and their reactions with the aquifer material. These results indicate a direct link between zones of anomalously high conductivity, oil-degrading microbial populations, acid production, and increased mineral dissolution observed through etching and high TDS concentrations. All this evidence further supports the conductive plume model at aged (i.e. mature) LNAPL sites (Sauck, 2000).

A detailed analysis of the conductive response is analyzed using Archie's Law (Archie, 1942). The results show elevated pore water saturations and pore water conductance necessary to produce the conductivity anomalies observed via the VRPs. At the locations of free phase LNAPL, these specific conductance estimates are greater than those measured in the field. This suggests another mechanism of conductance other than electrolytic may be responsible for the conductivity anomaly observed. The estimates from the residual phase LNAPL locations are supported by enhancements in TDS in the electrolyte.

The geoelectrical response is further investigated with respect to recharge. In this section of the study, the affects of seasonal precipitation events are correlated with the spatial and temporal variations in the geoelectrical response. These results reveal the conductivity response to recharge is dependent on the degree of LNAPL impaction. This study suggests that electrolytic conduction is very important to the conductivity profile observed at residual phase LNAPL locations while this mechanism of conductance is not enough to describe the results at the free phase locations. Finally, the response at the non-contaminated location suggests that saturation may be more important for the conductivity profile and not the TDS concentration of the electrolyte, as at the residual phase location.

The results presented in this study provide a detailed anatomy of the conductivity response at a mature LNAPL-impacted site. In conclusion, the geoelectrical response is anomalously conductive and is governed by the degree of LNAPL contamination and the products of the microbially-mediated degradation of the hydrocarbon. Furthermore, the

presence of either free phase LNAPL, or residual phase LNAPL affects the conductivity structure of the subsurface and its response to recharge events.

This investigation implies that geoelectrical methods can be used to locate zones of dynamic physical changes and guide biogeochemical analysis to these zones. Further biogeochemcial analysis may provide evidence to link these conductivity zones to processes resulting from biodegradation. Therefore, VRPs have the potential to monitor the natural biodegradation of petroleum hydrocarbons by measuring the conductivity profile and monitoring its response to recharge events. Furthermore, these results imply that VRPs can be used to guide active remediation efforts by targeting zones (i.e. the smear zone) where physical changes are occurring. Geochemists and environmental scientists can utilize these investigations to understand the dynamics, which affect the physical changes in the subsurface. Moreover, this study has increased the understanding of the geoelectrical response resulting from LNAPL degradation and provides relationships never before established. These results are fundamental to the development of robust geoelectrical models for the assessment of LNAPL-impacted sites and have the potential of increasing remediation effectiveness and cost savings by providing an understanding of how microbial modifications of LNAPL-impacted media alter the geoelectrical response.

5.1 References

Archie, G. E. The Electrical Resistivity Log as an Aid in Determining Some Reservoir Characteristics. Transactions of the American institute of Mining, Metallurgical and Petroleum Engineers, 146, 54-62. 1942.

Sauck, W. A. A model for the resistivity structure of LNAPL plumes and their environs in sandy sediments. Journal of Applied Geophysics, 44/2-3, 151-165. 2000.